

School of Doctoral Studies in Biological Sciences
University of South Bohemia in České Budějovice
Faculty of Science

**LEAF CUTICLE AS AN ARCHIVE OF INFORMATION ON
CO₂ SUPPLY**

Ph.D. Thesis

Mgr. Jitka Janová (Neuwirthová)

Supervisor: prof. Ing. Jiří Šantrůček, CSc

České Budějovice 2024

This thesis should be cited as:

Janová, J, 2024: Leaf cuticle as an archive of information on CO₂ supply. Ph.D. Thesis. University of South Bohemia, Faculty of Science, School of Doctoral Studies in Biological Sciences, České Budějovice, Czech Republic.

*** Annotation**

In this thesis, plant cuticle was not considered only as a protective barrier against water loss, but as a dynamic structure that reflects environmental conditions and may carry a trace of CO₂ concentration and its gradient within the leaf. We used the isotopic composition of epicuticular wax to reveal concentration of CO₂ in chloroplasts and gradient of CO₂ across the leaf of hypo- and amphistomatous plants, tested this new model in leaves with distinct anatomical structures and described the dynamics of epicuticular wax renewal in young and mature leaves.

*** Declaration**

I hereby declare that I am the author of this dissertation and that I have used only those sources and literature detailed in the list of references.

České Budějovice, 30.4. 2024

Jitka Janová

*** Financial support**

This work was funded by the Czech Science Foundation (18-14704S) and by the Grant agency of the University of South Bohemia (GAJU 017/2019/P). Access to IRMS and other facilities was supported by the Czech Research Infrastructure for Systems Biology C4SYS (Project No. LM2015055).

*** Acknowledgements**

First of all, I would like to acknowledge my supervisor Jiří Šantrůček, who guided me throughout my doctoral studies and whose door was always open to me. I also appreciate and thank all the members of the Department of Experimental Plant Biology who collaborated with me on any of the projects or just created a pleasant working atmosphere. Such an environment was very important for me, especially after returning from maternity leave, when I needed a fresh start. Last but not least I want to thank my family. To my parents who have always supported me and especially to my husband who gave me the strength to finish this work.

* List of articles and author's contribution

The thesis is based on the following original articles:

1. **Santrucek J; Schreiber L; Macková J; Vráblová M; Kveton J, Macek P, Neuwirthová J.** (2019). Partitioning of mesophyll conductance for CO₂ into intercellular and cellular components using carbon isotope composition of cuticles from opposite leaf sides. *Photosynthesis Research* 141, 33-51. DOI: 10.1007/s11120-019-00628-7, IF (2022) = 3.7

Jitka Janová prepared samples from second group of plants (11 species) included in this study, analyzed anatomical traits, isolated cuticles, extracted cuticular waxes and prepared samples for EA-IRMS analysis. She did the same, including gas chromatography analyses, with Ficus elastica plants growing under contrasting light conditions. She prepared sensitivity models for partitioning of r_m . She discussed the results and commented on the whole manuscript.

Jitka's percentile contribution was 20 %.

2. **Kubásek J; Kalistová T, Janová J; Askanbayeva B; Bednár J; Santrucek J** (2023) ¹³CO₂ labelling as a tool for elucidating the mechanism of cuticle development: a case of *Clusia rosea*. *New Phytologist* 238, 202-215. DOI: 10.1111/nph.18716, IF (2022) = 9.4

Jitka prepared together with J. Kubasek and J. Santrucek a design of the pilot experiment, she was responsible for collecting cuticular samples, preparing them for the analysis and evaluating the data. She discussed the results and commented on the whole manuscript.

Jitka's percentile contribution was 25 %.

3. **Janová J; Kubásek J; Grams TE; Zeisler-Diehl V; Schreiber L; Šantrůček J** (2024) Effect of light-induced changes in leaf anatomy on intercellular and cellular components of mesophyll resistance for CO₂ in *Fagus sylvatica*. Plant biology. DOI: 10.1111/plb.13655, IF (2022) = 3.9

Jitka designed together with J. Santrucek the experiment, together they did the field work, subsequently she prepared the samples for analysis (including leaf traits, EA-IRMS, GC-MS/FID). She analysed the data and wrote the article in co-operation with other co-authors.

Jitka's percentile contribution was 75 %.

4. **Askanbayeva B; Janová J; Kubásek J; Zeisler-Diehl V; Schreiber L; Muir CD; Šantrůček J** (2024). Amphistomy: stomata patterning inferred from ¹³C content and leaf-side specific deposition of epicuticular wax. Annals of Botany. IF (2022) = 4.2

Jitka prepared part of samples from the experiment (including wax isolation and preparing for GC and IRMS analysis) and wrote Carbon isotope parts of Material and methods. She discussed the results and commented on the whole manuscript.

Jitka's percentile contribution was 20 %.

*** Co-author agreement**

Jiří Šantrůček, the supervisor of this Ph.D. thesis and co-author of papers I, II, III and IV, fully acknowledges the stated contribution of Jitka Janová to these manuscripts.

.....

prof. Ing. Jiří Šantrůček, CSc

*** Content:**

1. General Introduction	- 1 -
1.1. Plant cuticle: structure and functions	- 2 -
1.2. Mesophyll conductance for CO ₂	- 15 -
1.3. Basics of discrimination of the heavy stable isotope ¹³ C by plants	- 23 -
2. Hypotheses and aims of the study	- 26 -
3. Summary and future prospects	- 28 -
4. Conclusions	- 32 -
5. References	- 33 -
Research articles	- 48 -
<i>Article I</i>	- 49 -
<i>Article II</i>	- 69 -
<i>Article III</i>	- 84 -
<i>Article IV</i>	- 87 -
* <i>Curriculum vitae</i>	

List of abbreviation

A_n	net rate of CO ₂ fixation in photosynthesis, $\mu\text{mol m}^{-2} \text{s}^{-1}$
c_a, c_i, c_c	CO ₂ concentration in the ambient atmosphere, in the substomatal cavity and in the chloroplast, respectively
CM	cuticular membrane
EW	epicuticular waxes
FA	fatty acids
g_{IAS}	gas phase of mesophyll conductance, $\text{mol m}^{-2} \text{s}^{-1}$
g_{liq}	liquid phase of mesophyll conductance, $\text{mol m}^{-2} \text{s}^{-1}$
g_m	mesophyll conductance, $\text{mol m}^{-2} \text{s}^{-1}$
g_s	stomatal conductance, $\text{mol m}^{-2} \text{s}^{-1}$
IAS	intercellular air space
IW	intracuticular waxes
MX	cuticle matrix
PPFD	photosynthetic photon flux density, $\mu\text{mol m}^{-2} \text{s}^{-1}$
r_{IAS}	gas phase of mesophyll resistance, $\text{m}^2 \text{s mol}^{-1}$
r_{liq}	liquid phase of mesophyll resistance, $\text{m}^2 \text{s mol}^{-1}$
r_m	mesophyll resistance, $\text{m}^2 \text{s mol}^{-1}$
r_s	stomatal resistance, $\text{m}^2 \text{s mol}^{-1}$
SD	stomatal density, number of stomata per cm^2
SI	stomatal index, number of stomata (cm^2) / number of all epidermal cell (cm^2), %
VLC	very long chain
Δ	shift in isotopic composition related to the source, ‰
δ	isotopic composition related to the standard, ‰

1. General Introduction

The primary carboxylation enzyme of C_3 plants, Ribulose-1,5-bisphosphate carboxylase/oxygenase (Rubisco), has a relatively low affinity for carbon dioxide. In addition to carboxylation, it also has oxygenation activity, i.e. it can bind oxygen instead of carbon dioxide. As a consequence, it functions at less than one-half of its maximum carboxylation capacity even with currently globally increasing atmospheric CO_2 concentrations (Evans & Von Caemmerer, 1996). Despite the current exponential increase in the concentration of CO_2 in the Earth's atmosphere, the transport of CO_2 from the atmosphere across the leaf and its sufficient concentration in the leaf chloroplasts (together with its carboxylation capacity) is one of the main limitations of the rate of photosynthesis and plant growth. Lack of CO_2 in chloroplasts creates selection pressure leading to adaptive changes in leaf anatomy, such as an increase in mesophyll permeability to CO_2 , which subsequently result in higher CO_2 concentrations around the Rubisco enzyme. Therefore, in order to understand and exploit these adaptive changes, we need a good understanding of the patterns of CO_2 fluxes across the leaf and the mechanisms regulating them.

The plants' leaves are covered with an extracellular polymeric membrane - the cuticle, which is very poorly (almost immeasurably) permeable to CO_2 . The flow of CO_2 into the leaf is, as currently understood, controlled almost exclusively by the diffusive resistance of the stomata and mesophyll. Our previous data suggest that both of these resistances, and the resulting deficiency in chloroplast CO_2 supply, may leave a trace in the chemical composition of the cuticle, specifically in the content of the naturally occurring stable carbon isotope, ^{13}C . Therefore, in this thesis I treat the cuticle in a somewhat unconventional way - primarily as a "marker" of diffusive CO_2 fluxes, not only as a barrier limiting water flux out and CO_2 flux into the leaf.

1.1. Plant cuticle: structure and functions

The plant cuticle, or cuticular membrane (CM), is an extracellular product of the epidermis. Its evolution is related to the conquest of terrestrial environment by plants around 450 million years ago, when plants were exposed to new abiotic and biotic stresses, i.e. desiccation, ultraviolet radiation, gravitation or pathogen infections (Kenrick & Crane, 1997; Bateman *et al.*, 1998). The CM is almost impermeable to gases and probably evolved prior or co-evolved together with stomata, where the gas exchange between plant and atmosphere occurs (Clark *et al.*, 2022). These evolutionary innovations went hand in hand with extended root system, vascular structures and development of intercellular air space (IAS) (Raven, 2002).

The CM is a thin, white to translucent membrane with the thickness in the range 1-10 μm (Riederer, 2007). It covers all living epidermal cells of the aerial parts of higher plants, i.e. not only leaves but also stems or fruits (Heredia, 2003), and forms the interface between the plant and the atmosphere (Riederer & Schreiber, 2001). Recently, the cuticle was also detected on the root tips, where it is an important protection against abiotic stresses during seedling establishment and lateral roots growth (Berhin *et al.*, 2019). On the leaf, we find the cuticle on both sides, adaxial (upper) and abaxial (lower), lining the stomata and extending into the substomatal cavity, where it covers the free epidermal cells (but not the mesophyll cells) (Osborn & Taylor, 1990) (Fig. 1).

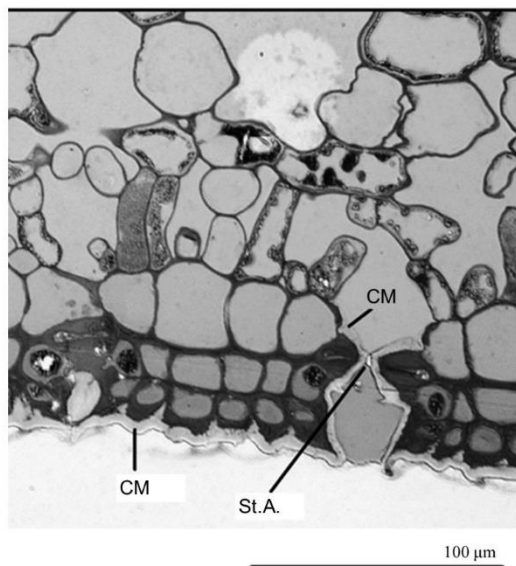


Fig. 1: Semi-thin section of *F. elastica* leaf with cross-section of stomal aperture (St.A.) in detail. The cuticular membrane (CM) covering the leaf surface covers also the surface of antestomatal chamber and guard cells and extends into the substomatal cavity. Author: Jitka Janová

The cuticle developed a unique supramolecular and dynamic assembly of molecules and macromolecules that perform multiple functions. It forms a major barrier to water loss (Schönherr & Mérida, 1981; Riederer, 1991), reflects UV radiation (Krauss *et al.*, 1997), protects leaves from pathogen attack (Serrano *et al.*, 2014; Kalistova & Janda, 2023), and helps in keeping the leaf dry and clean due to its hydrophobic nature, so called "lotus effect", respectively (Neinhuis & Barthlott, 1997; Watson *et al.*, 2014). This "multifunctionality" is given by its heterogeneous structure and variable chemical composition, which differs among plant species, organs, depends on the developmental stage and reflects biotic and abiotic factors (Knoche *et al.*, 2004; Szakiel *et al.*, 2012; Macková *et al.*, 2013; Serrano *et al.*, 2014). Indeed, any defects in cuticle biosynthetic pathways cause defects in cuticle assembly and affect organ growth and morphology (Reynoud *et al.*, 2021). The cuticle is not a rigid structure, it can change its thickness and chemical composition dynamically depending on the leaf environment; in particular, the surface layer of waxes is renewed as erosion occurs (see below in *Cuticle biosynthesis* section). Waxes deposited on the leaf surface continually could potentially imprint changes in the internal and external environment of the leaf including leaf internal CO₂ concentration (see below).

Cuticle composition

CM is an extracellular product of epidermis and is in direct contact with the underlying polysaccharide cell wall of the epidermis. Based on histochemical staining, the CM can be divided into two domains: dense, cutin-rich "*cuticular layer*" with polysaccharides, and "*cuticle proper*" which is enriched in waxes (Fig. 2) (Yeats & Rose, 2013). The intermingled polysaccharides in the cuticular layer come probably from the cell wall continuum (Fich *et al.*, 2016).

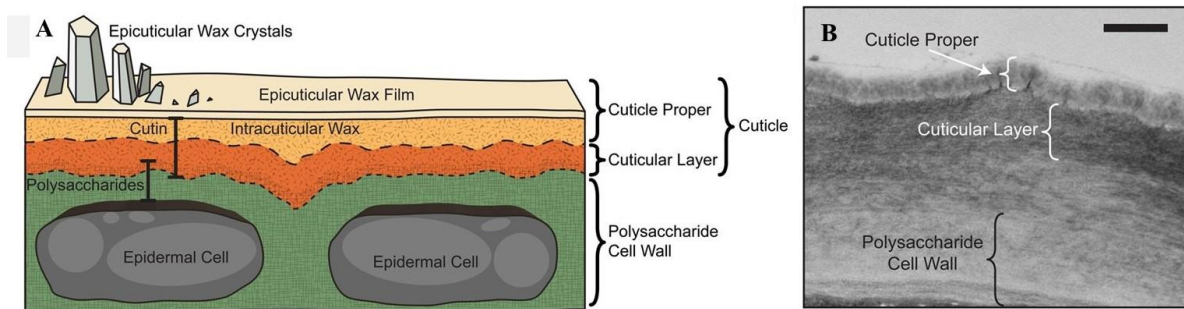


Fig. 2: (A) Schematic diagram with major structural features of the cuticle. (B) Transmission electron micrograph image of epidermal cell wall and cuticle of *Arabidopsis thaliana* stem. Bar = 0.5 μm (Yeats & Rose, 2013).

Generally, from the chemical point of view, the cuticle can be divided into two basic components:

- i. Cuticle matrix (MX) consisting of insoluble polymer and minor fraction of mixture of polysaccharides, amino acids and phenols (Nawrath, 2006). The polymer is formed from cutin and/or cutan and is the major component of the MX (making up 40 to 75% of the total MX weight) (Schreiber & Schönherr, 2009). Cutin is a network of oxidized C₁₆ and C₁₈ fatty acids and its derivatives¹ linked by an ester bond, forming a mechanically resistant network (Nawrath, 2006). The profile of cutin monomers vary among species, organs or developmental stages, and its chemical properties indicate the possibility of branching and cross-linking between different chains and dendrimers (Fich *et al.*, 2016). In order to analyse the chemical composition of cutin, it must first be depolymerised by ester cleaving acid-catalysed transesterification. Rarely, a highly resistant biopolymer remains after extraction and hydrolysis of the cuticle, which has been termed cutan or non-ester cutin (Schmidt & Schönherr, 1982; Nip *et al.*, 1986). Cutan is considered a minor cuticular component in most plant species, but there are documented cuticles with significant amounts of cutan, f. e. *Podocarpus* sp., *Agave americana*, *Clusia rosea*, *Clusia multiflora*, *Clivia miniata*, *Ficus elastica* or *Prunus laurocerasus* (Boom *et al.*, 2005; Gupta *et al.*, 2006; Guzmán-Delgado *et al.*, 2016). All above mentioned species have similar leaf morphological characteristics such as succulent or thick leaves with thick cuticle (Boom *et al.*, 2005; Leide *et al.*, 2020). The study of cutan composition requires employment of advanced spectroscopic and gas

¹ Monomers typically have a terminal hydroxyl (ω -OH) and one or more oxygen groups in the midchain, most commonly hydroxy or epoxy groups (Fich *et al.*, 2016).

chromatographic techniques, as described, f.e., in Leide et al. (2020). Nevertheless, the analyses of chemical composition do not provide us with information about the arrangement and structure of polymers in the MX. Nowadays, there are accessible methods for studying the intact polymer that employ several variations of solid-state nuclear magnetic resonance (Serra *et al.*, 2012).

ii. The second fraction, cuticular waxes, consist of a mixture of linear molecules with a long carbon chain (18 to 34 C) and various functional groups, mainly acids, alkanes, aldehydes, ketones, primary and secondary alcohols and esters (Samuels *et al.*, 2008; Yeats & Rose, 2013). Pentacyclic triterpenoids and small amounts of aromatic compounds may also be present (Jetter *et al.*, 2006; Samuels *et al.*, 2008). The amount of the loaded wax dispersed at the surface and within the cuticle vary across plant species as intra-species, depending on the organ, ecotype and growing conditions, with the range from 20 to 1300 $\mu\text{g} \cdot \text{cm}^{-2}$ (Schreiber & Riederer, 1996).

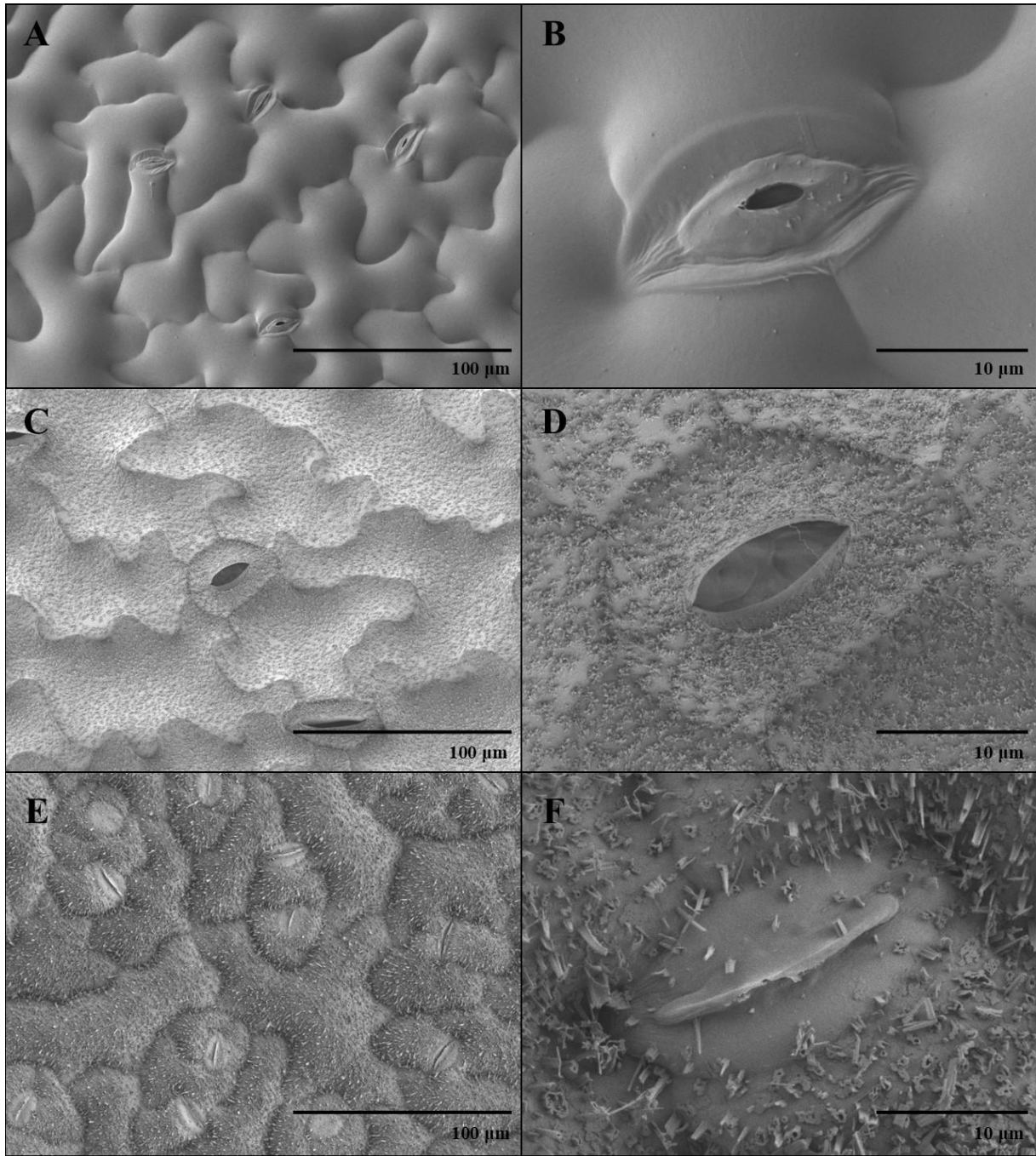


Fig. 3: Cryo-SEM visualisation of abaxial leaf side of *Arabidopsis thaliana* (thale cress, A-B), *Papaver somniferum* (breadseed poppy, C-D) and *Brassica napus* (rapeseed, E-F) with different EW arrangement. Authors: Kalistová and Janová.

Depending on their deposition, waxes are divided into intracuticular (IW), embedded in the cutin polymer, and epicuticular (or extracuticular) waxes (EW) deposited on the surface (Buschhaus & Jetter, 2011). Epicuticular waxes can form amorphous films or characteristic microcrystals visible with a scanning electron microscope (Fig.2 and 3) as described already more than 50 years ago by Amelunxen et al. (1967). They proposed five main classes of EW

structures: *Grains, rods and filaments, plates and scales, films and crusts, and fluid and greasy wax layers*. The classes were later divided into more subclasses as imaging technique improved and provided better resolution (Barthlott *et al.*, 1998). All waxes can be easily extracted by immersion the isolated CM² in a polar solvent such as chloroform or hexane (Post-Beittenmiller, 1996). However, enzymatic isolation of CM is not possible in all plant species, especially those with thin leaves and delicate membranes. In such case, the method of immersing whole fresh leaves into the solvents is used. Nevertheless, this method is not optimal, because it is necessary to choose such a “dipping-time” to obtain as much wax as possible (included IW) and still avoid solvent penetration into the leaf tissue and extraction of compounds from it. Recently, Vráblová *et al.* (2020) modified the method for enzymatic isolation for the model plant, *Arabidopsis thaliana*, which works well for other species as well, for example in *Brassica juncea* (Yadav *et al.*, 2023), *Papaver somniferum* or *Brassica napus* (Kalistová and Janová, not published).

Another option is selective mechanical removal of EW, which can be performed from the isolated CM or intact leaf by several methods: *Gum arabic* dissolved in water (Jetter & Schäffer, 2001), *cellulose acetate* dissolved in acetone (Silcox & Holloway, 1986), *collodion* (nitrocellulose) dissolved in diethyl ether:ethanol (Haas & Rentschler, 1984) or cryo-adhesive-based wax removal by a droplet of *glycerol* or *water* (Jeffree, 1996; Jetter *et al.*, 2000). For a comparison of methods and yields, see e.g. Jetter *et al.* (2000), Zeisler & Schreiber (2016) or Kalistová *et al.* (publication under preparation).

This selective wax isolation helps to understand the function of distinct parts in the function of the whole cuticle, for example regarding the main function, the barrier against water lost. It is known for a long time that after extraction of all waxes (EW and IW), the cuticular permeability to water increases by two to three orders of magnitude (Schönherr, 1976; Schönherr & Riederer, 1989; Schreiber & Schönherr, 2009). It was shown by selective removing of EW that the transpiration barrier is essentially formed by IW (Zeisler & Schreiber, 2016; Zeisler-Diehl *et al.*, 2018).

In general, the recent data showed that functions of the cuticle cannot be assessed solely by its chemical composition but arise from the spatial organization of molecules and

² In some plant species, the CM can be isolated by incubation in an enzymatic mixture of pectinase and cellulase (Schönherr & Riederer, 1986). The CM is then detached from the epidermis and can be dipped in the solvent.

macromolecules, i.e. from the 3D architecture (Reynoud *et al.*, 2021), and probably as well from the dynamics of synthesis and regeneration. I believe that the future research will go in this direction and reveal more information about CM functions that could be inspiring for people, such as manufacturers of functional materials.

Cuticle biosynthesis

The biosynthesis pathway of CM precursors is fairly well characterized even at the level of key genes and enzymes (Fig.4), but there are still a few white spaces, especially in the area of fatty acids (FA) and very long chain fatty acids (VLCFA) transfer and cuticle assembly. The beginning, synthesis of FA in plastids of the epidermal cells, is common to cuticle and wax precursors. It is catalysed by FA synthase complex (FAS) which adds acetyl moiety of malonyl-CoA (two-carbon activated part) to acyl primer repeatedly (8-9 times) to form 16- or 18-carbon long saturated FA (Kunst & Samuels, 2009; Ohlrogge *et al.*, 2015). The malonyl-CoA originate from the two-carbon acetyl in acetyl-CoA, which is formed from pyruvate by its oxidative decarboxylation catalysed by pyruvate dehydrogenase (Ohlrogge *et al.*, 2015). C16 and C18 FAs are consequently transported into the cytoplasm and endoplasmic reticulum (ER) by so far unknown mechanism. At the outer plastid membrane or ER (depending on the enzyme localization), FA chains are activated by long-chain acyl-coenzyme A synthases (LACSs) to FA-coenzyme A (FA-CoA) (Jessen *et al.*, 2015; Zhao *et al.*, 2021). At the ER, the biosynthesis pathway splits and continue separately for cutin and waxes.

The *cutin synthesis* proceeds in ER by ω -hydroxylation and/or hydroxylation to form oxygenated fatty acid-glycerol esters, termed monoacylglycerols, often in the presence of cytochrome P450 (CYP) enzymes (Pollard *et al.*, 2008; Fich *et al.*, 2016). The final step in cutin monomers synthesis is esterification of the precursors (Ohlrogge *et al.*, 2015).

The *wax synthesis* continues at the ER by elongating of the activated FA-CoA catalysed by enzyme FA elongase (FAE). FAE adds two carbons in each cycle to synthesize a very long chain (VLC) acyl-CoA (Samuels *et al.*, 2008), which are further modified via either the alcohol-forming pathway (generating primary alcohols and wax esters) or the alkane-forming pathway (producing alkanes, aldehydes, secondary alcohols, and ketones) (Ohlrogge *et al.*, 2015). Primary alcohols are produced from VLC acyl-CoAs by acyl desaturase ECERIFERUM17 (CER17) by conversion to monounsaturated FAs, which are subsequently reduced by fatty acyl-CoA reductase (FAR) (Yang *et al.*, 2017; Wang *et al.*, 2020). Primary

alcohols and VLC acyl-CoAs can further serve as precursors for wax synthase/acyl-CoA:diacylglycerol acyltransferase1 (WSD1) producing wax esters (Yeats & Rose, 2013; Ohlrogge *et al.*, 2015). The alkane forming pathway involves CER1/CER3/CYTB5 complex, which converts VLC acyl-CoAs to aldehydes and subsequently to alkanes (Yeats & Rose, 2013; Wang *et al.*, 2020). The later mentioned can be further hydroxylated to secondary alcohols and secondary oxidised to ketones by midchain alkane hydroxylase1 (MAH1) (Greer *et al.*, 2007; Samuels *et al.*, 2008).

The biggest uncertainties are about the transport mechanism of cutin monomers and VLCFA through the plasma membrane and cell wall into the CM. Almost certainly ABC (ATP-binding cassette) transporters from the G subfamily are involved in the traffic of some wax and cutin precursors through plasma membrane (Bessire *et al.*, 2011; Yeats & Rose, 2013; Ohlrogge *et al.*, 2015; Wang *et al.*, 2020). Another proposed option is the direct transfer of cutin monomers from the ER across plasma membrane at their point of touch (Samuels & McFarlane, 2012; Fich *et al.*, 2016). The following step is transport of hydrophobic cuticle precursors via the hydrophilic polysaccharide cell wall, which might be facilitated by some of lipid transfer proteins (LTPs) (Edstam *et al.*, 2011; Yeats & Rose, 2013; Ohlrogge *et al.*, 2015; Salminen *et al.*, 2016) or spontaneously with the water similarly to the steam distillation mechanism (Neinhuis *et al.*, 2001).

The final step, assembly of functional cuticle, occurs in the cuticle layer. Cutin monomers are cross-linked with ester bonds between carboxyl group of one fatty acid and the primary or secondary hydroxyl group of another one forming polyester matrix (Ohlrogge *et al.*, 2015). There are two proposed mechanisms of the polymerisation: via enzymatic pathway (Yeats & Rose, 2013; Fich *et al.*, 2016; Segado *et al.*, 2020) or with the help of cutinosomes, spherical nanostructures capable of self-assembly only through physicochemical processes (Heredia-Guerrero *et al.*, 2008; Stępiński *et al.*, 2020; Xin & Herburger, 2021).

The cuticular matrix is synthesized early in leaf development³ and is not renewed for the rest of ontogeny (Riederer & Schönherr, 1988; Kubásek *et al.*, 2023). In contrast cuticular waxes are gradually eroded by wind or rain and are thus constantly renewed. Gao *et al.* (2012) determined the wax renewal time in timothy, *Phleum pratense*, to be 2-3 days for C16 and C18 acids, 5-16 days for waxes with carbon chain lengths C22-C26, and 71-128 days for the

³ The base of cuticle, procuticle, covers the very earliest epidermal cells in the shoot apices and leaf primordia. It is an electron-dense layer approximately 20 nm thick visible with transmission electron microscopy (Jeffree, 2007).

very long chain (VLC) component of waxes (C27 to C31). The composition of newly synthesized waxes may change in response to ontogenetic leaf development (Jetter & Schäffer, 2001) or seasonal conditions (Kerfourn & Garrec, 1992). We can conclude that wax synthesis is ongoing processes during the whole period of leaf growth (Prasad & Gülz, 1990; Hauke & Schreiber, 1998; Piasentier *et al.*, 2000; Jetter & Schäffer, 2001; Suh & Diefendorf, 2018). The wax may be re-deposited even in mature leaves within a period of days or weeks as is described in the literature (Koch *et al.*, 2004; Kahmen *et al.*, 2011; Gao *et al.*, 2012), in *Article II* (Kubásek *et al.*, 2023). Given this wax re-synthesis of waxes, we hypothesize that the extracted waxes carry a better signal about the external environment or changes in the external conditions compared to MX or whole CM. Therefore, we recommend using only extracted wax to estimating the CO₂ concentration profile inside the leaf, as we did in *Article III* (Janová *et al.*, 2024).

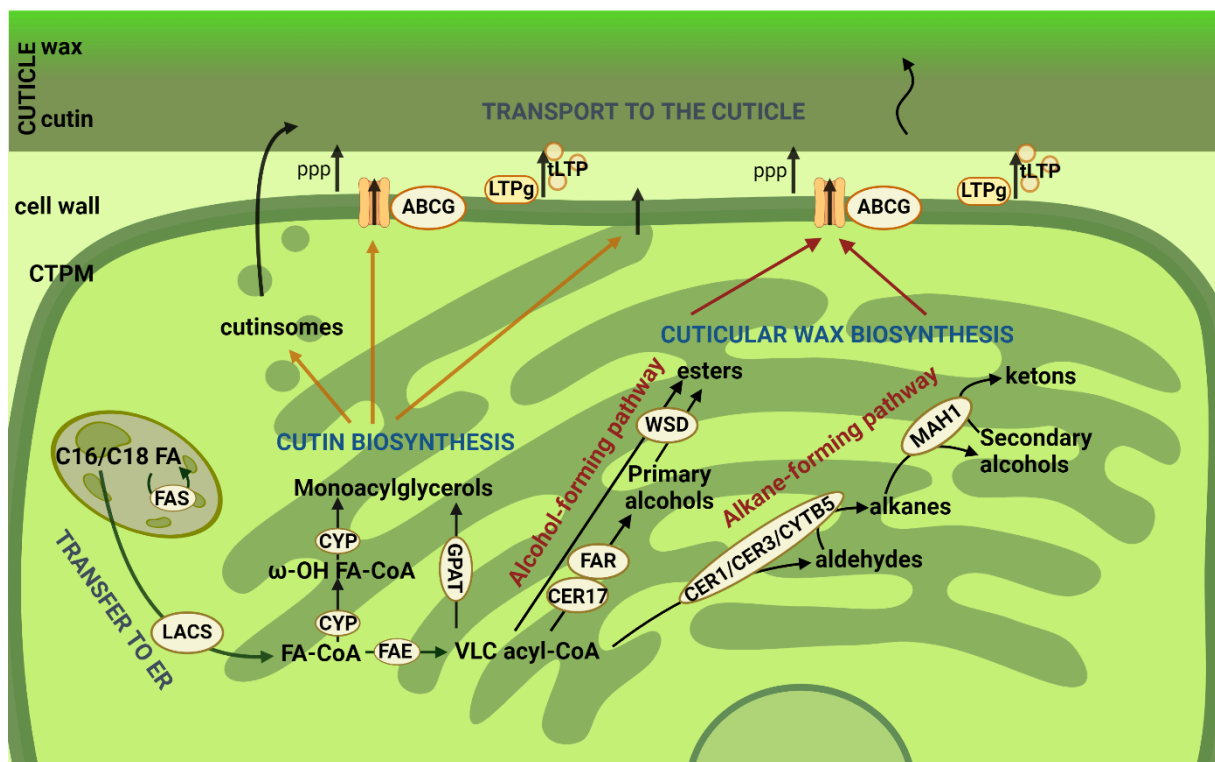


Fig. 4: Scheme of Cuticle biosynthesis showing crucial proteins: FA synthase complex (FAS), long-chain acyl-coenzyme A synthase (LACS), cytochrome P₄₅₀ enzymes (CYP), FA elongase (FAE), (GPAT), eceriferum17 (CER17), fatty acyl-CoA reductase (FAR), wax synthase/acyl-CoA:diacylglycerol acyltransferase (WSD), eceriferum1, eceriferum 3 and cytochrome B5 complex (CER1/CER3/CYTB5), midchain alkane hydroxylase 1 (MAH1), G subfamily of ATP-binding cassette (ABCG), lipid transfer proteins (LTPg and tLTP). Modified from Kalistova & Janda (2023). Created with BioRender.com.

Cuticle, leaf and stomata development

As mentioned above, colonisation of the land by plants was connected to the cuticle evolution. From the fossil findings we have evidence of the CM in all extinct embryophytes from bryophytes to angiosperms (Edwards, 1993; Haworth & McElwain, 2008; Budke *et al.*, 2012). Its main function may be protection against water loss, but this is far from the only feature, the CM also plays a crucial role in plant development. Morphological abnormalities, especially fusion of organs (leaves, floral organs), were observed in mutants with defective cuticle. Lolle *et al.* (1992) characterized a *fiddlehead* (*fdh*) mutant with fused leaves and floral organs. Histological analysis showed that the cell wall and cytoplasmic membrane remained intact, and leaf fusion was caused only by a change in cuticle structure (Fig. 5). Also, mutations in other genes of the cuticle/cuticular wax synthesis pathway led to a phenotype similar to *fdh* (e.g. the *eceriferum* group of mutants) indicating the importance of cuticle composition in plant development (Lolle *et al.*, 1998).

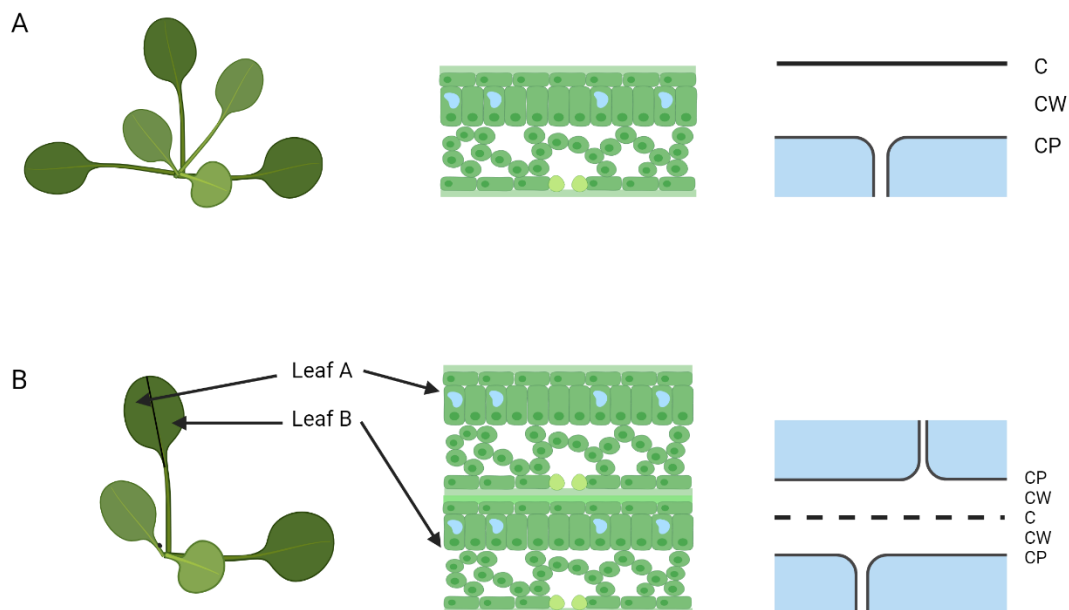


Fig. 5: Schematic illustration of developed leaves in: A) Wild type plants with normal cuticle. B) Mutant plant with defective cuticle causing leaf fusion. Schematic diagram of growth morphology (left), leaf cross-section (middle part) and epidermis ultrastructure (right). Abbreviations: C-cuticle; CW-cell wall; CP-cytoplasmic membrane. According to Tanaka & Machida (2006). Created with BioRender.com.

Another interesting interconnection seems to be between cuticle and stomata development. The fossil records indicate that cuticle evolved slightly prior or co-evolved together with stomata (Clark *et al.*, 2022). Some genes involved in cuticular wax and cutin biosynthesis are also known to be involved in the control of stomatal development in *A. thaliana*, enabling shared regulation pathway of stomatal development and cuticular properties. Gray *et al.* (2000) described the HIGH CARBON DIOXIDE (HIC) gene, which regulates stomatal development in response to CO₂ concentration⁴ and is homologous to the gene encoding a beta keto-acyl Co-A synthase involved in the synthesis of VLC fatty acids, i.e. in the synthesis of cuticle and waxes. The *hic* mutant failed in regulation of SD in response to changing c_a . Two other mutations in wax synthesis, *cer1* and *cer6*, also show a similar phenotype to *hic* mutants (Gray *et al.*, 2000). Aharoni *et al.* (2004) observed *shn* mutant with significantly increased wax amount and decreased SD compared to wild type. Finally, gene MYB16 encodes a transcription factor involved in cutin biosynthesis and is expressed in stomatal lineage ground cells. Its mutation breaks the one-cell spacing rule⁵ producing clustered, directly touching stomata, due to disruption of polarity during cell division (Yang *et al.*, 2022). As well our data of “stomatal mutants” (*StRNAi*, *epf1,2* and *tmm*) indicate that changes in SD positively correlate with the amount of epicuticular waxes by so far unknown mechanism which seems to be side specific (Fig. 6, Hronková *et al.*, under preparation). In barley (*Hordeum vulgare*), the wax-deficient *cer-g* (*glossy sheath5*) mutant shows the phenotype with stomatal clustering (Zeiger & Stebbins, 1972). Recent study on *cer-g* and related *cer-s* mutants suggested that YDA and BRX-domain factors control multiple epidermal specialisations including stomatal and cuticle development in barley (Liu *et al.*, 2022b).

⁴ Usually, increased ambient CO₂ concentration (c_a) leads to decreased SD on leaves.

⁵ „One-cell spacing rule“ ensures insertion of at least one pavement cell between stomata, which ensures proper pore function (Dow *et al.*, 2014).

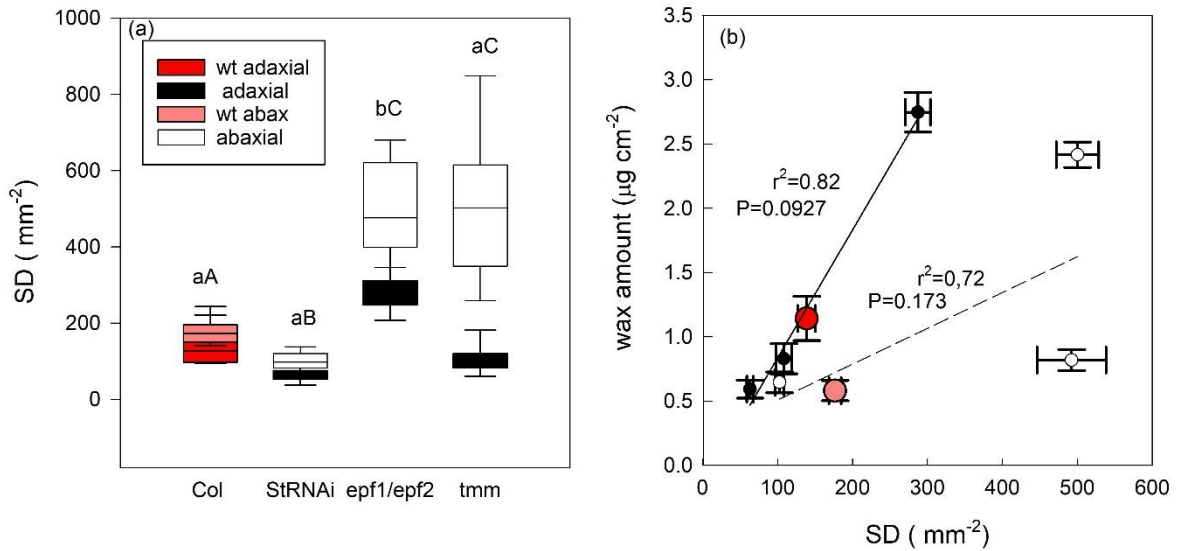


Fig. 6: (a) Stomatal density (SD) of wild type and three *A. thaliana* mutants (*StRNAi*, *epf1,2* and *tmm*) separately for adaxial (bold red for wt and black for mutants) and abaxial leaf side (light red for wt and white for mutants). Medians and standard errors are shown. (b) Correlation between wax amount and SD shown separately for adaxial (solid line) and abaxial leaf side (dashed line).

Previous studies suggest that information about the external environment (irradiance, CO_2 concentration) is perceived by photosynthetically active organs and transmitted to the newly forming leaves via a so far unknown systemic signal (see Fig. 7) (Lake *et al.*, 2001; Miyazawa *et al.*, 2006; Šantrůček *et al.*, 2014; Dutton *et al.*, 2019). Cuticular waxes could be involved in this pathway, e.g. depending on their composition they could influence the mobility of this signal (Bird & Gray, 2003; Engineer *et al.*, 2016). These hypothesis supports a fact, that stomatal cells' wax load probably differs from the pavement cells' wax composition (Karabourniotis *et al.*, 2001; Yu *et al.*, 2008), and thus the signal can be side-specific, varying with stomatal density. This area certainly deserves further research which would unravel the mechanism behind coordinating cuticle and stomatal development.

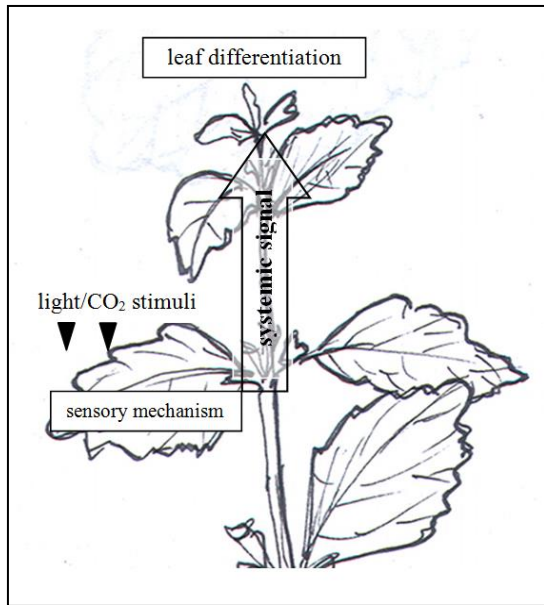


Fig. 7: Information about light conditions and atmospheric CO₂ concentration is perceived by the fully autotrophic leaves. The signals are further transmitted by an unknown systemic signal to the newly forming leaves, where they regulate SD/SI [J. Janová, adapted from Lake et al. (2002)].

1.2. Mesophyll conductance for CO₂

The main property of plant cuticle is its impermeability for gases, which means that it limits not only the loss of water from the leaf to the atmosphere, but also the uptake of CO₂ in the leaf and ultimately the chloroplast of the mesophyll cells. Thus, CO₂ must enter the leaf through the stomatal pores located in the epidermis and then through the mesophyll. Both structures represent barriers that significantly reduce the CO₂ concentration in the substomatal cavity (c_i) and subsequently in the chloroplast (c_c). The decrease in the concentration of c_c compared to its concentration in the air around the leaf (c_a) is caused by the carboxylation activity of the enzyme Rubisco. The magnitude of the concentration gradient depends on the rate of CO₂ assimilation and the rate of CO₂ transport and considerably affects the rate of photosynthesis (A_n) and thus plant growth (Evans *et al.*, 2009). CO₂ enters chloroplasts from the atmosphere through a process of diffusion, i.e. the spontaneous movement of molecules from the sites of their higher concentration to the sites of lower concentration. The flux density (J) for a particular compound indicates the number of molecules that move per unit area per unit time (e.g. mol·m⁻²·s⁻¹). The main driver of this process is the concentration gradient along the path, dc/dx (dc = concentration difference, dx = path length in the x-direction). The total flux density is then expressed as: $J = -D \cdot \frac{dc}{dx}$, where D is the diffusion coefficient (i.e., diffusivity) for a given molecule. The value of D depends on the temperature, and nature of the medium (Nobel, 2005). The integrated form of the equation of flux, J , is analogous to Ohm's law, where D/dx is called conductance, g , and denoted dc is the difference in concentration at the beginning and end of the diffusion path.

During its journey from the atmosphere, CO₂ must overcome a series of diffusion barriers, the main ones being the stomata and the path from the sub-stomatal cavity to the mesophyll cells, in whose chloroplasts CO₂ is biochemically fixed. These diffusion barriers can be described by two quantities: i) resistances (r ; m² s mol (CO₂)⁻¹) which can be added in a series; or ii) the inverse value, conductance ($g = 1/r_m$; mol (CO₂) m⁻² s⁻¹), which is added when the diffusion pathways are arranged in parallel and is more convenient due to its linear relation with flux, such as A_n (Fig. 8).

At present, relatively much is known about the control of the stomatal conductance (g_s) and its effect on the flow of gases (i.e. not only CO₂ from the atmosphere inside the leaf, but also water evaporation in the opposite direction), for recent reviews see (Buckley & Mott, 2013; Engineer *et al.*, 2016; Lawson & Matthews, 2020; Li *et al.*, 2022). The magnitude of g_s is determined by the size, opening and density/distribution of the stomata. The number of

stomata per leaf is determined early during the leaf ontogeny (Simmons & Bergmann, 2016). We have fairly good understanding of stomatal development at the molecular level [for recent review see Chen *et al.* (2020) or Zoulias *et al.* (2018)] and the influence of environment, i.e. irradiation, CO₂ concentration, temperature or relative humidity, on stomatal development (Xu *et al.*, 2016; Driesen *et al.*, 2020; Han *et al.*, 2021). Moreover, we can quantify instantaneous g_s using gas-exchange measurements of transpiration and photosynthesis rates and calculate both g_s and c_i (Gaastra, 1959) and thus monitor the regulation of g_s in response to, e.g., changes in irradiance, temperature, water stress, etc (Driesen *et al.*, 2020). In the long-term, we can calculate c_i integrated over the leaf lifespan from the isotopic composition ($\delta^{13}\text{C}$) of dry leaf tissue (Farquhar *et al.*, 1982).

On the other hand, mesophyll conductance is still understudied. The original assumption that g_m is infinitely large, as was assumed for simplicity when mathematical models of photosynthesis were constructed in the 1980s (Farquhar *et al.*, 1980, 1982), has been overcome. On the contrary, the concept of dynamics and plasticity of g_m is now generally accepted and the causes and especially the regulation of these are still being sought (Vrábl *et al.*, 2009; Flexas *et al.*, 2013; Liu *et al.*, 2022a). The value of g_m range between 0.05 and 0.45 mol (CO₂) m⁻² s⁻¹ and the variability is given by the plant species, leaf age or environmental conditions (Flexas *et al.*, 2008, 2012, 2018).

Mesophyll conductance, g_m , can be divided into two main parts: 1. gas-phase conductance (g_{IAS}), i.e. CO₂ transport through intercellular spaces; 2. liquid-phase conductance (g_{liq}), i.e. diffusion pathways in the cell wall and inside cells (see Fig. 8). Working with the resistances ($r = 1/g$) brings us possibility to sum the resistance arranged in series, so the total r_m can be expressed as: $r_m = r_{IAS} + r_{liq}$.

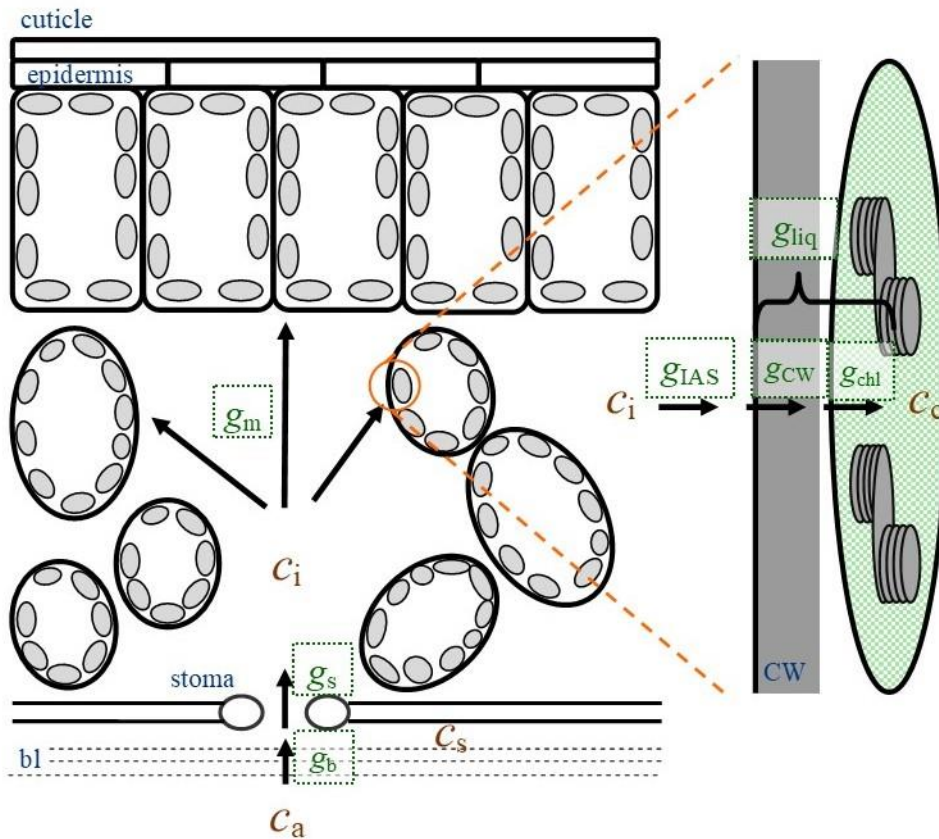


Fig. 8: The scheme of conductances (g) and concentrations (c) on CO₂ pathway from the ambient atmosphere (c_a) through unmixed leaf boundary layer (c_s), stomatal pore into the sub-stomatal cavity (c_i) and via the mesophyll into chloroplast (c_c). Three parts of mesophyll conductance (g_m) are displayed in detail in the right part of the picture: conductance through intercellular air space (g_{IAS}), conductance through cell wall (g_{cw}) and chloroplast's envelopes (g_{chl}). The two components mentioned later form together liquid part of mesophyll resistance (r_{liq}). The scheme also shows the boundary layer (bl) and the corresponding conductance (g_b), stomatal conductance (g_s), cell wall (CW), epidermal cells and cuticle.

Gas phase mesophyll conductance, g_{IAS}

The length and shape of the CO₂ diffusion pathway through the intercellular spaces is mainly influenced by leaf thickness, cell shape and mesophyll compactness. At the scale of a few cells, the g_{IAS} must be anisotropic, i.e., variable depending on the direction. It will vary with respect to the anatomy of the surrounding cells depending on whether it is a compact palisade parenchyma or cells of a more porous spongy parenchyma. g_{IAS} may also be affected by the density, distribution and size of the stomata. These leaf parameters may contribute to overall g_{IAS} , and they may also proportionally vary the importance of diffusion for CO₂ in the lateral direction (i.e. parallel to the epidermis) and across the leaf (Morison et al., 2005). Traditionally, a two-dimensional model has been used for simplification of the model of CO₂

flux through the leaf. However, as recently pointed out by Earles (2018), we should acknowledge the importance of 3D structure of IAS.

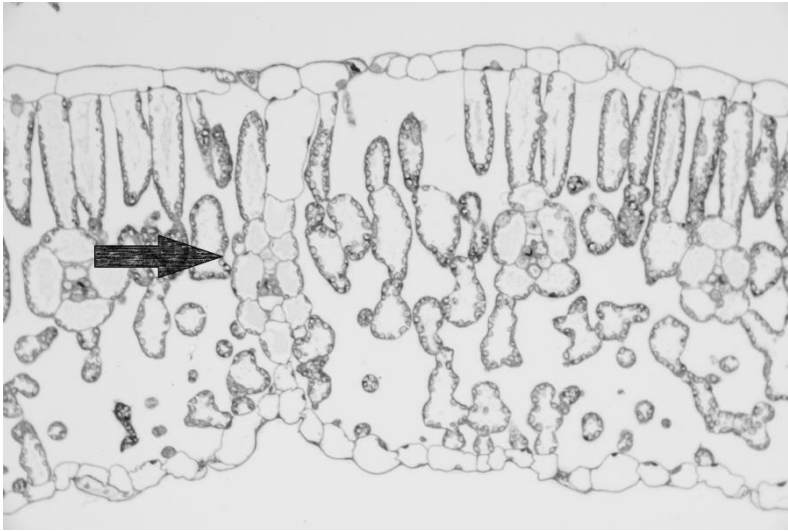


Fig. 9: A semi-thick leaf cross-section of heterobaric sunflower (*H. annuus*). The arrow shows bundle sheath extension connecting upper and lower epidermis, thus forming hermetically sealed compartments (author: Jitka Janová).

Some plant species have vascular bundle sheath extensions up to both epidermes, creating a physical barrier to lateral diffusion of gases within the leaf. This separates the individual compartments "served" in terms of gas exchange by their own group of stomata and hermetically isolates them from the adjacent compartments. Such a leaf is called a heterobaric leaf (examples of heterobaric plants are the grape vine, *Vitis vinifera*; the rough cocklebur, *Xanthium strumarium*; or the sunflower, *Helianthus annuus*, see Fig. 9) and the physical barriers affect the lateral diffusion of CO₂ in the IAS. Nevertheless, most plants are homobaric, do not form complete barriers and CO₂ diffusion can take place across the leaf in all directions (Terashima, 1992).

Liquid phase mesophyll conductance, g_{liq}

Liquid phase of g_m begins with the dissolution of CO₂ as it passes through the mesophyll cell wall, plasma membrane, cytoplasm and chloroplast envelopes into the stroma. The diffusion of CO₂ in the liquid phase is four orders of magnitude slower than in the gas phase and accounts for most of the mesophyll limitation (Mizokami *et al.*, 2022). Three main traits have been emphasized as the key factors responsible for g_{liq} : the chloroplast surface area exposed to the intercellular airspace per leaf area (S_c/S), mesophyll cell wall thickness (T_{cwm}), and chloroplast thickness (T_{chl}); however, their relative importance varies and is still largely unknown (Veromann-Jürgenson *et al.*, 2020). These physical features of leaf anatomy seem to

model the maximum g_m (Peguero-Pina *et al.*, 2017; Han *et al.*, 2018; Tosens & Laanisto, 2018). The above mentioned parameters vary considerably between plant species, but even within one species there is a great deal of variability when comparing individuals growing in different conditions, e.g. light intensity (Hanba *et al.*, 2002; Piel *et al.*, 2002; Warren *et al.*, 2007).

Techniques for measuring mesophyll conductance, g_m

Techniques for calculating total g_m (and thus c_c) are now available [for a review see Pons *et al.* (2009)], starting from Fick's law, we can define g_m as:

$$g_m = A_n / (c_i - c_c) \quad (1)$$

where $A_n = \text{CO}_2$ assimilation rate. There are two frequently used methods for estimating g_m (or r_m) which provide reliable and reproducible data; combinations of gas exchange measurements with (1) chlorophyll fluorescence or (2) ^{13}C isotope discrimination measurements (Pons *et al.*, 2009). There are other proposed but not widely accepted methods, i.e. curve-fitting method (exclusively from gas exchange measurement). For all mentioned methods, reliable gas exchange data are needed. Especially modulation of gas exchange by light or CO_2 availability can provide information on a wide range of biochemical and biophysical limitations on photosynthesis (Long & Bernacchi, 2003), and is essential for correct g_m measurements.

The first method is based on the relationship between the net CO_2 assimilation rate (A_n), rate of photosynthetic electron transport (J), and c_c . The model is based on Farquhar *et al.* (1980) as follows:

$$J = (A_n + R_L) \frac{4c_c + 8\Gamma^*}{c_c - \Gamma^*} \quad (2)$$

where R_L is the rate of mitochondrial respiration in the light and Γ^* is the CO_2 compensation point in the absence of R_L . The factor 4 denotes the minimum electron required for carboxylation. The flux rate J is calculated from fluorometry measurement according Genty *et al.* (1989) as follows:

$$J = \alpha \cdot \beta \cdot \text{PPFD} \cdot \phi_{\text{PSII}} \quad (3)$$

where ϕ_{PSII} is the photochemical yield of photosystem II estimated from fluorescence, PPFD is the photosynthetic photon flux density, α is the leaf absorptance and β denotes the

fraction of photons absorbed by PSII. With the knowledge of A_n (estimated from gas-exchange measurements) and c_c (combination of Eq. 2 and 3 and), g_m can be calculated according to Eq. 1. This original model includes some assumptions and simplifications which were corrected and implemented in the calculation during following decades (Di Marco *et al.*, 1990; Harley *et al.*, 1992; Flexas *et al.*, 2007; van der Putten *et al.*, 2018).

The second method, combinations of gas exchange measurements with ^{13}C isotope discrimination, was used first by Evans *et al.* (1986) and exploits the isotopic fractionation occurring during photosynthetic CO_2 fixation. More specifically, the isotopic composition of CO_2 changes on its pathway from the atmosphere to the chloroplasts's stroma due to the slower diffusion of $^{13}\text{CO}_2$ in comparison to lighter $^{12}\text{CO}_2$. In addition to this diffusional discrimination of ^{13}C , preferential carboxylation of $^{12}\text{CO}_2$ by enzyme Rubisco results in depletion of first assimilates (trioses) in ^{13}C isotope. The isotopic composition of primary sugars depends on and the c_c/c_a ratio and the fractionation factors (constants) during diffusion and carboxylation (Farquhar *et al.*, 1982). For the physical background of fractionation see the section *Basics of discrimination of heavy stable isotope ^{13}C by plants* below. Comparison of the modelled ^{13}C discrimination assuming zero mesophyll resistance with the experimentally measured discrimination allows calculation of c_c . Again, the knowledge of c_c , based on ^{13}C fractionation measurements and calculation, and A_n and c_i , estimated from gas-exchange measurements, allow calculation of g_m .

Unfortunately, there is no direct method to measure the resistance of the individual leaf structures on the CO_2 pathway, and so we cannot fully assess their relative contribution to the total mesophyll resistance. Both of the mentioned models neglect the complexity of the leaf anatomy and simplify the leaf interior to a 2D plane with one average CO_2 source, the atmosphere in the substomatal cavities. Separate measurements of the effect of intercellular spaces on CO_2 diffusion were attempted in the 1990s by Parkhurst and Mott (1990). They compared the rate of net photosynthesis (A_n) as a function of CO_2 partial pressure in the substomatal cavity (p_i) in normal air and in an artificial gas mixture - helox - in which nitrogen is replaced by helium. Because of the lower average molecular weight of helox than air, the mean free path of molecules, and thus CO_2 diffusion, is 2.3 times faster in helox, so that the g_{IAS} is proportionally larger in the helox atmosphere than in air. Higher diffusive conductance led to an increase in A_n at a constant p_i by 3-37% in hypostomatic leaves (having the stomata exclusively on the abaxial leaf side) and by -2 to 7% for the amphistomatic leaves (with stomata on both leaf sides) (see Fig. 10). It can therefore be concluded that the effect

of g_{IAS} is more significant in leaves with stomata exclusively on the abaxial leaf side, where the pathway for gas exchange is longer. Other important roles may be played by leaf anatomical characteristics, such as leaf thickness, the size of the intercellular air space (IAS) or the stomatal density (SD).

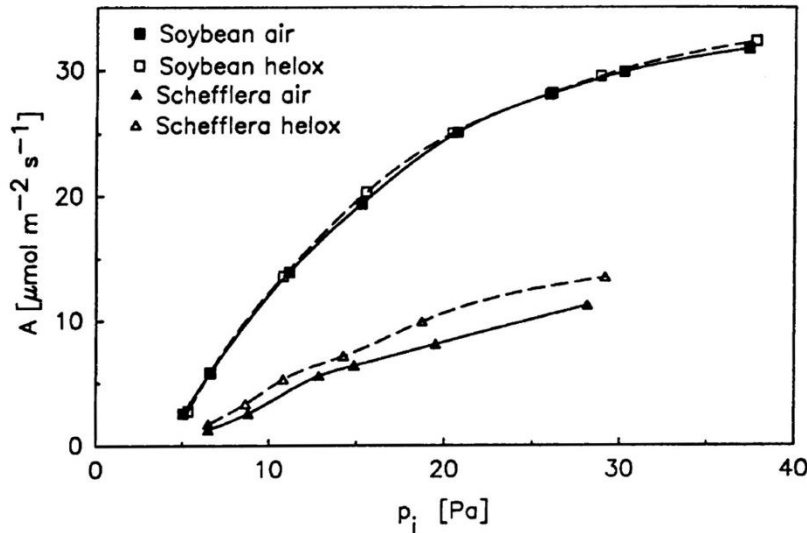


Fig. 10: $A-p_i$ curves for amphistomatous *soybean* (*Glycine max*) and hypostomatous *Schefflera*. Gas measurement in normal air and in helox is shown (Parkhurst & Mott, 1990).

Syvertsen et al. (1995) suggested a model for estimating r_{IAS} and r_{liq} derived from leaf anatomical traits (e.g. LMA, proportion of intercellular air space or leaf thickness). This model showed a contribution of r_{IAS} over r_m between 23 and 48 % for three analysed hypostomatous species (*Citrus*, *Macadamia* and *Prunus*). It should be noted that r_m and its fractions were not measured directly, only modelled from the leaves' cross-sections.

The other proposed technique uses pulsed photoacoustics to measure oxygen diffusion as a proxy for CO_2 diffusion in liquid phase of the mesophyll. The photoacoustic method tracks leaf photosynthesis as pressure waves caused by the conversion of absorbed light to heat and oxygen evolution in the photosystem II. Comparison of photoacoustics data (r_{liq}) and total r_m calculated from photosynthetic rate showed that 92 % of r_m belongs to r_{liq} , and the remaining 8 % to r_{IAS} . (Gorton et al., 2003).

Recently, Earles et al. (2018) and Theroux-Rancourt and Gilbert (2017) pointed out the importance of the 3D complexity of leaves. By introducing tortuosity, lateral path length reflecting stomatal patchiness, and IAS connectivity into a model for g_{IAS} , they found an average reduction in g_{IAS} by 3.5 % in C_3 plants and of 37 % in plants with CAM metabolism (Earles et al., 2018). Their 3D image-processing technique can provide detailed information

about the CO₂ pathway through the leaf mesophyll, but it requires x-ray microcomputed tomography imaging and is time-consuming.

We proposed another possibility for quantifying the proportion of r_{IAS} and r_{liq} using the occurrence of stable carbon isotopes (¹²C and ¹³C) in cuticular membrane (CM) and waxes extracted separately from the upper (adaxial) and lower (abaxial) leaf side. This method is based on ¹³C isotope discrimination during diffusion and photosynthetic carboxylation, which are proportional to the local CO₂ concentration (Farquhar *et al.*, 1982). For the basics of carbon fractionation see model derivation, method description and results in the *Article I* (Šantrůček *et al.*, 2019) and *Article III* (Janová *et al.*, 2024).

1.3. Basics of discrimination of the heavy stable isotope ^{13}C by plants

Since I worked with stable carbon isotopes (^{12}C , ^{13}C) throughout the whole PhD study and we used analysis of ^{13}C distribution ($\delta^{13}\text{C}$) in all reported papers, the following section introduces the basic concepts and laws of isotopic fractionation in terrestrial plants.

There are two stable isotopes of carbon in the Earth's atmosphere, 98.89% of ^{12}C and 1.11% of one neutron heavier ^{13}C . Plant tissues are depleted in ^{13}C content compared to the atmosphere, which is due to discrimination of $^{13}\text{CO}_2$ mainly during the carboxylation reaction, and partly also during diffusion of CO_2 through stomata and mesophyll. Farquhar et al. (1982) discovered the correlation of the carbon isotope ratio ($^{13}\text{C}/^{12}\text{C}$) in plant biomass with the CO_2 concentration in the intercellular air space, c_i . This helped to understand the observations that the degree of ^{13}C depletion is related to environmental conditions affecting stomatal conductance and leaf photosynthetic rate, e.g. water availability or irradiance: both A_n and g affect c_i .

During the journey of carbon dioxide from the atmosphere to the chloroplasts, the relative abundance of $^{13}\text{CO}_2$ and $^{12}\text{CO}_2$ molecules changes, so the isotopic signal changes. The content of the different isotopic forms (isotopologues) of CO_2 is measurable, is denoted by the Greek letter δ , which expresses the relative difference in ^{13}C isotope content between the sample and the standard, and is given in per mill (Urey, 1948).

$$\delta^{13}\text{C} = \left(\frac{R_{\text{sample}}}{R_{\text{standard}}} - 1 \right) \cdot 1000 (\text{‰}) \quad (4)$$

where R is isotopic ratio⁶.

The change in isotope ratio in course of a reaction can also be expressed as a big delta, Δ , which indicates the change in isotope ratio in the product (i.e. the plant) compared to the initial substrate (i.e. the atmosphere). Thus, unlike δ , Δ does not refer to the international isotope standard but to the source. If we know the δ values of the plant tissue and of the atmosphere, we can calculate Δ as:

$$\Delta = \frac{\delta_a - \delta_p}{1 + \delta_p/1000} \quad (5)$$

⁶ $R = (\text{minor isotope abundance})/(\text{major isotope abundance})$, i.e. $^{13}\text{C}/^{12}\text{C}$ in the case of carbon
 R_{standard} is the ratio of minor and major isotope abundances in the internationally used standard (V)PeeDee Belemnite, $R_{\text{standard}} (^{13}\text{C}/^{12}\text{C}) = 1,1180 \cdot 10^{-2}$

The change in the isotope composition of plant versus the atmosphere (Δ) is due to **(i) kinetic isotope fractionation of CO₂ during diffusion in a gaseous environment**; CO₂ molecules enter the leaf interior from the atmosphere by diffusion through stomata, with heavier molecules diffusing more slowly than lighter ones, causing a depletion in ¹³CO₂ that can be quantified by a fractionation factor of $\varepsilon_a = 4.4 \text{ ‰}$ (O’Leary *et al.*, 1981). In the case of diffusion in the boundary layer, the fractionation factor is smaller due to laminar flow, with an empirical measurement of $\varepsilon_h = 2.9 \text{ ‰}$.

(ii) a small fractionation also occurs during **dissolution of CO₂ in water**, which is required for transport through the water saturated cell wall ($\varepsilon_s = 1.1 \text{ ‰}$) and during diffusion through the cell wall and cytosol ($\varepsilon_w = 0.7 \text{ ‰}$) (O’Leary *et al.*, 1981).

iii) kinetic isotope fractionation during photosynthetic CO₂ fixation; the enzyme Rubisco (ribulose-1,5-bisphosphate carboxylase, oxygenase) mediates the binding of the CO₂ molecule to the five-carbon sugar ribulose-1,5-bisphosphate (RUBP) in the chloroplast stroma. Because of the extra neutron, ¹³CO₂ is less likely to seed the Rubisco reaction centre and the product is therefore depleted of ¹³C by a factor of 30 ‰ ($\varepsilon_b = 30\text{‰}$). This mode of carboxylation is present in so-called C₃ plants, but even in these plants approximately 5-10 % of the carbon is obtained by another carboxylation enzyme, phosphoenolpyruvate carboxylase (PEPC) (Farquhar & Richards, 1984). The latter has a much smaller fractionation factor, about 2 ‰, and therefore the weighted average value of the photosynthetic carboxylation fractionation factor $\varepsilon_R = 27\text{‰}$ ($\varepsilon_R = 30 \cdot 0.9 + 2 \cdot 0.1 = 27.2 \text{ ‰}$) is usually used in carbon discrimination calculations in C₃ plants (O’Leary, 1993). This fractionation factor is not at all or only minimally dependent on pH (Roeske & O’Leary, 1984) or temperature (Christeller & Laing, 1976). Nevertheless, the variability in discrimination between plant species and among individuals is considerable. Vogel (1980) compared 351 plant species in the family *Poaceae* and measured $\delta^{13}\text{C}$ values ranging from -22‰ to -34‰ for C₃ plants and -9‰ to -16‰ for C₄ plants (Fig. 11).

These variations were attributed already in the 1980s to the factors of the external environment affecting the carbon dioxide concentration inside the leaf (c_i). Farquhar, O’Leary and Berry (1982) derived a relationship between Δ and the ratio of c_a (atmospheric CO₂ concentration) to c_i as:

$$\Delta^{13}\text{C} = a \cdot \frac{c_a - c_i}{c_a} + b \cdot \frac{c_i}{c_a} \quad (6)$$

The resulting equation contains the following assumptions: i) the internal conductance of the leaf for CO₂ is infinitely large (and thus the CO₂ concentration in the intercellular compartments c_i is equal to the concentration at the carboxylation site inside the chloroplasts c_c); ii) the conductance of the boundary layer of air above the leaf is large and therefore c_a is very close to the concentration on the leaf surface, c_s ; iii) the contribution of photorespiration and respiration to isotope discrimination is negligible. Thus, it is clear from Eq. 6 that the shift in carbon isotope composition between c_a and the assimilates (trioses or even polysaccharides, e.g. cellulose, if we consider post-photosynthetic discrimination to be negligible), Δ , depends on a single physiological parameter, namely the CO₂ concentration inside the leaf (Farquhar *et al.*, 1982).

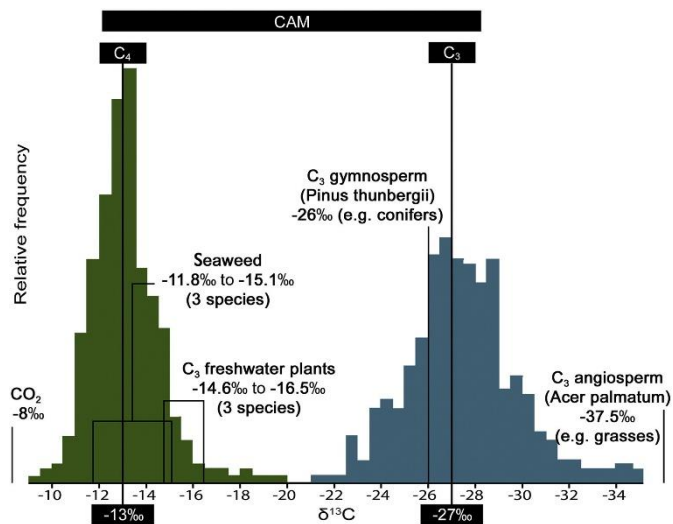


Fig. 11: Variation of $\delta^{13}C$ values among and between plant species with different carbon metabolism (C₃, C₄ or CAM). App. 1000 plant species were included. [Histogram adapted from O'Leary (1988) and Glaser (2005) by (Reiffarth *et al.*, 2016)].

2. Hypotheses and aims of the study

My PhD work was based on study of plant cuticle which was used as a marker of environmental conditions and leaf internal constraints in transport of CO₂. Four main hypotheses and goals were as listed:

Hypothesis 1:

Carbon isotope composition ($\delta^{13}\text{C}$) of leaf cuticles from the opposite leaf sides reflects the CO₂ concentration difference across the hypostomatous leaf.

Goal: To test the hypothesis that the CO₂ concentration gradient across the hypostomatous leaf can be detected from the difference in $\delta^{13}\text{C}$ between the adaxial and abaxial cuticular waxes. $\delta^{13}\text{C}$ of wax was suggested to reflect the CO₂ concentration in plastids and/or endoplasmic reticulum of epidermal cells, alternatively in chloroplast adjacent to the respective epidermis. The objective was to develop a model of CO₂ isotopic fractionation along its pathway from the abaxial (stomatous) to the adaxial (astomatous) leaf side and to apply the model in estimation of the proportion of gas and liquid phase of mesophyll resistance (r_m) for CO₂ transport.

The experimental outcomes of goal 1 were used in *Article I*.

Hypothesis 2:

*The CO₂ concentration in chloroplasts calculated from $\delta^{13}\text{C}$ of epicuticular waxes on opposite leaf sides can be used to estimate the mesophyll resistance for CO₂ transport integrated over the growing season. Leaves in the canopy profile of *Fagus sylvatica* adjust their anatomy and mesophyll resistance to light environment.*

Goal: To test the model developed under the first goal with leaves grown under light gradient. Contrasting environment modulate leaf anatomy and thus presumably the ratio of gas to liquid phase of mesophyll resistance. The validity of the new method had to be verified by independent measurements of r_m using conventional isotopic and gas exchange techniques.

The experimental outcomes of goal 2 were used in *Article III*.

Hypothesis 3:

In amphistomatic leaves, the CO₂ concentration is the same or similar in chloroplasts adjacent to adaxial and abaxial epidermes. Therefore, δ¹³C of the opposite epicuticular waxes should also approach similar values.

Goal: To investigate potential link between carbon isotope composition (δ¹³C) of cuticular waxes and fraction of stomata on the adaxial (upper) leaf side in the total number of stomata on both leaf sides, the so-called amphistomy level.

The experimental outcomes of goal 3 were used in *Article IV*.

Hypothesis 4:

The cuticular wax is renewed throughout the life of the leaf.

Goal: Because we consider cuticular membrane as carriers of environmental and leaf internal information, it was necessary to look at the dynamics of the cuticular membrane (individually for matrix and cuticular wax) in young and fully developed mature leaves to determine whether regeneration or renewal of each component occurs during leaf life and how timely the information is.

The experimental outcomes of goal 4 were used in *Article II*.

3. Summary and future prospects

A presence of a distinctive layer on the surface of leaves and fruits was noticed already fourth century BC by Greek botanist Theophrastus (Domínguez *et al.*, 2011). For the first time, the cuticular membrane was isolated in the 19th century by Brongniart (1830, 1834) and Henslow (1831). The structure of the cuticle was gradually revealed during the 20th century, and this research has moved us to the current concept of cuticular membrane (CM) perception as a complex structure bearing information on the leaf internal and ambient environments as described above (Fig. 2) (Domínguez *et al.*, 2011).

Nowadays it is clear that plant cuticle is not a rigid structure creating merely an interphase between plant and atmosphere. From the historical viewpoint it was studied mainly for its water-resistant properties, but lately the approach became more integrative, highlighting many unresolved mysteries regarding cuticle biogenesis, structure and functions (González-Valenzuela *et al.*, 2023). In this thesis, we considered cuticle as an archive of information on CO₂ concentration in a distinct part of the leaf, the opposite epidermes. Based on the information in form of the ¹³C/¹²C ratio, we attempted to quantify the time integrated mesophyll resistance and partition it into the gas and the liquid phase (Šantrůček *et al.*, 2019; Janová *et al.*, 2024). This model was developed as a micro-analogy of Evans' model for measurements of r_m (Evans *et al.*, 1986) and assumes that the carbon isotope composition of CM reflects the CO₂ concentration in chloroplasts of mesophyll cells next to the epidermis.

We showed in *Article I* and *III* that, indeed, most of 40 investigated hypostomatous plants species have CM and wax on the adaxial leaf side enriched in ¹³C compared with CM and wax obtained from the abaxial leaf side. This indicates lower c_c in plastids of the upper epidermal cells and, therefore, a transverse CO₂ gradient across the leaf. In case of *Fagus sylvatica* leaves growing under a light gradient, we showed that in the sun exposed leaves approximately 6 % of total mesophyll resistance (r_m) is accounted to gas phase (r_{IAS}), the remaining 94 % is attributable to transport resistances inside the cell (r_{liq}). In shaded leaves the r_{IAS} to r_{liq} ratio is higher, about 15 to 85. Although the sun-adapted leaves are thicker, more compact and have higher leaf mass per area (LMA), their total r_m is lower compared to leaves growing in the shade. This is probably caused by higher chloroplast surface area exposed to the intercellular airspace per leaf area (S_c/S) and higher stomatal density.

Our model published in Šantrůček et al. (2019) assumes that the isotopic signal is not influenced by other carbon sources, such as assimilates in storage organs, which could interfere, especially if the whole cuticular membrane (including matrix) is used for the isotopic analyses. The CM is synthesised early in the leaf ontogeny when the leaf is fully or (in the later phase of growth) partly heterotrophic and has to rely on other leaves or reserves. However as we confirmed in a model plant (Kubásek et al., 2023), cuticular wax is renewed during the whole leaf life-span and so it is a better medium to preserve the actual information on leaf environment and better candidate to work with, as we did in the *Article III* (Janová et al., 2024). Another pitfall of this model may be the complexity and variability of wax composition, which typically consist of different substance classes: alkanes, aldehydes, alcohols, and others (see above in the *Cuticle composition* section) (Samuels et al., 2008; Yeats & Rose, 2013) and often varies between adaxial and abaxial leaf side. Even though there are often one or two dominant classes in different plant species or families (Jetter et al., 2006), there could be differences in fractionation of ^{13}C during the synthesis of individual compounds (Hayes, 2001), which may increase variance in the observed isotopic polarity across the leaf. We respected the variability of wax composition and employed compound-specific isotopic analyses in our two recent works (*Article II* and *IV*). Future extensions of this work should therefore focus on compound-specific IRMS and use isotopic fractionation of individual major wax compounds.

The change in chemical composition of cuticular wax during the season is known at least for some plant species (Prasad & Gülz, 1990; Gülz et al., 1992; Hauke & Schreiber, 1998; Piasentier et al., 2000; Suh & Diefendorf, 2018). Labelling with heavy isotopes (stable or radioactive) moved the knowledge about the real dynamics and turn-over of distinct compounds (Kahmen et al., 2011; Gao et al., 2012). In *Article II* (Kubásek et al., 2023), we applied method of ^{13}C pulse labelling on perennial *Clusia rosea* plants and tracked the isotopic signal in cutin matrix (MX), and in intra- and epicuticular wax, respectively. We compared young leaves (whose leaf area reached final size after the labelling) with mature, fully grown leaves. From the data it is obvious that only young leaves incorporate new carbon into their MX. In contrast, waxes were synthesized in young and mature leaves with same dynamics. Furthermore, it was shown that the newly synthesised wax is deposited in the intracuticular wax layer first and, with a delay, it appears also in the epicuticular wax.

In the future, I plan to do a similar experiment with monocot plant species, as *Zea mays* or *Clivia miniata*. Their leaves grow ongoingly on the base so there are leaf sections of

different age and ontogenetical phase. It should be readily apparent at what point the cuticle matrix synthesis stopped and confirm ongoing deposition of fresh carbon in the intra- or epicuticular wax. This wax dynamic supports a hypothesis that CM could be involved in the perception of ambient atmosphere (CO₂ concentration, light availability), thus influencing a hypothetical systemic signal affecting development of new leaves. It also appears that wax composition can differ not only between the adaxial and abaxial leaf sides⁷ (Jetter *et al.*, 2000), but also between stomatal cells and pavement cells (Karabourniotis *et al.*, 2001; Šantrůček *et al.*, 2004; Yu *et al.*, 2008). This could be given by the absence of chloroplasts in pavement cells which means that pyruvate, the first step in cuticle synthesis, has to come from freshly assimilated carbon in adjoined mesophyll cell, probably through secondary plasmodesmata connecting cell which belong to different cell lineages (Voitsekhovskaja *et al.*, 2021) or is a product of the glycolysis (process of glucose degradation) in the cytosol of epidermal cell (Ohlrogge *et al.*, 2015). In contrast, stomatal guard cells contain chloroplasts and mature guard cells are not connected to the surrounding cells (functional plasmodesmata were detected only during its development) (Wille & Lucas, 1984; Mumm *et al.*, 2011). Single-cell transcriptomics could provide a tool to investigate gene expression in stomata and pavements cells (Liu *et al.*, 2020; Lopez-Anido *et al.*, 2021; Berrío *et al.*, 2022) and to observe potential differences in expression of genes involved in cuticle or cuticular wax synthesis.

In *Article IV* (Askanbayeva *et al.*, 2024), advantages and costs of amphistomy vs. hypostomy were studied. We quantified benefits of access of CO₂ through stomata on the adaxial leaf surface using ¹³C abundance in the adaxial and abaxial epicuticular wax. We showed that increased amphistomy level (ASL, fraction of adaxial in all stomata) in the sun-exposed amphistomatous leaves reduces the CO₂ gradient across the leaf mesophyll and that stomata and epicuticular wax deposition follow similar leaf-side patterning.

In summary, my study of plant cuticle started with a model explaining differences in carbon isotope composition of epicuticular wax on the opposite leaf sides in terms of CO₂ gradient across the leaf. The model was used for partitioning the mesophyll resistance into the gas- and liquid phases and studying the CO₂ fluxes inside leaves. Over time, my research has moved towards the multifunctionality of the cuticle, which has increasingly fascinated me, followed by the study of cuticle dynamics, the interaction between the cuticle and stomatal development, and more recently toward the role of the cuticle in plant immunity (not shown

⁷ This specificity of wax composition on leaf side is species-dependent and is not a general rule.

in this thesis). In any case, there are a lot of interesting, unknown and unexplored phenomena around the plant cuticle, the knowledge of which can help us (as I deeply believe) in many areas. For example, to breed plants with lower r_m and optimal SD, and thus higher water use efficiency, to produce cultivars more resistant to various pathogens, or to develop new water-proof materials used in the textile industry.

4. Conclusions

H1: The isotopic composition of cuticular wax extracted separately from the adaxial and abaxial leaf sides allow us to estimate CO₂ concentrations in chloroplast of adjacent to the respective epidermis. In case of hypostomatous leaves, this concentration is lower at the proximity of astomatous adaxial leaf side.

H2: The leaf anatomy altered by light availability influences the flux of CO₂ through the leaf. Thicker sun-adapted leaves of *Fagus sylvatica* with higher leaf mass per area and stomatal density have lower r_m than thinner and less compact shade-adapted leaves. The r_m was estimated by two methods: i) the conventional technique combining on-line ¹³C discrimination with gas exchange measurements, ii) the new technique which is based on the isotopic composition of epicuticular wax harvested from the adaxial and abaxial leaf sides. The r_m value obtained by this method is integrated over the time of leaf development (wax deposition). The proportion of r_{IAS} to r_{liq} varied along the light gradient with r_{IAS} higher in shaded leaves ($r_{IAS} = 15\%$) compared with sun-exposed leaves (were $r_{IAS} = 5.5\%$).

H3: Fraction of adaxial in all stomata (amphistomy level ASL) increase in amphistomatous leaves with higher growing irradiance. Hand in hand with this, the difference in isotopic composition of epicuticular waxes on the abaxial and adaxial leaf sides is reduced, suggesting a similar or equal CO₂ concentration in chloroplasts near both epidermes. These results show at least one benefit of amphistomy, which is reduction of stomatal and mesophyll resistances and consequently a higher supply of CO₂ in chloroplasts.

H4: The cuticular matrix (MX) is synthesized only during early the leaf ontogeny. No freshly assimilated carbon is incorporated into the MX of mature leaves of *Clusia rosea* plants. In contrast, waxes (both epi- and intra-cuticular) are continuously synthesized in young but also in mature, fully developed leaves.

5. References

Aharoni A, Dixit S, Jetter R, Thoenes E, Van Arkel G, Pereira A. 2004. The SHINE clade of AP2 Domain Transcription Factors Activates Wax Biosynthesis, Alters Cuticle Properties, and Confers Drought Tolerance when Overexpressed in Arabidopsis W inside a box sign. *Plant Cell* **16**.

Amelunxen F, Morgenroth K, Picksak T. 1967. Untersuchungen an der Epidermis mit dem Stereoscan Elektronenmikroskop. *Zeitschrift für Pflanzenphysiologie* **57**: 79–95.

Askanbayeva B, Janová J, Kubásek J, Zeisler-Diehl V, Schreiber L, Muir C, Šatnrůček J. 2024. Amphistomy: stomata patterning inferred from ¹³C content and leaf–side specific deposition of epicuticular wax. *Annals of Botany*.

Barthlott W, Neinhuis C, Cutler D, Ditsch F, Meusel I, Theisen I, Wilhelmi H. 1998. Classification and terminology of plant epicuticular waxes. *Botanical Journal of the Linnean Society* **126**.

Bateman RM, Crane PR, Dimichele WA, Kenrick PR, Rowe NP, Speck T, Stein WE. 1998. Early evolution of land plants: Phylogeny, physiology, and ecology of the primary terrestrial radiation. *Annual Review of Ecology and Systematics* **29**.

Berhin A, de Bellis D, Franke RB, Buono RA, Nowack MK, Nawrath C. 2019. The Root Cap Cuticle: A Cell Wall Structure for Seedling Establishment and Lateral Root Formation. *Cell* **176**.

Berrío RT, Verstaen K, Vandamme N, Pevernagie J, Achon I, van Duyse J, van Isterdael G, Saeys Y, de Veylder L, Inzé D, et al. 2022. Single-cell transcriptomics sheds light on the identity and metabolism of developing leaf cells. *Plant Physiology* **188**.

Bessire M, Borel S, Fabre G, Carrac L, Efremova N, Yephremov A, Cao Y, Jetter R, Jacquat AC, Métraux JP, et al. 2011. A member of the PLEIOTROPIC DRUG RESISTANCE family of ATP binding cassette transporters is required for the formation of a functional cuticle in Arabidopsis. *Plant Cell* **23**.

Bird SM, Gray JE. 2003. Signals from the cuticle affect epidermal cell differentiation. *New Phytologist* **157**.

Boom A, Sinnige Damsté JS, De Leeuw JW. 2005. Cutan, a common aliphatic biopolymer in cuticles of drought-adapted plants. *Organic Geochemistry* **36**.

Brongniart A. 1830. Recherches sur la structure et sur les fonctions des feuilles. *Annales Des Sciences Naturelles 1st Series* **21**: 420–457.

Brongniart A. 1834. Sur l'épiderme des plantes. Nouvelles recherches sur la structure de l'épiderme des vegetaux. *Annales Des Sciences Naturelles 2nd Series* **1**: 65–71.

Buckley TN, Mott KA. 2013. Modelling stomatal conductance in response to environmental factors. *Plant, Cell and Environment* **36**.

Budke JM, Goffinet B, Jones CS. 2012. The cuticle on the gametophyte calyptra matures before the sporophyte cuticle in the moss *Funaria hygrometrica* (Funariaceae). *American Journal of Botany* **99**.

Buschhaus C, Jetter R. 2011. Composition differences between epicuticular and intracuticular wax substructures: How do plants seal their epidermal surfaces? *Journal of Experimental Botany* **62**.

Chen L, Wu Z, Hou S. 2020. SPEECHLESS Speaks Loudly in Stomatal Development. *Frontiers in Plant Science* **11**.

Christeller JT, Laing W a. 1976. Isotope Discrimination by Ribulose 1,5-Diphosphate Carboxylase: No Effect of Temperature or HCO₃ Concentration. *Plant physiology* **57**.

Clark JW, Harris BJ, Hetherington AJ, Hurtado-Castano N, Brench RA, Casson S, Williams TA, Gray JE, Hetherington AM. 2022. The origin and evolution of stomata. *Current Biology* **32**.

Domínguez E, Heredia-Guerrero JA, Heredia A. 2011. The biophysical design of plant cuticles: an overview. *New Phytologist* **189**: 938–949.

Dow GJ, Berry JA, Bergmann DC. 2014. The physiological importance of developmental mechanisms that enforce proper stomatal spacing in *Arabidopsis thaliana*. *New Phytologist* **201**.

Driesen E, Van den Ende W, De Proft M, Saeys W. 2020. Influence of environmental factors light, CO₂, temperature, and relative humidity on stomatal opening and development: A review. *Agronomy* **10**.

Dutton C, Hōrak H, Hepworth C, Mitchell A, Ton J, Hunt L, Gray JE. 2019. Bacterial infection systemically suppresses stomatal density. *Plant Cell and Environment* **42**.

Earles JM, Th roux-Rancourt G, Roddy AB, Gilbert ME, McElrone AJ, Brodersen CR. 2018. Beyond porosity: 3D leaf intercellular airspace traits that impact mesophyll conductance. *Plant Physiology* **178**.

Edstam MM, Viitanen L, Salminen TA, Edqvist J. 2011. Evolutionary history of the non-specific lipid transfer proteins. *Molecular Plant* **4**.

Edwards D. 1993. Cells and tissues in the vegetative sporophytes of early land plants. *New Phytologist* **125**.

Engineer CB, Hashimoto-Sugimoto M, Negi J, Israelsson-Nordstr m M, Azoulay-Shemer T, Rappel W-J, Iba K, Schroeder JI. 2016. CO₂ Sensing and CO₂ Regulation of Stomatal Conductance: Advances and Open Questions. *Trends in Plant Science* **21**: 16–30.

Evans JR, Von Caemmerer S. 1996. Carbon dioxide diffusion inside leaves. *Plant Physiology* **110**.

Evans JR, Kaldenhoff R, Genty B, Terashima I. 2009. Resistances along the CO₂ diffusion pathway inside leaves. *Journal of Experimental Botany* **60**.

Evans J, Sharkey T, Berry J, Farquhar G. 1986. Carbon Isotope Discrimination measured Concurrently with Gas Exchange to Investigate CO₂ Diffusion in Leaves of Higher Plants. *Functional Plant Biology* **13**.

Farquhar GD, von Caemmerer S, Berry JA. 1980. A biochemical model of photosynthetic CO₂ assimilation in leaves of C₃ species. *Planta* **149**.

Farquhar G, O'Leary M, Berry J. 1982. On the Relationship Between Carbon Isotope Discrimination and the Intercellular Carbon Dioxide Concentration in Leaves. *Functional Plant Biology* **9**: 121.

Farquhar GD, Richards RA. 1984. Isotopic composition of plant carbon correlates with water-use efficiency of wheat genotypes. *Australian Journal of Plant Physiology* **11**.

Fich EA, Segerson NA, Rose JKC. 2016. The Plant Polyester Cutin: Biosynthesis, Structure, and Biological Roles. *Annual Review of Plant Biology* **67**.

Flexas J, Barbour MM, Brendel O, Cabrera HM, Carriqu  M, D az-Espejo A, Douthe C, Dreyer E, Ferrio JP, Gago J, et al. 2012. Mesophyll diffusion conductance to CO₂: An unappreciated central player in photosynthesis. *Plant Science* **193–194**.

Flexas J, Cano FJ, Carriquí M, Coopman RE, Mizokami Y, Tholen D, Xiong D. 2018. CO₂ Diffusion Inside Photosynthetic Organs.

Flexas J, Diaz-Espejo A, Galmés J, Kaldenhoff R, Medrano H, Ribas-Carbo M. 2007. Rapid variations of mesophyll conductance in response to changes in CO₂ concentration around leaves. *Plant, Cell and Environment* **30**.

Flexas J, Niinemets Ü, Gallé A, Barbour MM, Centritto M, Diaz-Espejo A, Douthe C, Galmés J, Ribas-Carbo M, Rodriguez PL, et al. 2013. Diffusional conductances to CO₂ as a target for increasing photosynthesis and photosynthetic water-use efficiency. *Photosynthesis Research* **117**.

Flexas J, Ribas-Carbó M, Diaz-Espejo A, Galmés J, Medrano H. 2008. Mesophyll conductance to CO₂: Current knowledge and future prospects. *Plant, Cell and Environment* **31**.

Gaastra P. 1959. Photosynthesis of crop plants as influenced by light, carbon dioxide, temperature, and stomatal diffusion resistance.

Gao L, Burnier A, Huang Y. 2012. Quantifying instantaneous regeneration rates of plant leaf waxes using stable hydrogen isotope labeling. *Rapid Communications in Mass Spectrometry* **26**.

Genty B, Briantais JM, Baker NR. 1989. The relationship between the quantum yield of photosynthetic electron transport and quenching of chlorophyll fluorescence. *Biochimica et Biophysica Acta - General Subjects* **990**.

Glaser B. 2005. Compound-specific stable-isotope ($\delta^{13}\text{C}$) analysis in soil science. *Journal of Plant Nutrition and Soil Science* **168**.

González-Valenzuela L, Renard J, Depège-Fargeix N, Ingram G. 2023. The plant cuticle. *Current Biology* **33**: R210–R214.

Gorton HL, Herbert SK, Vogelmann TC. 2003. Photoacoustic analysis indicates that chloroplast movement does not alter liquid-phase CO₂ diffusion in leaves of *Alocasia brisbanensis*. *Plant Physiology* **132**.

Gray JE, Holroyd GH, Van Der Lee FM, Bahrami AR, Sijmons PC, Woodward FI, Schuch W, Hetherington AM. 2000. The HIC signalling pathway links CO₂ perception to stomatal development. *Nature* **408**.

Greer S, Wen M, Bird D, Wu X, Samuels L, Kunst L, Jetter R. 2007. The cytochrome P450 enzyme CYP96A15 is the midchain alkane hydroxylase responsible for formation of secondary alcohols and ketones in stem cuticular wax of arabidopsis. *Plant Physiology* **145**.

Gülz PG, Müller E, Prasad RBN. 1992. Surface Structures and Chemical Composition of Epicuticular Waxes During Leaf Development of *Fagus Sylvatica* L. *Zeitschrift für Naturforschung - Section C Journal of Biosciences* **47**.

Gupta NS, Collinson ME, Briggs DEG, Evershed RP, Pancost RD. 2006. Reinvestigation of the occurrence of cutan in plants: implications for the leaf fossil record. *Paleobiology* **32**.

Guzmán-Delgado P, Graça J, Cabral V, Gil L, Fernández V. 2016. The presence of cutan limits the interpretation of cuticular chemistry and structure: *Ficus elastica* leaf as an example. *Physiologia Plantarum* **157**.

Haas K, Rentschler I. 1984. Discrimination between epicuticular and intracuticular wax in blackberry leaves: Ultrastructural and chemical evidence. *Plant Science Letters* **36**.

Han SK, Kwak JM, Qi X. 2021. Stomatal Lineage Control by Developmental Program and Environmental Cues. *Frontiers in Plant Science* **12**.

Han J, Lei Z, Flexas J, Zhang Y, Carriquí M, Zhang W, Zhang Y. 2018. Mesophyll conductance in cotton bracts: Anatomically determined internal CO₂ diffusion constraints on photosynthesis. *Journal of Experimental Botany* **69**.

Hanba YT, Kogami H, Terashima I. 2002. The effect of growth irradiance on leaf anatomy and photosynthesis in *Acer* species differing in light demand. *Plant, Cell and Environment* **25**.

Harley PC, Loreto F, Marco G Di, Sharkey TD. 1992. Theoretical considerations when estimating the mesophyll conductance to CO₂ flux by analysis of the response of photosynthesis to CO₂. *Plant Physiology* **98**.

Hauke V, Schreiber L. 1998. Ontogenetic and seasonal development of wax composition and cuticular transpiration of ivy (*Hedera helix* L.) sun and shade leaves. *Planta* **207**.

Haworth M, McElwain J. 2008. Hot, dry, wet, cold or toxic? Revisiting the ecological significance of leaf and cuticular micromorphology. *Palaeogeography, Palaeoclimatology, Palaeoecology* **262**.

Hayes JM. 2001. Fractionation of Carbon and Hydrogen Isotopes in Biosynthetic Processes. *Reviews in Mineralogy and Geochemistry* **43**: 225–277.

Henslow JS. 1831. *On the examination of a hybrid digitalis*. Cambridge: Printed by J. Smith, printer to The University.

Heredia A. 2003. Biophysical and biochemical characteristics of cutin, a plant barrier biopolymer. *Biochimica et Biophysica Acta - General Subjects* **1620**.

Heredia-Guerrero JA, Benítez JJ, Heredia A. 2008. Self-assembled polyhydroxy fatty acids vesicles: A mechanism for plant cutin synthesis. *BioEssays* **30**.

Janová J, Kubásek J, Grams TEE, Zeisler-Diehl V, Schreiber L, Šantrůček J. 2024. Effect of light-induced changes in leaf anatomy on intercellular and cellular components of mesophyll resistance for CO₂ in *Fagus sylvatica*. *Plant Biology*.

Jeffree CE. 1996. The Fine Structure of the Plant Cuticle. In: *Biology of the Plant Cuticle*. Oxford, UK: Blackwell Publishing Ltd, 11–125.

Jeffree CE. 2007. The Fine Structure of the Plant Cuticle. In: *Annual Plant Reviews*.

Jessen D, Roth C, Wiermer M, Fulda M. 2015. Two activities of long-chain acyl-coenzyme a synthetase are involved in lipid trafficking between the endoplasmic reticulum and the plastid in *arabidopsis*. *Plant Physiology* **167**.

Jetter R, Kunst L, Samuels AL. 2006. Composition of Plant Cuticular Waxes. In: *Annual Plant Reviews*. 145–181.

Jetter R, Schäffer S. 2001. Chemical composition of the *Prunus laurocerasus* leaf surface. Dynamic changes of the epicuticular wax film during leaf development. *Plant Physiology* **126**.

Jetter R, Schäffer S, Riederer M. 2000. Leaf cuticular waxes are arranged in chemically and mechanically distinct layers: Evidence from *Prunus laurocerasus* L. *Plant, Cell and Environment* **23**.

Kahmen A, Dawson TE, Vieth A, Sachse D. 2011. Leaf wax n-alkane δD values are determined early in the ontogeny of *Populus trichocarpa* leaves when grown under controlled environmental conditions. *Plant, Cell and Environment* **34**.

Kalistova T, Janda M. 2023. Could a cuticle be an active component of plant immunity? *Biologia plantarum* **67**: 322–333.

Karabourniotis G, Tzobanoglou D, Nikolopoulos D, Liakopoulos G. 2001. Epicuticular phenolics over guard cells: Exploitation for in situ stomatal counting by fluorescence microscopy and combined image analysis. *Annals of Botany* **87**.

Kenrick P, Crane PR. 1997. The origin and early evolution of plants on land. *Nature* **389**.

Kerfourn C, Garrec JP. 1992. Modifications in the alkane composition of cuticular waxes from spruce needles (*Picea abies*) and ivy leaves (*Hedera helix*) exposed to ozone fumigation and acid fog: comparison with needles from declining spruce trees . *Canadian Journal of Botany* **70**.

Knoche M, Beyer M, Peschel S, Oparlakov B, Bukovac MJ. 2004. Changes in strain and deposition of cuticle in developing sweet cherry fruit. *Physiologia Plantarum* **120**.

Koch K, Neinhuis C, Ensikat HJ, Barthlott W. 2004. Self assembly of epicuticular waxes on living plant surfaces imaged by atomic force microscopy (AFM). *Journal of Experimental Botany* **55**.

Krauss P, Markstädter C, Riederer M. 1997. Attenuation of UV radiation by plant cuticles from woody species. *Plant, Cell and Environment* **20**.

Kubásek J, Kalistová T, Janová J, Askanbayeva B, Bednář J, Šantrůček J. 2023. ¹³CO₂ labelling as a tool for elucidating the mechanism of cuticle development: a case of *Clusia rosea*. *New Phytologist* **238**.

Kunst L, Samuels L. 2009. Plant cuticles shine: advances in wax biosynthesis and export. *Current Opinion in Plant Biology* **12**.

Lake JA, Quick WP, Beerling DJ, Woodward FI. 2001. Signals from mature to new leaves. *Nature* **411**.

Lake JA, Woodward FI, Quick WP. 2002. Long-distance CO₂ signalling in plants. *Journal of Experimental Botany* **53**.

Lawson T, Matthews J. 2020. Guard Cell Metabolism and Stomatal Function. *Annual Review of Plant Biology* **71**.

Leide J, Nierop KGJ, Deininger AC, Staiger S, Riederer M, De Leeuw JW. 2020. Leaf cuticle analyses: Implications for the existence of cutan/non-ester cutin and its biosynthetic origin. *Annals of Botany* **126**.

Li S lan, Tan T ting, Fan Y fang, Raza MA, Wang Z lin, Wang B bei, Zhang J wei, Tan X ming, Chen P, Shafiq I, et al. 2022. Responses of leaf stomatal and mesophyll conductance to abiotic stress factors. *Journal of Integrative Agriculture* **21**.

Liu T, Barbour MM, Yu D, Rao S, Song X. 2022a. Mesophyll conductance exerts a significant limitation on photosynthesis during light induction. *New Phytologist* **233**.

Liu L, Jose SB, Campoli C, Bayer MM, Sánchez-Diaz MA, McAllister T, Zhou Y, Eskan M, Milne L, Schreiber M, et al. 2022b. Conserved signalling components coordinate epidermal patterning and cuticle deposition in barley. *Nature Communications* **13**.

Liu Z, Zhou Y, Guo J, Li J, Tian Z, Zhu Z, Wang J, Wu R, Zhang B, Hu Y, et al. 2020. Global Dynamic Molecular Profiling of Stomatal Lineage Cell Development by Single-Cell RNA Sequencing. *Molecular Plant* **13**.

Lolle SJ, Cheung AY, Sussex IM. 1992. Fiddlehead: An Arabidopsis mutant constitutively expressing an organ fusion program that involves interactions between epidermal cells. *Developmental Biology* **152**.

Lolle SJ, Hsu W, Pruitt RE. 1998. Genetic analysis of organ fusion in Arabidopsis thaliana. *Genetics* **149**.

Long SP, Bernacchi CJ. 2003. Gas exchange measurements, what can they tell us about the underlying limitations to photosynthesis? Procedures and sources of error. *Journal of Experimental Botany* **54**.

Lopez-Anido CB, Vatén A, Smoot NK, Sharma N, Guo V, Gong Y, Anleu Gil MX, Weimer AK, Bergmann DC. 2021. Single-cell resolution of lineage trajectories in the Arabidopsis stomatal lineage and developing leaf. *Developmental Cell* **56**.

Macková J, Vašková M, Macek P, Hronková M, Schreiber L, Šantrůček J. 2013. Plant response to drought stress simulated by ABA application: Changes in chemical composition of cuticular waxes. *Environmental and Experimental Botany* **86**.

Di Marco G, Manes F, Tricoli D, Vitale E. 1990. Fluorescence Parameters Measured Concurrently with Net Photosynthesis to Investigate Chloroplastic CO₂ Concentration in Leaves of Quercus ilex L. *Journal of Plant Physiology* **136**.

Miyazawa SI, Livingston NJ, Turpin DH. 2006. Stomatal development in new leaves is related to the stomatal conductance of mature leaves in poplar (*Populus trichocarpax* P. deltoides). In: *Journal of Experimental Botany*.

Mizokami Y, Oguchi R, Sugiura D, Yamori W, Noguchi K, Terashima I. 2022. Cost-benefit analysis of mesophyll conductance: diversities of anatomical, biochemical and environmental determinants. *Annals of Botany* **130**.

Morison JIL, Gallouët E, Lawson T, Cornic G, Herbin R, Baker NR. 2005. Lateral diffusion of CO₂ in leaves is not sufficient to support photosynthesis. *Plant Physiology* **139**.

Mumm P, Wolf T, Fromm J, Roelfsema MRG, Marten I. 2011. Cell Type-Specific Regulation of Ion Channels Within the Maize Stomatal Complex. *Plant and Cell Physiology* **52**: 1365–1375.

Nawrath C. 2006. Unraveling the complex network of cuticular structure and function. *Current Opinion in Plant Biology* **9**.

Neinhuis C, Barthlott W. 1997. Characterization and distribution of water-repellent, self-cleaning plant surfaces. *Annals of Botany* **79**.

Neinhuis C, Koch K, Barthlott W. 2001. Movement and regeneration of epicuticular waxes through plant cuticles. *Planta* **213**.

Nip M, Tegelaar EW, de Leeuw JW, Schenck PA, Holloway PJ. 1986. A new non-saponifiable highly aliphatic and resistant biopolymer in plant cuticles - Evidence from pyrolysis and ¹³C-NMR analysis of present-day and fossil plants. *Naturwissenschaften* **73**.

Nobel PS. 2005. *Physicochemical and Environmental Plant Physiology, Third Edition*.

Ohlrogge J, Browse J, Jaworski J, Somerville C. 2015. Lipids. In: Buchanan BB, Grussem W, Jones RL, eds. *Biochemistry and Molecular Biology of Plants*. Hoboken: Wiley Blackwell, 337–400.

O’Leary MH. 1988. Carbon Isotopes in Photosynthesis. *BioScience* **38**.

O’Leary MH. 1993. Biochemical Basis of Carbon Isotope Fractionation. In: *Stable Isotopes and Plant Carbon-water Relations*.

O’Leary MH, Rife JE, Slater JD. 1981. Kinetic and Isotope Effect Studies of Maize Phosphoenolpyruvate Carboxylase. *Biochemistry* **20**.

Osborn JM, Taylor TN. 1990. Morphological and Ultrastructural Studies of Plant Cuticular Membranes. I. Sun and Shade Leaves of *Quercus velutina* (Fagaceae). *Botanical Gazette* **151**.

Parkhurst DF, Mott KA. 1990. Intercellular diffusion limits to CO₂ uptake in leaves: Studies in air and helox. *Plant Physiology* **94**.

Peguero-Pina JJ, Sancho-Knapik D, Gil-Pelegrín E. 2017. Ancient cell structural traits and photosynthesis in today's environment. *Journal of Experimental Botany* **68**.

Piasentier E, Bovolenta S, Malossini F. 2000. The n-alkane concentrations in buds and leaves of browsed broadleaf trees. *Journal of Agricultural Science* **135**.

Piel C, Frak E, Le Roux X, Genty B. 2002. Effect of local irradiance on CO₂ transfer conductance of mesophyll in walnut. *Journal of Experimental Botany* **53**.

Pollard M, Beisson F, Li Y, Ohlrogge JB. 2008. Building lipid barriers: biosynthesis of cutin and suberin. *Trends in Plant Science* **13**.

Pons TL, Flexas J, Von Caemmerer S, Evans JR, Genty B, Ribas-Carbo M, Brugnoli E. 2009. Estimating mesophyll conductance to CO₂: Methodology, potential errors, and recommendations. *Journal of Experimental Botany* **60**.

Post-Beittenmiller D. 1996. Biochemistry and molecular biology of wax production in plants. *Annual Review of Plant Physiology and Plant Molecular Biology* **47**.

Prasad RBN, Gülz PG. 1990. Developmental and Seasonal variations in the epicuticular waxes of beech leaves (*fagus sylvatica* l.). *Zeitschrift fur Naturforschung - Section C Journal of Biosciences* **45**.

van der Putten PEL, Yin X, Struik PC. 2018. Calibration matters: On the procedure of using the chlorophyll fluorescence method to estimate mesophyll conductance. *Journal of Plant Physiology* **220**.

Raven JA. 2002. Selection pressures on stomatal evolution. *New Phytologist* **153**.

Reiffarth DG, Petticrew EL, Owens PN, Lobb DA. 2016. Sources of variability in fatty acid (FA) biomarkers in the application of compound-specific stable isotopes (CSSIs) to soil and sediment fingerprinting and tracing: A review. *Science of the Total Environment* **565**.

Reynoud N, Petit J, Bres C, Lahaye M, Rothan C, Marion D, Bakan B. 2021. The Complex Architecture of Plant Cuticles and Its Relation to Multiple Biological Functions. *Frontiers in Plant Science* **12**.

Riederer M. 1991. Cuticle as Barrier between Terrestrial Plants and the Atmosphere - Significance of Growth-Structure for Cuticular Permeability. *Naturwissenschaften* **78**: 201–208.

Riederer M. 2007. Introduction: Biology of the Plant Cuticle. In: Annual Plant Reviews.

Riederer M, Schönherr J. 1988. Development of plant cuticles: fine structure and cutin composition of *Clivia miniata* Reg. leaves. *Planta* **174**.

Riederer M, Schreiber L. 2001. Protecting against water loss: Analysis of the barrier properties of plant cuticles. In: Journal of Experimental Botany.

Roeske CA, O'Leary MH. 1984. Carbon Isotope Effects on the Enzyme-Catalyzed Carboxylation of Ribulose Bisphosphate. *Biochemistry* **23**.

Salminen TA, Blomqvist K, Edqvist J. 2016. Lipid transfer proteins: classification, nomenclature, structure, and function. *Planta* **244**.

Samuels L, Kunst L, Jetter R. 2008. Sealing plant surfaces: Cuticular wax formation by epidermal cells. *Annual Review of Plant Biology* **59**.

Samuels L, McFarlane HE. 2012. Plant cell wall secretion and lipid traffic at membrane contact sites of the cell cortex. *Protoplasma* **249**.

Šantrůček J, Schreiber L, Macková J, Vráblová M, Květoň J, Macek P, Neuwirthová J. 2019. Partitioning of mesophyll conductance for CO₂ into intercellular and cellular components using carbon isotope composition of cuticles from opposite leaf sides. *Photosynthesis Research* **141**.

Šantrůček J, Šimánová E, Karbulková J, Šimková M, Schreiber L. 2004. A new technique for measurement of water permeability of stomatous cuticular membranes isolated from *Hedera helix* leaves. *Journal of Experimental Botany* **55**.

Šantrůček J, Vráblová M, Šimková M, Hronková M, Drtinová M, Květoň J, Vrábl D, Kubásek J, Macková J, Wiesnerová D, et al. 2014. Stomatal and pavement cell density linked to leaf internal CO₂ concentration. *Annals of Botany* **114**.

Schmidt HW, Schönherr J. 1982. Development of plant cuticles: occurrence and role of non-ester bonds in cutin of *Clivia miniata* Reg. leaves. *Planta* **156**.

Schönherr J. 1976. Water permeability of isolated cuticular membranes: The effect of cuticular waxes on diffusion of water. *Planta* **131**.

Schönherr J, Mérida T. 1981. Water permeability of plant cuticular membranes: the effects of humidity and temperature on the permeability of non-isolated cuticles of onion bulb scales. *Plant, Cell & Environment* **4**.

Schönherr J, Riederer M. 1986. Plant cuticles sorb lipophilic compounds during enzymatic isolation. *Plant, Cell & Environment* **9**.

Schönherr J, Riederer M. 1989. Foliar penetration and accumulation of organic chemicals in plant cuticles. *Reviews of Environmental Contamination and Toxicology* **108**.

Schreiber L, Riederer M. 1996. Ecophysiology of cuticular transpiration: Comparative investigation of cuticular water permeability of plant species from different habitats. *Oecologia* **107**.

Schreiber L, Schönherr J. 2009. *Water and Solute Permeability of Plant Cuticles*.

Segado P, Heredia-Guerrero JA, Heredia A, Domínguez E. 2020. Cutinsomes and CUTIN SYNTHASE1 function sequentially in tomato fruit cutin deposition1[OPEN]. *Plant Physiology* **183**.

Serra O, Chatterjee S, Huang W, Stark RE. 2012. Mini-review: What nuclear magnetic resonance can tell us about protective tissues. *Plant Science* **195**.

Serrano M, Coluccia F, Torres M, L'Haridon F, Métraux JP. 2014. The cuticle and plant defense to pathogens. *Frontiers in Plant Science* **5**.

Silcox D, Holloway PJ. 1986. A simple method for the removal and assessment of foliar deposits of agrochemicals using cellulose acetate film stripping. *Aspects of Applied Biology* **11**: 13–17.

Simmons AR, Bergmann DC. 2016. Transcriptional control of cell fate in the stomatal lineage. *Current Opinion in Plant Biology* **29**.

Stępiński D, Kwiatkowska M, Wojtczak A, Polit JT, Domínguez E, Heredia A, Popłońska K. 2020. The Role of Cutinsomes in Plant Cuticle Formation. *Cells* **9**.

Suh YJ, Diefendorf AF. 2018. Seasonal and canopy height variation in n-alkanes and their carbon isotopes in a temperate forest. *Organic Geochemistry* **116**.

Syvertsen JP, Lloyd J, McConchie C, Kriedemann PE, Farquhar GD. 1995. On the relationship between leaf anatomy and CO₂ diffusion through the mesophyll of hypostomatous leaves. *Plant, Cell & Environment* **18**.

Szakiel A, Paćzkowski C, Pensec F, Bertsch C. 2012. Fruit cuticular waxes as a source of biologically active triterpenoids. *Phytochemistry Reviews* **11**.

Tanaka H, Machida Y. 2006. The cuticle and cellular interactions. In: Riederer M, Müller C, eds. *Biology of the Plant Cuticle*. Oxford: Blackwell Publishing Ltd, 312–333.

Terashima I. 1992. Anatomy of non-uniform leaf photosynthesis. *Photosynthesis Research* **31**: 195–212.

Théroux-Rancourt G, Gilbert ME. 2017. The light response of mesophyll conductance is controlled by structure across leaf profiles. *Plant Cell and Environment* **40**.

Tosens T, Laanisto L. 2018. Mesophyll conductance and accurate photosynthetic carbon gain calculations. *Journal of Experimental Botany* **69**.

Urey HC. 1948. Oxygen isotopes in nature and in the laboratory. *Science* **108**.

Veromann-Jürgenson LL, Brodribb TJ, Niinemets Ü, Tosens T. 2020. Variability in the chloroplast area lining the intercellular airspace and cell walls drives mesophyll conductance in gymnosperms. *Journal of Experimental Botany* **71**.

Vogel JC. 1980. Fractionation of the Carbon Isotopes During Photosynthesis. In: *Fractionation of the Carbon Isotopes During Photosynthesis*.

Voitsekhovskaja O V., Melnikova AN, Demchenko KN, Ivanova AN, Dmitrieva VA, Maksimova AI, Lohaus G, Tomos AD, Tyutereva E V., Koroleva OA. 2021. Leaf Epidermis: The Ambiguous Symplastic Domain. *Frontiers in Plant Science* **12**.

Vrábl D, Vašková M, Hronková M, Flexas J, Šantrůček J. 2009. Mesophyll conductance to CO₂ transport estimated by two independent methods: Effect of variable CO₂ concentration and abscisic acid. *Journal of Experimental Botany* **60**.

Vráblová M, Vrábl D, Sokolová B, Marková D, Hronková M. 2020. A modified method for enzymatic isolation of and subsequent wax extraction from *Arabidopsis thaliana* leaf cuticle. *Plant Methods* **16**: 129.

Wang X, Kong L, Zhi P, Chang C. 2020. Update on cuticular wax biosynthesis and its roles in plant disease resistance. *International Journal of Molecular Sciences* **21**.

Warren CR, Löw M, Matyssek R, Tausz M. 2007. Internal conductance to CO₂ transfer of adult *Fagus sylvatica*: Variation between sun and shade leaves and due to free-air ozone fumigation. *Environmental and Experimental Botany* **59**.

Watson GS, Gellender M, Watson JA. 2014. Self-propulsion of dew drops on lotus leaves: A potential mechanism for self cleaning. *Biofouling* **30**.

Wille AC, Lucas WJ. 1984. Ultrastructural and histochemical studies on guard cells. *Planta* **160**.

Xin A, Herburger K. 2021. Mini Review: Transport of Hydrophobic Polymers Into the Plant Apoplast. *Frontiers in Plant Science* **11**.

Xu Z, Jiang Y, Jia B, Zhou G. 2016. Elevated-CO₂ response of stomata and its dependence on environmental factors. *Frontiers in Plant Science* **7**.

Yadav K, Arya M, Prakash S, Jha BS, Manchanda P, Kumar A, Deswal R. 2023. Brassica juncea leaf cuticle contains xylose and mannose (xylomannan) which inhibit ice recrystallization on the leaf surface. *Planta* **258**.

Yang SL, Tran N, Tsai MY, Ho CMK. 2022. Misregulation of MYB16 expression causes stomatal cluster formation by disrupting polarity during asymmetric cell divisions. *Plant Cell* **34**.

Yang X, Zhao H, Kosma DK, Tomasi P, Dyer JM, Li R, Liu X, Wang Z, Parsons EP, Jenks MA, et al. 2017. The Acyl desaturase CER17 is involved in producing Wax unsaturated primary Alcohols and cutin monomers. *Plant Physiology* **173**.

Yeats TH, Rose JKC. 2013. The formation and function of plant cuticles. *Plant Physiology* **163**.

Yu MML, Konorov SO, Schulze HG, Blades MW, Turner RFB, Jetter R. 2008. In situ analysis by microspectroscopy reveals triterpenoid compositional patterns within leaf cuticles of *Prunus laurocerasus*. *Planta* **227**.

Zeiger E, Stebbins GL. 1972. Developmental Genetics in Barley: A Mutant for Stomatal Development. *American Journal of Botany* **59**.

Zeisler V, Schreiber L. 2016. Epicuticular wax on cherry laurel (*Prunus laurocerasus*) leaves does not constitute the cuticular transpiration barrier. *Planta* **243**.

Zeisler-Diehl V, Müller Y, Schreiber L. 2018. Epicuticular wax on leaf cuticles does not establish the transpiration barrier, which is essentially formed by intracuticular wax. *Journal of Plant Physiology* **227**.

Zhao H, Kosma DK, Lü S. 2021. Functional Role of Long-Chain Acyl-CoA Synthetases in Plant Development and Stress Responses. *Frontiers in Plant Science* **12**.

Zoulias N, Harrison EL, Casson SA, Gray JE. 2018. Molecular control of stomatal development. *Biochemical Journal* **475**.

Research articles

Article I

Partitioning of mesophyll conductance for CO₂ into intercellular and cellular components using carbon isotope composition of cuticles from opposite leaf sides

Santrucek J; Schreiber L; Macková J; Vráblová M; Kveton J, Macek P, Neuwirthová J.

(2019).

Photosynthesis Research **141**, 33-51. DOI: 10.1007/s11120-019-00628-7



Partitioning of mesophyll conductance for CO₂ into intercellular and cellular components using carbon isotope composition of cuticles from opposite leaf sides

J. Šantrůček¹ · L. Schreiber² · J. Macková³ · M. Vráblová^{1,4} · J. Květoň^{1,5} · P. Macek^{1,3} · J. Neuwirthová¹

Received: 4 June 2018 / Accepted: 14 February 2019 / Published online: 26 February 2019
© Springer Nature B.V. 2019

Abstract

We suggest a new technique for estimating the relative drawdown of CO₂ concentration (c) in the intercellular air space (IAS) across hypostomatous leaves (expressed as the ratio c_d/c_b , where the indexes d and b denote the adaxial and abaxial edges, respectively, of IAS), based on the carbon isotope composition ($\delta^{13}\text{C}$) of leaf cuticular membranes (CMs), cuticular waxes (WXs) or epicuticular waxes (EWXs) isolated from opposite leaf sides. The relative drawdown in the intracellular liquid phase (i.e., the ratio c_c/c_{bd} , where c_c and c_{bd} stand for mean CO₂ concentrations in chloroplasts and in the IAS), the fraction of intercellular resistance in the total mesophyll resistance (r_{IAS}/r_m), leaf thickness, and leaf mass per area (LMA) were also assessed. We show in a conceptual model that the upper (adaxial) side of a hypostomatous leaf should be enriched in ^{13}C compared to the lower (abaxial) side. CM, WX, and/or EWX isolated from 40 hypostomatous C₃ species were ^{13}C depleted relative to bulk leaf tissue by 2.01–2.85‰. The difference in $\delta^{13}\text{C}$ between the abaxial and adaxial leaf sides ($\delta^{13}\text{C}_{AB} - \delta^{13}\text{C}_{AD}$, Δ_{b-d}), ranged from -2.22 to $+0.71$ ‰ (-0.09 ± 0.54 ‰, mean \pm SD) in CM and from -7.95 to 0.89 ‰ (-1.17 ± 1.40 ‰) in WX. In contrast, two tested amphistomatous species showed no significant Δ_{b-d} difference in WX. Δ_{b-d} correlated negatively with LMA and leaf thickness of hypostomatous leaves, which indicates that the mesophyll air space imposes a non-negligible resistance to CO₂ diffusion. $\delta^{13}\text{C}$ of EWX and 30-C aldehyde in WX reveal a stronger CO₂ drawdown than bulk WX or CM. Mean values of c_d/c_b and c_c/c_{bd} were 0.90 ± 0.12 and 0.66 ± 0.11 , respectively, across 14 investigated species in which wax was isolated and analyzed. The diffusion resistance of IAS contributed $20 \pm 14\%$ to total mesophyll resistance and reflects species-specific and environmentally-induced differences in leaf functional anatomy.

Keywords Leaf mesophyll · CO₂ diffusion · Mesophyll conductance · Cuticle · Waxes · Carbon isotope discrimination · Leaf traits

Electronic supplementary material The online version of this article (<https://doi.org/10.1007/s11120-019-00628-7>) contains supplementary material, which is available to authorized users.

✉ J. Šantrůček
jsan@umbr.cas.cz

- ¹ Faculty of Science, University of South Bohemia, Branišovská 31, 37005 Ceske Budejovice, Czech Republic
- ² Institute for Cellular & Molecular Botany - IZMB, University of Bonn, Kirschallee 1, 53115 Bonn, Germany
- ³ Biology Centre ASCR, Institute of Soil Biology, Na Sádkách 702/7, 37005 Ceske Budejovice, Czech Republic
- ⁴ Institute of Environmental Technology, VSB - Technical University of Ostrava, 17. listopadu 15, 70833 Ostrava, Czech Republic
- ⁵ Institute of Experimental Botany, Academy of Sciences of the Czech Republic, 16502 Prague, Czech Republic

Introduction

Photosynthetic fixation of CO₂ in the stroma of chloroplasts creates a concentration gradient, driving CO₂ diffusion from the ambient atmosphere through stomata, across the substomatal cavity, intercellular air space (IAS), cell wall, plasmalemma, intracellular aqueous, and lipid phases toward chloroplasts, and through chloroplast envelopes to the ultimate sink of CO₂, Ribulose-1,5-bisphosphate carboxylase (Rubisco) in the stroma. All the various leaf and cell structures represent diffusion barriers, shaping the leaf internal CO₂ gradient and imposing limitations on photosynthetic CO₂ assimilation (Niinemets et al. 2009). The less permeable to CO₂ the barrier is, the steeper the gradient that is generated during steady-state photosynthesis. In amphistomatous leaves, CO₂ can be supplied through stomata on both

leaf sides and thus distributes more evenly across the cross-section of the leaf (Muir et al. 2014; Parkhurst 1994), whereas in hypostomatous leaves, which have stomata on the lower leaf side only, gradients in CO₂ concentration across the mesophyll will be more pronounced. In tightly packed and thick sclerophyllous, succulent or sun-adapted leaves, even steeper CO₂ gradients can be expected (Maxwell et al. 1997; Hassiotou et al. 2009).

The CO₂ concentration in the substomatal cavity (c_i) can be estimated from data obtained by conventional gas exchange techniques (von Caemmerer and Farquhar 1981) or from direct measurements on amphistomatous leaves (Tominaga et al. 2018; Sharkey et al. 1982). Recent progress in estimation of the leaf internal CO₂ gradients relies on on-line measurements combining gas exchange with stable isotope or chlorophyll fluorescence techniques (Flexas et al. 2008; Pons et al. 2009). These methods yield instantaneous leaf internal (chloroplast) CO₂ concentration and diffusion conductance for CO₂, which may vary with environmental parameters, leaf anatomy and plant species (Warren et al. 2007; Tholen et al. 2012; Flexas et al. 2012; Vrabl et al. 2009; Schauffele et al. 2011). Alternatively, carbon isotope analyses of primary or secondary assimilates or leaf dry mass have been used frequently for the estimation of c_i integrated over the period during which the carbon was assimilated (Farquhar and Richards 1984; Cernusak et al. 2013). This technique is based on a robust model comparing ¹³C depletion in leaf biomass to that of CO₂ in ambient air (i.e., ¹³C discrimination: $\Delta^{13}\text{C}$) to the ratio of substomatal and ambient CO₂ concentrations, c_i/c_a (Farquhar and Richards 1984). Often a simplified model of $\Delta^{13}\text{C}$ is employed, which assumes that discrimination in photorespiration and respiration is negligible and that the leaf internal CO₂ concentration gradient (the difference between substomatal cavity and chloroplasts, $c_i - c_c$) is insignificantly small and thus the leaf internal (mesophyll) conductance to CO₂ (g_m) infinitely high. However, recent results have shown that the mesophyll conductance can be comparable in magnitude and variability to stomatal conductance (Flexas et al. 2008; Warren 2008). Attempts to partition g_m into conductances in the gas phase (IAS) and aqueous and lipid phase (cellular including cell wall and membranes), respectively, have been rare. Parkhurst and Mott (1990) found a substantial increase of photosynthetic rate (by up to 27%) in hypostomatous plants when air was substituted by helox (a mixture of helium and oxygen in which diffusion of CO₂ is 2.3 times faster as in air). Visualization of the lateral diffusion of CO₂ in the leaf interior (Lawson and Morison 2006; Pieruschka et al. 2006), as well as 3D modeling of CO₂ transport (Xiao and Zhu 2017; Aalto and Juurola 2002) can also help in estimation of diffusion barriers in the IAS. Lloyd et al. (1992) formalized the contribution of both gas phase and liquid phase conductance to the deviation between the measured (real) and the modeled

(assuming infinitely high g_m) carbon isotope discrimination. However, the practical means suitable for their separate determination are still missing. In this study, we investigated carbon isotope fractionation within the leaf with the aim to find out whether the CO₂ concentration gradient across the leaf is imprinted in the isotopic composition of cuticles from opposite leaf sides and, in turn, how a $\delta^{13}\text{C}$ difference between cuticles could be used to quantify the gradient.

In terrestrial plants, both abaxial and adaxial leaf sides are covered by cuticular membranes (CMs), which protect them from water loss but also decrease CO₂ availability (Kerstiens 1996; Schreiber and Riederer 1996; Yeats and Rose 2013; Schreiber 2010). The cuticle is an extracellular product of the epidermis and is composed of three main parts: (1) cutin polymer, (2) polysaccharide microfibrils forming the cuticular matrix (MX) together with cutin, and (3) waxes that are embedded in the matrix and deposited at the outer surface of the cuticle (Jeffree 2006; Kunst and Samuels 2003). Wax production is localized in epidermal cells and includes fatty acid synthesis in plastids and underlying mesophyll chloroplasts and subsequent elongation and differentiation (Chikaraishi et al. 2004; Kunst and Samuels 2003). As mentioned previously, carbon isotope discrimination ($\Delta^{13}\text{C}$) and CO₂ concentration in (or near) chloroplasts are closely related. Therefore we assume that $\Delta^{13}\text{C}$ of cuticle and/or wax isolated from the abaxial stomatous leaf side reflects the CO₂ concentration in chloroplasts near the stomata. In turn, the isotopic composition of cuticle and/or its components isolated from the adaxial side of a hypostomatous leaf should indicate a lower CO₂ concentration in chloroplasts close to the astomatous adaxial epidermis.

Here we test (i) whether the difference in ¹³C content ($\delta^{13}\text{C}$) of cuticles or waxes from opposite leaf sides is consistent with the assumed gradient of CO₂ across hypostomatous leaves and (ii) whether it can yield information on intercellular (gas phase) and cellular (liquid and membrane phase) CO₂ drawdown and partitioning of the mesophyll resistance to CO₂ diffusion. The internal CO₂ drawdowns in leaves of 40 hypostomatous C₃ species are compared. Finally, we ask (iii) how the CO₂ concentration drawdown across the IAS correlates with selected leaf anatomical traits.

Materials and methods

Collection of plant material

Fully developed leaves of 23 hypostomatous C₃ species were collected in glasshouses of a botanical garden (at the University of Bonn, Germany) and were used for a first screening study on CMs isolated from opposite leaf sides. In the second campaign, eight hypostomatous C₃ species growing in open air were collected in a tropical forest of north-west

Belize (near Orange Walk) and their cuticles isolated. All these species are listed in Table 1. The third set of eight glasshouse-grown C₃ species (*Ficus elastica*, *Ficus lyrata*, *Hoya carnosa*, *Hedera helix*, *Clivia miniata*, *Yucca gloriosa*, *Zamioculcas zamiifolia*, and *Stephanotis floribunda*) was used for isolation of adaxial and abaxial epicuticular waxes (EWXs) directly from detached leaves (glasshouse of the University of South Bohemia, Ceske Budejovice, Czech Republic). Another five plant species (*C. miniata*, *Monstera*

deliciosa, *Schefflera actinophylla*, *Prunus laurocerasus*, *Z. zamiifolia*) grown in the same glasshouse were selected for more detailed study where CM, MX, and WX were isolated and analyzed. As CO₂ drawdown across the leaf mesophyll into chloroplasts is likely to increase with irradiation in the growth environment, leaves from two *F. elastica* plants grown for 5 years indoors in contrasting light conditions (less than 30 μmol m⁻² s⁻¹ and ~300 μmol m⁻² s⁻¹) were also used for analyses. Side-specific chemical composition

Table 1 List of species collected in a glasshouse (Bonn, Germany) and in the field (near Orange Walk, Belize) from which cuticles (CM) from both leaf sides were successfully isolated, and their leaf anatomical traits and δ¹³C values

Species	Leaf disc				Abax CM		Adax CM	Ab – Ad
	δ ¹³ C (‰)	d (mm)	LMA (g m ⁻²)	f _{IAS}	δ ¹³ C (‰)	SD (mm ⁻²)	δ ¹³ C (‰)	δ _{AB} – δ _{AD} (‰)
Germany, Bonn								
<i>Buxus sempervirens</i>	-30.67	0.333	110.1	0.160	-32.86	129.2	-32.52	-0.34
<i>Camellia sinensis</i>	-31.94	0.330	89.9	0.161	-33.65	163.2	-33.57	-0.08
<i>Citrus × aurantium</i>	-27.38	0.337	144.8	0.170	-31.38	513.9	-30.48	-0.89
<i>Citrus × limon</i>	-29.42	0.278	83.0	0.139	-34.00	508.0	-33.89	-0.11
<i>Citrus × myrtifolia</i>	-28.73	0.296	123.6	0.122	-33.00	246.0	-33.03	0.04
<i>Clivia miniata</i>	-26.85	0.680	84.4	0.286	-28.84	22.3	-28.73	-0.11
<i>Clusia</i> sp.	-29.43	0.466	132.6	0.134	-35.06	72.8	-34.78	-0.28
<i>Coffea arabica</i>	-35.22	0.155	38.9	0.303	-34.78	130.8	-35.55	0.77
<i>Cotyledon orbiculata</i> ^a	-24.60	5.698	15.3	0.134	-29.79	27.2	-28.30	-1.49
<i>Euonymus japonicus</i>	-31.89	0.268	93.8	0.202	-34.78	275.6	-35.25	0.47
<i>Forsythia suspensa</i>	-31.48	0.291	56.3	0.176	-33.72	203.2	-34.43	0.71
<i>Ginkgo biloba</i>	-30.82	0.309	59.8	0.297	-32.20	-	-32.81	0.61
<i>Ilex aquifolium</i>	-30.47	0.424	115.2	0.304	-33.01	145.6	-32.04	-0.97
<i>Ligustrum vulgare</i>	-30.81	0.353	79.0	0.234	-32.10	285.6	-32.51	0.41
<i>Monstera deliciosa</i>	-33.24	0.430	45.9	0.273	-35.96	30.1	-35.04	-0.93
<i>Oncidium excavatum</i>	-27.84	0.658	109.7	0.082	-30.93	99.6	-30.69	-0.24
<i>Prunus laurocerasus</i>	-28.86	0.338	119.7	0.262	-32.09	192.0	-31.97	-0.12
<i>Schefflera actinophylla</i>	-28.06	0.375	98.5	0.162	-29.41	176.8	-29.22	-0.20
<i>Syringa vulgaris</i> ^a	-31.14	0.255	69.5	0.157	-34.10	162.8	-33.76	-0.35
<i>Sobralia macrantha</i>	-31.38	0.393	76.1	0.091	-34.38	63.6	-34.04	-0.34
<i>Stephanotis floribunda</i>	-28.57	0.552	116.3	0.335	-33.73	149.0	-32.39	-1.35
<i>Taxus baccata</i>	-26.51	0.448	146.6	0.235	-27.53	78.8	-27.89	0.35
<i>Vinca major</i>	-32.45	0.210	37.8	0.294	-35.22	82.8	-35.20	-0.03
Belize								
<i>Annona muricata</i>	-31.51				-31.26		-31.34	0.08
Apocynaceae ^b	-29.69				-28.11		-27.08	-1.02
<i>Cecropia obtusifolia</i>	-27.25				-28.48		-28.19	-0.30
<i>Ficus ovalis</i>	-30.38				-31.76		-30.98	-0.79
Myrsinaceae ^b	-28.57				-28.64		-29.03	0.38
<i>Terminalia catappa</i>	-28.58				-30.98		-30.83	-0.14
<i>Thevetia ahouai</i>	-32.09				-32.49		-32.01	-0.48
<i>Xiphidium caeruleum</i>	-27.51				-30.85		-31.18	0.33

Means of 5–7 individual measurements are shown

dLeaf thickness, LMA leaf mass per area, f_{IAS} fraction of intercellular air space in total leaf volume, SD stomatal density

^aAmphistomatous species with adaxial/abaxial stomatal density ratio less than 1/3

^bNon-identified species

of wax and the compound-specific $\delta^{13}\text{C}$ of 30-C aldehyde (triacontanal) were determined. All the above-mentioned plants grew at low elevation (less than 400 m a.s.l.). In order to compare the results with high elevation-grown plants, which are known for their low ratio of leaf internal to ambient CO_2 concentration and greater mesophyll thickness (Körner 1999), three species of the genus *Polylepis* (*P. rugulosa*, *P. tarapacana* and *P. tomentella*) were collected in their natural habitats in Bolivia and Chile at 4300 m a.s.l. All 40 investigated species are listed in Tables 1 and 2. At least 12 leaf discs (diameter 2 cm) were punched from the central part of leaf laminae. Half of them were dried and ground, and their isotopic carbon composition was determined. The other half was used for cuticle isolation. In *Polylepis* and *Taxus*, leaf margins were cut off and central parts were used for cuticle isolation and carbon isotope analysis. To test the hypothesis that CO_2 gradient across the leaf is 'imprinted' in the isotopic composition of cuticles, we followed the advice of one reviewer to analyze wax also from amphistomatous species with presumably a zero or small difference between CO_2 concentrations in the opposite leaf-side substomatal cavities. We collected leaves of tulip (*Tulipa* sp.) and lilac (*Syringa vulgaris*) together with hypostomatous cherry laurel (*P. laurocerasus*) grown in common garden.

Leaf anatomical traits

Before the leaf traits were measured and wax extracted, the collected leaves were gently surface washed with distilled water and stored in plastic bags for several hours in order

to remove the atmospheric leaf surface depositions and to hydrate the leaves. Leaf thickness (d , mm) was measured using a manual micrometer screw. Stomatal density (mm^{-2}) was determined with ImageJ software on photographs of isolated cuticles taken with an optical microscope (Olympus BX61). Dry mass per unit leaf area (LMA, mg cm^{-2}) was calculated as $\text{LMA} = M_d/A$, where A (cm^2) is the projected area of the leaf discs and M_d (mg) is their dry mass (dried at 70°C to constant weight).

The volume fraction of leaf IAS (f_{IAS}) was estimated by vacuum infiltration of the leaf discs using distilled water. The variable f_{IAS} was calculated as the difference between the mass of a leaf disc after and before infiltration with water, normalized to the mass of the infiltrated disc, $f_{\text{IAS}} = 1 - (M_f/M_i)$, where M_f and M_i are fresh mass of the disc before and after infiltration, respectively. The leaf characteristics were estimated in the first set of 23 species and in *F. elastica* only.

Isolation of cuticular membranes (CMs)

CM were isolated by immersing leaf discs or central leaf parts in an aqueous solution of 2% (v/v) cellulase (Cellulast, Novo Nordisk, Bagsvared, Denmark) and 2% (v/v) pectinase (Trenolin Super DF, Erbslöh, Geisenheim, Germany) in 0.01 M citric buffer (Merck, Germany; pH 3.0, adjusted with KOH). Sodium azide (NaN_3 , Fluka, Neu-Ulm, Germany, 0.1 mM in final solution) was added to the enzymatic solution to prevent microbial growth. The detailed procedure is described in Schönherr and Riederer (1986).

Table 2 Carbon isotope composition of bulk leaf mass (whole discs) and of cuticular waxes (WXs) isolated from opposite sides of hypostomatous leaves

Species	Leaf disc $\delta^{13}\text{C}$ (‰)	Abaxial WX $\delta^{13}\text{C}$ (‰)	Adaxial WX $\delta^{13}\text{C}$ (‰)	Abax – Adax $\delta^{13}\text{C}$ (‰)
<i>Clivia miniata</i> ^a	−30.23	−33.76	−33.41	−0.35
<i>Ficus lyrata</i>	−26.45	−34.38	−33.54	−0.84
<i>Ficus elastica</i>	−28.23	−32.54	−27.86	−4.68
<i>Hedera helix</i>	−28.42	−31.67	−32.21	0.54
<i>Hoya carnosa</i>	−28.44	−27.33	−28.22	0.89
<i>Monstera deliciosa</i> ^a	−29.70	−40.13	−32.18	−7.95
<i>Prunus laurocerasus</i> ^a	−29.54	−32.81	−31.77	−1.04
<i>Stephanotis floribunda</i>	−29.97	−37.51	−35.28	−2.23
<i>Schefflera</i> sp. <i>actinophylla</i> ^a	−30.40	−38.13	−35.91	−2.22
<i>Yucca gloriosa</i>	−29.27	−28.69	−28.22	−0.47
<i>Zamioculcas zamiifolia</i> ^a	−30.37	−32.87	−29.81	−3.06
<i>Polylepis rugulosa</i> ^a	−23.84	−24.41	−23.73	−0.68
<i>Polylepis tarapacana</i> ^a	−24.56	−24.65	−23.94	−0.71
<i>Polylepis tomentella</i> ^a	−24.54	−25.55	−24.88	−0.67

$\delta^{13}\text{C}$ values are shown for 11 species grown in a glasshouse (Ceske Budejovice, Czech Republic) and 3 *Polylepis* species collected in their natural high-mountain habitat (Bolivia, Chile, 4300 m a.s.l.). Means of three to eight measurements are shown

^aDenotes species where total wax extracted from isolated cuticles was analyzed

Isolated CM from adaxial and abaxial leaf sides were separated, carefully washed with deionized water, air-dried and stored at room temperature.

Wax extraction

Five to ten CM isolated from adaxial and abaxial leaf sides of *C. miniata*, *H. carnosus*, *H. helix*, *P. laurocerasus*, *S. actinophylla*, and three *Polylepis* species (*P. rugulosa*, *P. tarapacana*, and *P. tomentella*) were immersed in 1 ml of chloroform (CHCl₃, Merck, Darmstadt, Germany) for 1 min. Wax from *F. elastica* grown under different light regimes was extracted from isolated CM submersed and shaken in chloroform overnight. The wax was used also for compound-specific isotopic analyses. EWX from *F. elastica*, *F. lyrata*, *M. deliciosa*, *S. floribunda*, *Y. gloriosa*, and *Z. zamiifolia* leaves was extracted directly from the leaf surface using a glass funnel pressed with its orifice to the leaf surface, filled with chloroform and shaken for about 30 s. Extracted waxes (WX) were dried on ignited silica sand. The whole amount of sand was transferred to a tin capsule and used for isotope analysis. Wax-free polymer matrix membranes (MX) were air-dried and stored at room temperature.

Carbon isotope analysis

Five sample types were used for carbon isotope analysis: leaf disc, CM, MX, WX, and EWX. The last four samples were analyzed separately for adaxial and abaxial leaf sides. All samples represent bulk material composed of a number of chemical compounds. The carbon isotope composition was determined using an elemental analyzer (EA1110, ThermoQuest Italy) linked to DeltaXLplus (ThermoFinnigan, Bremen, Germany). The ¹³C content (δ¹³C) was calculated as the difference in relative abundance of ¹³C normalized to that in VPDB (Vienna Pee Dee Belemnite) standard as δ¹³C = (R_{sample} - R_{VPDB})/R_{VPDB}, where R stands for the ratio of carbon isotopes (¹³C/¹²C). The standard deviation of δ¹³C determination in standard samples was lower than 0.1‰.

For compound-specific analyses of *F. elastica* wax we used IRMS interfaced with GC. The gas chromatograph (Trace GC Ultra, Thermo Fisher Scientific, Inc., USA) was equipped with a DB-5ms column (Agilent Technologies, USA; 30 m × 0.32 mm, film thickness 0.2 μm) and connected via an Isolink (with a pyrolysis furnace heated to 1000 °C) and Conflo IV interface to IRMS (Delta V Advantage, Thermo Fisher Scientific, Inc., USA). 1 μl of waxes solved in chloroform was injected into a splitless injector held at 50 °C. The oven temperature program started at the initial temperature of 50 °C for 2 min, followed by a ramp of 40 °C min⁻¹ to 200 °C, held for 2 min, and continued by increasing the temperature at 3 °C min⁻¹ to 310 °C, where it was held for another 30 min.

Estimation of CO₂ concentration relative drawdowns in the leaf interior (c_d/c_b and c_e/c_{bd}) and partitioning of mesophyll conductance

Details concerning the development of the formula relating CO₂ drawdown across the leaf to ¹³C content in adaxial and abaxial cuticles are presented in the Appendix. Equation 20 shows that the drawdown, expressed as the ratio of CO₂ concentrations at the distal (astomatous, adaxial) and proximal (stomatous, abaxial) sides of IAS, c_d/c_b, (i) decreases from one to zero when the difference in isotopic composition of cuticles from the opposite leaf sides, δ_{AB} - δ_{AD}, rises in absolute value (becomes more negative) and (ii) is proportional to the depletion of leaf tissue in ¹³C compared to air entering the leaf (δ_L - δ_b):

$$\frac{c_d}{c_b} = 1 - \frac{1}{1 + \frac{\delta_L - \delta_b + a}{\delta_{AB} - \delta_{AD}}}, \quad (1)$$

where *a* is the isotopic fractionation factor during diffusion of CO₂ in still air (4.4‰) (note that instead of denoting the CO₂ concentration in the intercellular space and/or substomatal cavity as *c_i*, as is commonly the case, we distinguish between CO₂ concentrations in abaxial substomatal cavities, *c_b*, and in adaxial IAS, *c_d*). The *c_d/c_b* values should range from 0 to 1 in photosynthesizing hypostomatous leaves (see simulation in Fig. 1a); lower values indicate a steeper drop in CO₂ concentration across the leaf and a higher diffusion resistance for CO₂ in the IAS. Several assumptions were made for the development of the relationship. First, we assume that assimilates ending up in cuticles from opposite leaf sides (mainly lipids with more than 16 carbon atoms in the chain) are synthesized in chloroplasts adjacent to the respective epidermis (and not transported transversely across the leaf) and record the δ¹³C and concentration of chloroplastic CO₂ in their ¹³C composition. Second, we assume that (i) the post-photosynthetic ¹³C fractionation during synthesis of individual cuticular compounds (long-chain aliphatics, aldehydes, ketones, acids, esters etc.) is not leaf side-specific and (ii) that cuticles on both leaf sides have identical compositions. Compound-specific ¹³C analyses eliminate part (ii) of the second assumption. Finally, we assumed that all investigated plants grew in an ambient atmosphere with δ_a of -8‰ and that the ¹³C content in substomatal air (δ_b) was reduced to -9.1‰ due to diffusion through stomata (when *c_b/c_a* was set to 0.75, which is typical for C₃ plants). The latter assumption has only a small or negligible impact on calculation of *c_d/c_b* (Fig. 1). We are aware that in photosynthesizing leaf, the intercellular bulk air is enriched in ¹³C compared to the free atmosphere due to Rubisco fractionation (Farquhar et al. 1982). The value of δ_b = -9.1‰ contradicts this fact because here we consider

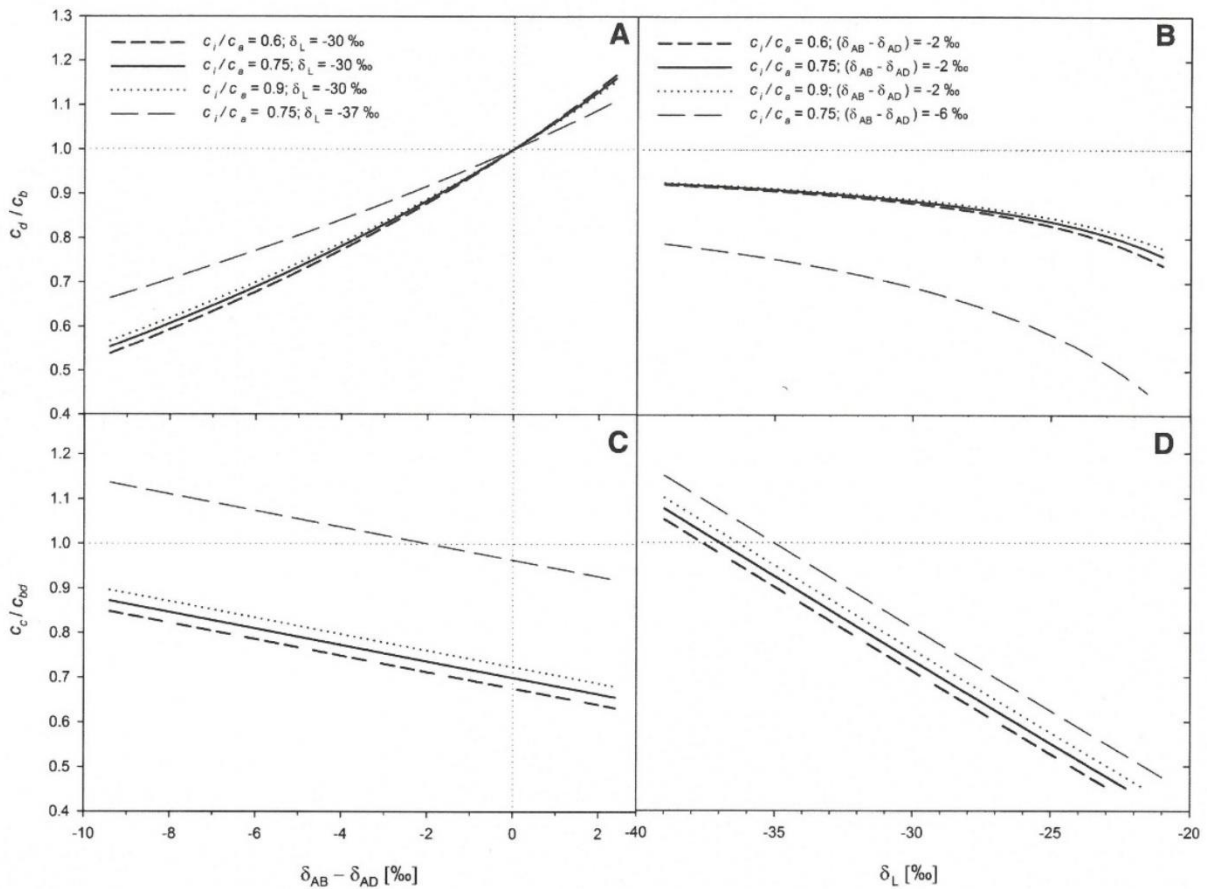


Fig. 1 Relative diminutions in CO₂ concentration transversally across the IAS of hypostomatous leaves (c_d/c_b) and across the cellular liquid phase (c_c/c_{bd}) and their sensitivity to differences in ¹³C composition of cuticles ($\delta_{AB} - \delta_{AD}$) and to the ¹³C content (δ_L) of bulk leaf mass. Equations 1 and 2 were used for modeling of c_d/c_b (a, b) and c_c/c_{bd}

(c, d), respectively, with c_i/c_a in the typical range for C₃ plants (0.6 to 0.9). Typical and extreme values recorded in our measurements were assigned to δ_L (−30‰ and −37‰, respectively) and to $\delta_{AB} - \delta_{AD}$ (−2‰ and −6‰, respectively)

only the partial effect of diffusion for assessment of this ‘boundary’ value: we assume that only the diffusion resistance of stomata is responsible for the reduction of CO₂ concentration across the stomatal pore ($c_a - c_b$) as well as for the change in carbon isotope composition ($\delta_a - \delta_b$). Rubisco CO₂ fixation accompanied by isotopic fractionation which takes place deeper in IAS as well as backward diffusion of ¹³CO₂ from the astomatous IAS side are not considered here for the simplicity reasons. Nevertheless, an arbitrary value of $\delta_b = -8‰$ (fractionation by Rubisco compensates for the isotopic effect of diffusion) does not increase c_d/c_b by more than 0.01 and c_c/c_{bd} (see below) by more than 0.04 compared to $\delta_b = -9.1‰$.

The relative drop of CO₂ concentration from the IAS across the cell wall and intracellular structures into chloroplasts, c_c/c_{bd} , was calculated using relationship (24):

$$\frac{c_c}{c_{bd}} = \frac{\delta_b - \delta_L - a_w(1 + \delta_L) - 0.5(\delta_{AB} - \delta_{AD})}{(b - a_w)(1 + \delta_L)}, \quad (2)$$

where c_c is the CO₂ concentration at carboxylation sites in the chloroplast, c_{bd} the average intercellular CO₂ concentration, b the isotopic fractionation during Rubisco carboxylation ($b = 30‰$), and a_w the fractionation during dissolution and diffusion of CO₂ in water ($a_w = 1.8‰$, for details see Farquhar and Lloyd 1993). Additionally, we assumed that the drawdown of CO₂ from the cell surface to the stroma (c_c/c_d) is the same on the adaxial and abaxial sides of the mesophyll ($c_{cb}/c_b = c_{cd}/c_d$). Relationship (2) and the simulation shown in Fig. 1c, d predict that the cellular CO₂ drawdown will be more pronounced (c_c/c_{bd} will be lower) in leaves that are relatively less depleted in ¹³C (have a less

negative $\delta^{13}\text{C}$ value) and at the same time have a high absolute value (more negative) of $\delta_{\text{AB}} - \delta_{\text{AD}}$.

The partitioning of the mesophyll resistance into intercellular (IAS) and cellular (liquid phase) fractions may be estimated by combining the drawdowns within the IAS across the leaf and from the IAS to the stroma, respectively [see Eqs. (27a), (27b) and (27c), (27d):

$$\frac{r_{\text{IAS}}}{r_m} \cong \frac{1}{1 + \frac{1 - \frac{c_c}{c_b}}{1 - \frac{c_d}{c_b}}}, \quad (3)$$

$$\frac{g_{\text{IAS}}}{g_m} \cong 1 + \frac{1 - \frac{c_c}{c_b}}{1 - \frac{c_d}{c_b}}, \quad (4)$$

$$\frac{r_{\text{liq}}}{r_m} \cong \frac{1}{1 + \frac{1 - \frac{c_d}{c_b}}{1 - \frac{c_c}{c_b}}}, \quad (5)$$

$$\frac{g_{\text{liq}}}{g_m} \cong 1 + \frac{1 - \frac{c_d}{c_b}}{1 - \frac{c_c}{c_b}}. \quad (6)$$

A sensitivity analysis shows that the IAS is responsible for 0–50% of total mesophyll resistance when $\delta_{\text{AB}} - \delta_{\text{AD}}$ ranges from zero to about -4‰ in a leaf with $\delta_L = -30\text{‰}$ (Fig. 2a). For a more ^{13}C -depleted leaf ($\delta_L = -37\text{‰}$), however, the same impact of the IAS on r_m can be indicated by $\delta_{\text{AB}} - \delta_{\text{AD}}$ ranging from zero to just some tenths of 1‰ ($\sim -0.7\text{‰}$). In turn, at a given value of $\delta_{\text{AB}} - \delta_{\text{AD}}$, the

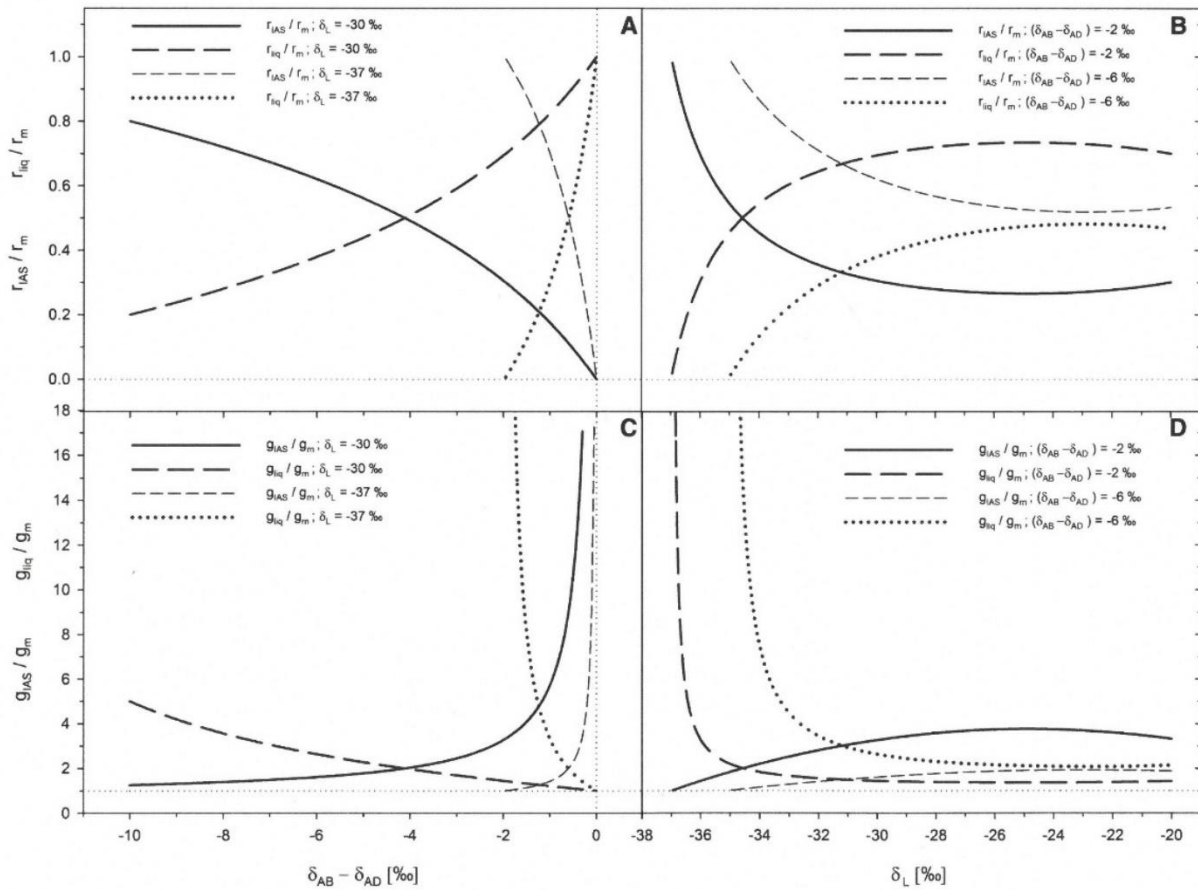


Fig. 2 Modeled partitioning of mesophyll diffusive resistance and conductance for CO_2 into their gas- and liquid-phase components based on ^{13}C enrichment of adaxial against abaxial cuticle ($\delta_{\text{AB}} - \delta_{\text{AD}}$) and on ^{13}C content in leaf dry mass (δ_L). Equations 3–6

and parameter values typical for C_3 plants ($c_i/c_a = 0.75$) were used in simulated partitioning of mesophyll resistance (a, b) and conductance (c, d)

portion of r_{IAS} increases while that of r_{liq} rapidly falls with increasing leaf ^{13}C depletion (Fig. 2b).

Sample size and statistics

In the initial study with material from the glasshouse in Bonn, 7 leaf discs and 7 abaxial and adaxial CM from each of 23 plant species were measured for leaf thickness, LMA, f_{IAS} , stomatal density, and isotopic composition. With the material sampled in Belize, Czech Republic and Bolivia and Chile we analyzed the isotopic composition only, not the leaf anatomical traits. In the analyses of isotopic composition, one pooled sample of leaf discs (discs from four to eight leaves) and one sample of CM and/or WX from each leaf side were prepared, or alternatively only the leaf disc and the leaf side-specific EWX were analyzed in each species. In the more detailed study with CM, 5–24 replications from each plant and sample type (leaf disc, CM, MX, and WX from both abaxial and adaxial leaf side) were measured. To avoid pseudo-replications, the MX samples were not included in statistical analyses. Each sample was measured by IRMS in two analytical replicates. Data were analyzed using two-way ANOVA with species and sample type as factors. The Tukey HSD test was used for post-hoc comparisons. For comparison of the isotopic composition of leaf disc and CM and comparison of adaxial and abaxial CM, respectively, paired t -tests were used. All results given are means \pm 1 SD.

Results

Isotopic enrichment of the adaxial leaf surface

The carbon isotope composition of leaves (δ_L) ranged from -23.84‰ (*P. rugulosa*) to -35.22‰ (*C. arabica*), which indicates that all species investigated here were using predominantly the C_3 type of CO_2 fixation. CM isolated from both sides of the same leaf were ^{13}C depleted (more negative δ) compared to the bulk leaf disc (paired t -test, $t = 14.38$, $P < 0.001$; Table 1). The depletion of CM relative to bulk leaf material, averaged over all species, was $2.01 \pm 1.33\text{‰}$ (mean \pm 1 SD); waxes (WX) were depleted even more than CM ($2.85 \pm 2.75\text{‰}$). In the whole dataset, including the detailed study with *F. elastica*, adaxial CM, WX, and EWX were less depleted in ^{13}C than their abaxial counterparts by $0.09 \pm 0.54\text{‰}$, $0.88 \pm 1.59\text{‰}$ and $1.17 \pm 1.40\text{‰}$, respectively. However, 10 out of 31 species did not exhibit relative ^{13}C enrichment of the upper CM compared to the lower CM as expected but, on the contrary, their upper cuticle was more depleted than the lower one. Two out of 14 species showed the same trend in WX. The $\delta^{13}C$ values of bulk leaf tissue and CM from the opposite leaf sides are summarized in Table 1 (Bonn glasshouse and Belize field collections);

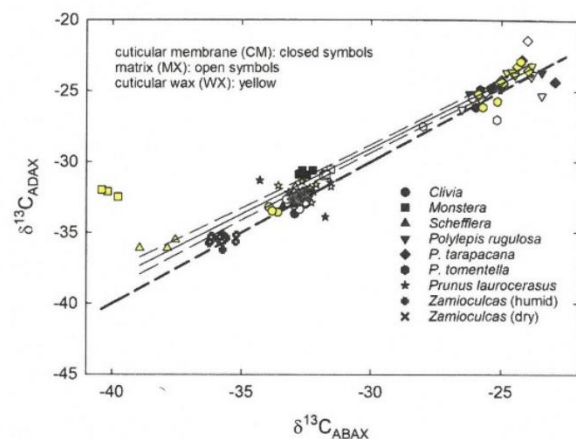


Fig. 3 The relationship between ^{13}C content ($\delta^{13}C$) in adaxial and abaxial cuticle, cuticular matrix, and wax in eight hypostomatous species. Symbols indicate measurements with bulk cuticular membranes (CMs) isolated from opposite leaf sides, cuticular waxes (WXs) extracted from CM with chloroform, and cuticular matrix (MX). The thick dashed line indicates the 1:1 relationship. The thin lines show linear regression and 95% confidence intervals for WX (yellow symbols)

$\delta^{13}C$ values of WX are shown in Table 2. The greater difference between δ_{AB} and δ_{AD} in WX than in CM or MX (note the greater abundance of yellow points above the 1:1 line in Fig. 3) led us to study total and EWX from *F. elastica* more extensively, including the determination of compound-specific $\delta^{13}C$.

Leaf internal CO_2 gradients

The differences in $\delta^{13}C$ between abaxial and adaxial cuticles ($\delta_{AB} - \delta_{AD}$) and $\delta^{13}C$ values of leaf discs (δ_L) were used in calculations of (i) the relative drawdown of CO_2 concentration across the leaf air space (IAS), c_d/c_b , and (ii) the CO_2 gradient from cell walls into the chloroplasts, c_c/c_{bd} , using Eqs. (1) and (2), respectively. Gradients (relative drawdowns) of CO_2 plotted in Fig. 4 yield average values across all species in which wax was isolated and analyzed of 0.90 ± 0.12 in the IAS and 0.66 ± 0.11 within cells (dotted lines in Fig. 4) with medians of 0.94 and 0.68, respectively. Extreme values of c_d/c_b and c_c/c_{bd} were found in *M. deliciosa* ($c_d/c_b = 0.60$) and in the three *Polylepis* species ($c_c/c_{bd} = 0.51$), which indicates that the CO_2 concentration at the astomatous side of the IAS can be reduced by up to 40% compared to that in substomatal cavities and the intracellular structures of *Polylepis* can reduce the CO_2 concentration by up to one-half of that at the cell walls. While the cuticle data did not reveal any relationship between IAS and cellular CO_2 gradients, the wax data show that the IAS drawdown increases with a

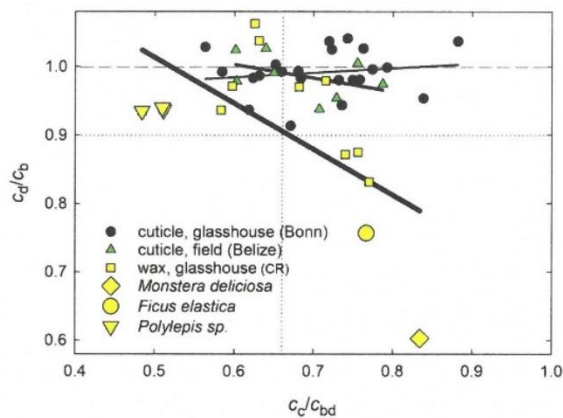


Fig. 4 Relationship between relative drawdown of CO₂ concentrations across the leaf air space, c_d/c_b , and across the cell wall-chloroplast pathway, c_c/c_{bd} . Results are shown for 31 plant species grown in a glasshouse (closed circles and thin regression line) or in the open (upward pointing triangles and half-thick line), calculated from the $\delta^{13}C$ of cuticular membranes from opposite leaf sides. In addition, data for cuticular waxes isolated from adaxial and abaxial leaf sides of 14 plant species are shown (yellow squares and large symbols, thick regression line, see Table 2 for the list of species). The large symbols mark out three genera with extremely low c_d/c_b and c_c/c_{bd} . The dotted lines indicate average values across all species in which wax was analyzed

decreasing drop of CO₂ inside the cells and vice versa (thick line in Fig. 4). Results from *F. elastica* show that neither CM nor WX differed isotopically between opposite leaf sides (Fig. 5a, b). Nevertheless, EWX and especially 30-C aldehyde were significantly less depleted on the adaxial side and indicated $c_d/c_b < 1$. The decrease of c_d/c_b below 1 was even more pronounced in the thicker leaves adapted to high irradiance (sun-exposed leaves in Fig. 5b). Based on the 30-C aldehyde data, both components of CO₂ drawdown inside the sun-exposed *F. elastica* leaves were of about the same magnitude (~0.78, Fig. 5b, d). The cell (liquid phase) relative drawdown ($1 - c_c/c_{bd}$) also increased in sunny compared to shaded leaves (Fig. 5c, d).

Mesophyll resistance partitioning

Only the samples that were less depleted on the adaxial than on the abaxial side were used for the calculation of the resistance partitioning in order to avoid a bias caused by physiologically irrelevant or infinitely high values. The diffusive resistance for CO₂ in the IAS averaged across all species comprised between 16.7% and 23.0% of the total mesophyll resistance while the cellular resistance explained the residual part (83.3–77.1%) when WX and EWX data were used for

calculations (Table 3). Accordingly, the conductance of IAS (g_{IAS}) was between 12.6 and 7.9 times higher and cellular conductance (g_{liq}) between 1.2 and 1.4 times higher than the total mesophyll conductance, provided that g_{IAS} and g_{liq} are arranged in series. High coefficients of variation (~0.7 and 0.2 for IAS and cell interior, respectively) represent mainly the high interspecific variability (Table 3).

¹³C discrimination and CO₂ drawdowns related to leaf anatomical traits

The isotopic composition of the entire leaf discs correlated with leaf thickness ($R^2 = 0.37, P < 0.001$); thicker leaves were less depleted in ¹³C than thinner leaves (Fig. 6a). Further, δ_L correlated positively with LMA ($R^2 = 0.65, P < 0.001$), with extremes in *Cotyledon* (open circle in Fig. 6b). Interestingly, there was neither a correlation between δ_L and f_{IAS} ($P = 0.25$) nor between stomatal density and δ_L ($P = 0.80$). Both the drawdown in the IAS and that from the cell walls to chloroplasts increased with rising LMA (Fig. 7). Thicker and denser leaves were more deprived in CO₂ at the distal stomatous IAS (Figs. 7a, 8a) and also in chloroplasts (Fig. 7b) than thinner and less densely packed leaves. The transversal drawdown also correlated weakly with stomatal density (Fig. 8b).

Leaves grown at extremely high elevations

For *Polylepis* species, δ_L ranged from -23.84‰ to -24.54‰ for *P. rugulosa* and *P. tomentella*, respectively. The abaxial cuticle was significantly more depleted in ¹³C than the adaxial one (paired *t*-test, $t = 3.76, P < 0.01$). The mean values of $\delta_{AB} - \delta_{AD}$ for CM and WX were -0.32‰ and -0.69‰, respectively, which corresponds to CO₂ drawdowns in the IAS (c_d/c_b) of 0.97 and 0.94, respectively, and cellular CO₂ drawdowns (c_c/c_{bd}) of 0.50 and 0.49, respectively (Fig. 4). The latter data indicate a remarkably low CO₂ concentration in chloroplasts of high-mountain plants.

Amphistomatous leaves

We analyzed the relevant isotopic and anatomical parameters in leaves of one herbaceous and one woody amphistomatous species, tulip (*Tulipa* sp.) and lilac (*S. vulgaris*), respectively. While tulip has almost identical stomatal density on both leaf sides, stomata on abaxial side of lilac leaf outnumbered those of adaxial side by a factor of five (see inset in Fig. 9). Equi-stomatal tulip leaves yielded almost identical $\delta^{13}C$ of adaxial and abaxial wax (Fig. 9). In spite of the apparently reduced CO₂ access from sunlit side of lilac leaf due to less abundant stomata, $\delta^{13}C$ of wax washed out by chloroform from both leaf sides was also indistinguishable. In contrast,

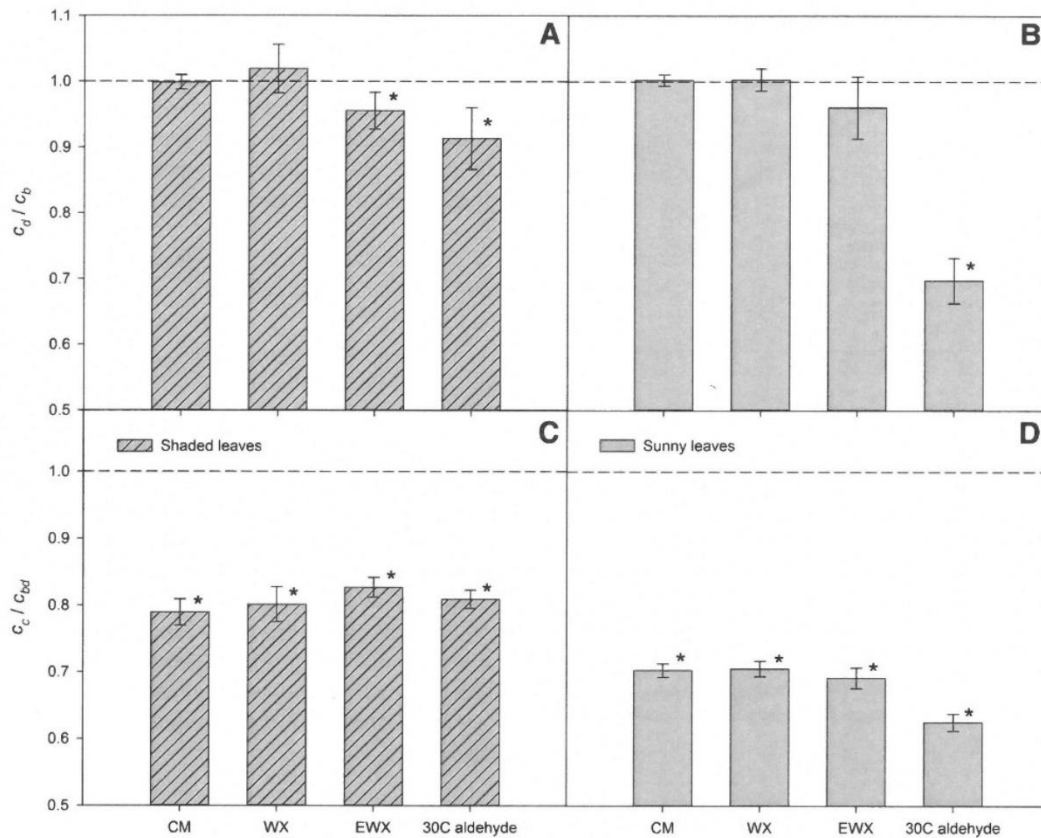


Fig. 5 CO₂ drawdowns across intercellular air space (IAS), c_d/c_b , and from IAS across cell wall into chloroplast stroma, c_c/c_{bd} , in hypostomatous *Ficus elastica* leaves estimated from various types of cuticular material taken from opposite leaf sides. CM, WX, EWX and 30-C aldehyde indicate samples taken for analyses from the same leaf: bulk cuticular membrane (CM), total cuticular wax (WX)

extracted with chloroform from CM, epicuticular wax (EWX) collected from the leaf surface by short-time chloroform extraction, and triacontanal (30-C aldehyde in WX). Data from plants grown in a glasshouse and adapted to shady (a, c, irradiance $30 \mu\text{mol m}^{-2} \text{s}^{-1}$) or sunny (b, d, $300 \mu\text{mol m}^{-2} \text{s}^{-1}$) conditions are shown. The asterisks indicate significant reduction from c_d/c_b and $c_c/c_{bd} = 1$

Table 3 Relative ¹³C content in leaf bulk mass (δ_L), differences in ¹³C content between abaxial and adaxial cuticles ($\delta_{AB} - \delta_{AD}$), calculated CO₂ drawdowns and fractional contributions to the overall resistance for CO₂ diffusion inside the leaf

	δ_L	$\delta_{AB} - \delta_{AD}$	c_d/c_b	c_c/c_{bd}	r_{IAS}/r_m (%)	r_{liq}/r_m (%)	g_{IAS}/g_m	g_{liq}/g_m	n	n_{sp}
CM	-30.32 ± 2.80	-0.09 ± 0.54	0.99 ± 0.03	0.72 ± 0.08	8.77 ± 7.61	91.03 ± 7.61	25.81 ± 27.87	1.11 ± 0.10	32	32
WX	-30.15 ± 2.55	-0.88 ± 1.59	0.95 ± 0.08	0.72 ± 0.10	16.70 ± 12.12	83.30 ± 12.12	12.57 ± 18.27	1.23 ± 0.21	20	5
EWX	-29.98 ± 3.43	-1.17 ± 1.40	0.93 ± 0.09	0.74 ± 0.09	22.95 ± 15.36	77.05 ± 15.36	7.93 ± 7.64	1.36 ± 0.31	17	6

c_d/c_b indicates CO₂ drawdown across the intercellular air space (IAS), from substomatal cavities to the adaxial side of hypostomatous leaves, c_c/c_{bd} is the ratio of CO₂ concentrations in chloroplast stroma and the IAS, r_{IAS}/r_m and r_{liq}/r_m are percentages of the total resistance in the mesophyll to CO₂ diffusion located in the gas and liquid phases, respectively, g_{IAS}/g_m and g_{liq}/g_m are analogous fractions expressed as conductances. n denotes number of measurements (each from two to eight IRMS analyses) performed with the number of species indicated (n_{sp}). Analyses were carried out with whole cuticular membranes (CMs), extracted total cuticular wax (WX) or collected epicuticular wax (EWX). Only those samples with a negative $\delta_{AB} - \delta_{AD}$ were used because they allowed calculations of CO₂ drawdown and partitioning of resistances. Average values ± 1 SD are shown

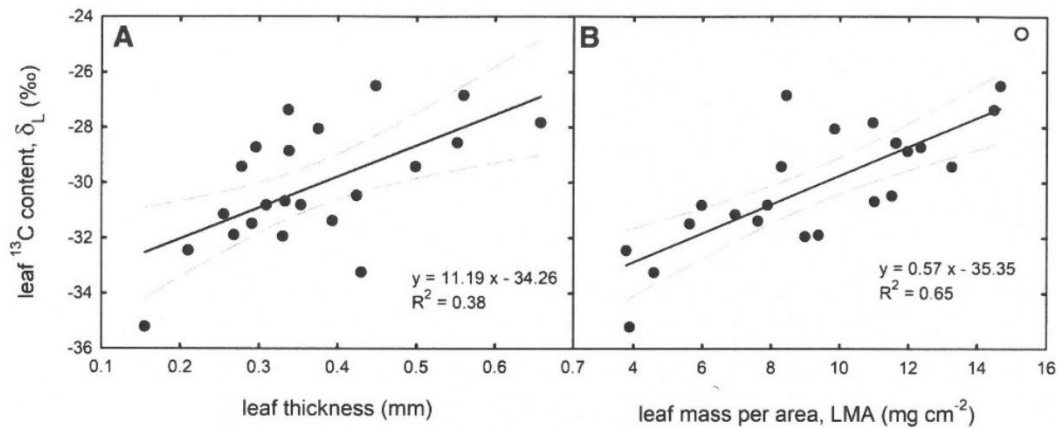


Fig. 6 The relationships between carbon isotope composition of the entire leaf disc (δ_L) and leaf thickness (**a**) or leaf mass per area (**b**). Both correlations are significant ($P < 0.001$). Points show values obtained from analyses of cuticular membranes of 23 plant species

(collected in Bonn's Botanical Garden). The open circle in **b** shows values for *Cotyledon orbiculata*, a succulent plant species with leaf water storage tissue, leaf thickness 5.7 mm and abax/adax stomatal density of 27/10 mm⁻². Dashed lines indicate 95% confidence intervals

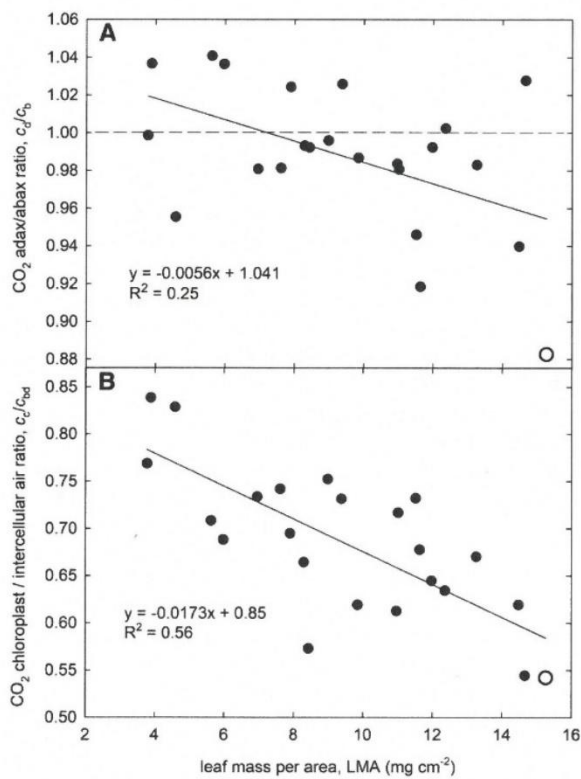


Fig. 7 The relationship between relative CO₂ drawdown across the leaf, c_d/c_b , and leaf dry mass per area, LMA (**a**) and between chloroplast to mesophyll air space CO₂ concentration ratio, c_c/c_{bd} , and LMA (**b**). Values were calculated from differences in isotopic composition of isolated abaxial and adaxial cuticular membranes and leaf discs of 23 hypostomatous C₃ species. Open circles represent the amphistomatous succulent *Cotyledon orbiculata*

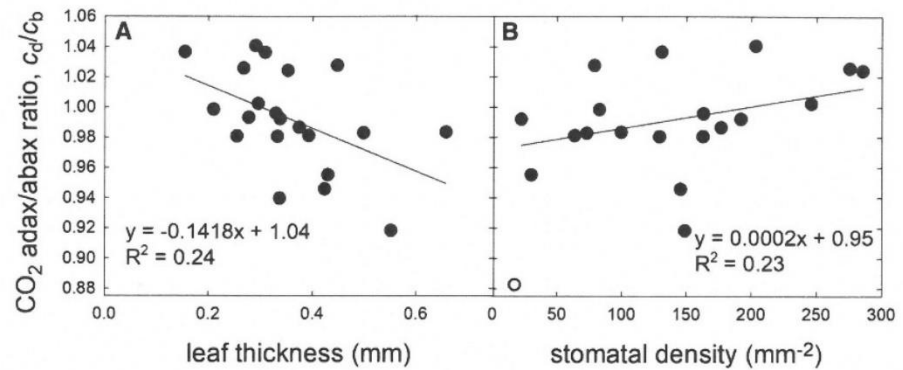
hypostomatous cherry laurel collected at the same time and environment showed pronounced $\delta_{AB} - \delta_{AD}$ values (Fig. 9).

Discussion

We have used the ¹³C content of assimilates deposited in the cuticles on opposite leaf sides to estimate the CO₂ transverse gradient across the leaf and the partitioning of air- and liquid-phase components of the leaf's internal conductance for CO₂. This is a novel technique, which could help with modeling 3D leaf photosynthesis and understanding anatomical adaptations. However, it employs several assumptions whose rationale has to be considered and tested.

In the majority of plant species investigated here, the adaxial cuticle was enriched (less depleted) compared to the abaxial one, as suggested by our hypothesis. On average, the enrichment translates to only 1% drawdown of CO₂ across the leaf; i.e., CO₂ concentration at the adaxial edge of the IAS in hypostomatous leaves was 1% lower than in the substomatal cavities (Table 3). This is an unexpectedly low value for hypostomatous leaves, where the mean increment in photosynthesis rate due to increased diffusivity when the IAS was filled with helox was 12% for seven species (Parkhurst and Mott 1990). We can see at least three possible reasons why the drawdown could be underestimated when calculated using Eq. (1) and CM data. First, different lipid compounds in the cuticle bear different ¹³C signals and their abundance differs between adaxial and abaxial cuticles (see Table S1 in Supplementary Information for our model plant *F. elastica*;

Fig. 8 Relationship of CO_2 drawdown across the leaf intercellular air space (c_d/c_b) to leaf thickness (a) and to stomatal density (b). Points show values of c_d/c_b calculated for 19–21 hypostomatous C_3 species. Regression lines and coefficients of determination are shown



cf. Mackova et al. 2013). In addition to cutin monomers, there are dozens of very long-chain linear and cyclic compounds forming wax and their ^{13}C content may be modified according to their biosynthetic pathway (Chikaraishi et al. 2004). Second, the wax composition across the cuticle is heterogeneous—intracuticular wax differs from the epicuticular one in chemical composition (Buschhaus and Jetter 2011); hence, $\delta^{13}\text{C}$ of the extracted wax may differ based on the method of extraction. Indeed, at the point of complete extraction of wax, after hours of immersion of isolated cuticles in chloroform, we did not detect any difference between δ_{AB} and δ_{AD} or found even a positive one in several species. For example, *F. elastica* bulk cuticle or total wax did not show any leaf-side specificity for $\delta^{13}\text{C}$, while EWX did, and the difference was even more pronounced when a single compound (30-C aldehyde) was

analyzed (Fig. 5). Third, the backward diffusion of $^{13}\text{CO}_2$ from the enriched adaxial IAS towards stomata could reduce the gradient in isotopic composition of the leaf internal air and diminish the difference in isotopic composition of cuticles ($\delta_{\text{AB}} - \delta_{\text{AD}}$).

Isotopic composition of leaf, cuticle and of isolated waxes

The plant cuticle, an extracellular product of epidermal cells, is composed of cutin, a polymer matrix interlocked with polysaccharide microfibrils, and embedded waxes that can be deposited dynamically during leaf development (Jetter and Schaffer 2001). The cuticle is usually depleted in ^{13}C relative to leaf tissue. The depletion of total lipids extracted from the leaf surface relative to the total leaf tissue ranges from 1.9 to 9‰ with an average of 4.5‰ in C_3 plants (Chikaraishi and Naraoka 2001; Zhou et al. 2015). In our study, depletion of CM relative to bulk leaf tissue averaged at 2.0‰ and mean depletion of waxes relative to bulk leaf tissue ranged from $-0.8‰$ (enrichment) to 7.5‰ for both leaf sides. Such depletion is associated with isotopic fractionation during the oxidation of pyruvate to acetyl-coenzyme A and with biosynthetic pathways of lipid compounds, e.g., for acetogenic lipids via fatty acid biosynthesis and for polyisoprenoid lipids via the mevalonic and methylerythritol phosphate pathway (Chikaraishi et al. 2004). The kinetic isotope effect during wax biosynthesis can differ among plant groups but it is relatively insensitive to environmental factors (Chikaraishi and Naraoka 2003). Therefore, we assume that biosynthetic pathways of cuticle and waxes are species-specific rather than leaf side-specific. As waxes are highly variable among species with regard to their proportion in overall cuticle mass (20–60%, Schreiber and Riederer 1996), the isotopic signal of bulk CM is affected by MX, WX, and EWX according to their isotopic mass balance (Hobbie and Werner 2004).

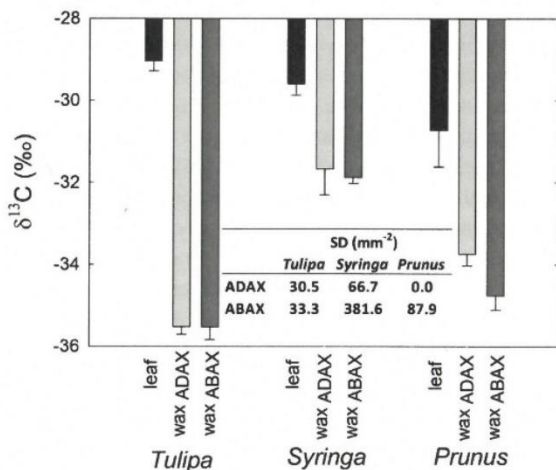


Fig. 9 ^{13}C content ($\delta^{13}\text{C}$) in leaf dry mass and adaxial and abaxial cuticular wax isolated from leaves of two amphistomatous (*Tulipa*, *Syringa*) and one hypostomatous (*Prunus*) species. The inset table indicates stomatal densities (SDs) on both leaf sides of these species. All three species were collected in spring (May) in common garden. Means and standard deviations are shown ($n=3$)

Leaf-side specificity in isotopic composition of cuticle and waxes

The adaxial astomatous cuticle was enriched in ^{13}C relative to the abaxial stomatous cuticle in two-thirds of our species; however, the effect was stronger in WX and especially EWX (Fig. 3). A possible explanation is that the composition of intra- and EWXs may differ. It was shown that primary alcohols, diols and cyclic wax constituents accumulate in the intracuticular wax, and alkanes and secondary alcohols in the epicuticular layer (Buschhaus and Jetter 2011). The reasons for this heterogeneity of wax composition have not been resolved yet but it is known that the epicuticular layer represents a dynamic deposit being eroded by rain, wind or mechanical abrasion during the whole life of the leaf and that it is replenished by freshly synthesized wax with a fast turnover (Jetter and Schaffer 2001; Gao et al. 2012). Therefore, the uppermost surface probably reflects the actual conditions of wax precursor synthesis in plastids and chloroplasts. Conversely, the primary cuticle in leaves of some deciduous tree species is probably synthesized from stored or imported carbon skeletons lacking the leaf-side specificity (Tipple and Ehleringer 2018).

Why does the hypothesis of ^{13}C enrichment of the adaxial bulk cuticle fail in about one-third of the investigated species? The individual wax compounds can be synthesized and deposited in various proportions on adaxial and abaxial leaf sides (see Table S1 in Supplementary) and, if they differ in ^{13}C content, this will affect $\delta^{13}\text{C}$ of bulk cuticle and wax in a leaf side-specific way. The effect of differences in wax composition between the leaf sides or between intra- and EWXs can be experimentally removed by compound-specific $\delta^{13}\text{C}$ analyses. Our data on ^{13}C enrichment of 30-C aldehyde isolated from the adaxial side of *F. elastica* leaves support the view that there is a CO_2 drawdown across the leaf. Other wax compounds and plant species remain to be investigated before we can fully understand the mechanisms behind any leaf-side specificity of isotopic wax composition.

Amphistomatous leaves allow CO_2 access from both leaf sides and, therefore, the CO_2 concentration gradient should be less pronounced than in the species with hypostomatous leaves. If our hypothesis is valid, we can expect less (if any) ^{13}C enrichment of the adaxial cuticle in amphistomatous species, especially under shaded conditions or in species with upright vertical leaf orientation letting both leaf sides to be irradiated similarly. Indeed, we did not find any pronounced difference in $\delta^{13}\text{C}$ of wax between both leaf sides in two amphistomatous species (Fig. 9). The screening over broad spectrum of species with various degree of amphistomy could shed more light on the CO_2 gradients and on ecological significance of amphistomy (Muir 2015).

Leaf anatomy and CO_2 drawdowns in mesophyll

Mesophyll conductance for CO_2 diffusion (g_m), one of the main constraints of leaf photosynthetic productivity (e.g., Niinemets et al. 2009), consists of intercellular and cellular components (g_{IAS} , g_{liq}). The proportion of chloroplast surface facing intercellular spaces and cell wall thickness are likely the main anatomical determinants of the cellular component (e.g., Tomas et al. 2013). The intercellular component g_{IAS} , which is considered to be high compared to g_{liq} (Evans et al. 2009), is often overlooked due to the absence of a fast and easy way to determine it. Results from the method we suggest here indicate the existence of a CO_2 drawdown across hypostomatous leaves constituting between 8 and 23% of the overall mesophyll resistance, depending on the cuticle component analyzed (Table 3). Is the drawdown we found here real? Which leaf anatomical components underlie r_{IAS} ? The distance CO_2 molecules have to diffuse before entering mesophyll cells depends on leaf thickness and the tortuosity (lateral diffusion) of the diffusion pathway, determined by the density with which the cells are packed and by the density of stomatal pores. Therefore, leaf thickness, leaf mass per area (LMA) or the proportion of IAS, as well as stomatal density are good candidates for explaining the variability in the c_d/c_b drawdown. In fact, the relative CO_2 concentration difference between abaxial and adaxial sides of the IAS (calculated from CM only) correlated with LMA (Fig. 7a), and weakly with leaf thickness and stomatal density (Fig. 8a, b). Consistent with our observations (Fig. 6), leaf thickness and LMA are known for their relationship with ^{13}C discrimination in bulk leaf dry mass (Rumman et al. 2018; Ramirez-Valiente et al. 2010), which can be explained by a reduction of chloroplast CO_2 concentration c_c in proportion to both anatomical parameters.

Conclusions and perspectives

The leaf-side specificity in carbon isotopic composition of EWX, and especially in the compound-specific ^{13}C signature, could serve as a marker of relative CO_2 drawdown across the leaf caused by the diffusive resistance of intercellular spaces. The drawdown-based partitioning of mesophyll resistance to CO_2 diffusion could shed more light on leaf 3D-photosynthesis and adaptations of the traits affecting chloroplast access to CO_2 and water loss to various environmental constraints. EWX collection and $\delta^{13}\text{C}$ analyses are both potentially high-throughput techniques which can yield extensive databases of the leaf internal CO_2 transport characteristics, although only in terms of relative gradients and fractions.

Acknowledgements Thanks are due to Marie Šimková for stomata counting, Marcel Rejmánek (Davis, USA) for determination of tropical plant species collected in Belize and Jiří Šetlík for IRMS analyses. We also thank Lucas Cernusak (Cairns, AU) for valuable comments and Gerhard Kerstiens (Lancaster, UK) for language revisions. Special thanks are due to Graham Farquhar for opening the field of stable isotopes to JS and for valuable critical comments to this manuscript.

Funding This work was supported by the Czech Science Foundation (18-14704S). Access to IRMS and other facilities was supported by the Czech Research Infrastructure for Systems Biology C4SYS (Project No. LM2015055). PM was supported by MEYS Project No. LM2015078.

Compliance with ethical standards

Conflict of interest The authors declare that they have no conflict of interest.

Estimation of CO₂ concentration drawdown across the leaf

Photosynthesis integrated over the leaf profile and ¹³C discrimination

Positive values of net carbon fixation in leaf photosynthesis require CO₂ molecules to enter the leaf along a downward CO₂ concentration gradient from the atmosphere (c_a) to mesophyll chloroplasts (c_c). On the way, CO₂ passes through the laminar boundary layer of air and stomatal pore, diffuses from the substomatal cavity through the IAS of mesophyll, dissolves in water saturating cell walls and finally enters chloroplasts of photosynthesizing cells, where it is assimilated. In hypostomatous leaves where the astomatous leaf surface faces the sun, palisade parenchyma adjoining the upper (adaxial) epidermis is the ultimate end of the CO₂ pathway. However, portions of net CO₂ influx are consumed by mesophyll cells adjoining the stomatous epidermis and in ‘deeper’ mesophyll layers before reaching the palisade cells. Assuming in first approximation that the CO₂ carboxylation takes place at the sun lit adaxial leaf side, net photosynthesis is proportional to the CO₂ concentration difference between the IAS adjoining abaxial and adaxial leaf sides ($c_b - c_d$) and to the mean value of IAS conductance for CO₂ diffusion between the stomatal cavity and adaxial leaf side (g_{IAS}):

$$A = g_{IAS} \cdot (c_b - c_d) \quad (7)$$

(for more rigorous integration of A across the leaf on a volume basis see Appendix 1 in Lloyd et al. 1992). Assimilates synthesized in chloroplasts located at opposite leaf sides serve as precursors for long-chain aliphatics presumably deposited in the adjacent cuticle. Here we search for the relationship between CO₂ concentration drawdown across the leaf and carbon isotopic composition of cuticles at the

opposite leaf sides. Two parts of the overall CO₂ concentration drawdown in mesophyll may be distinguished: the transversal one across the IAS (c_d/c_b) and one in the cellular liquid phase (c_c/c_d or c_c/c_b where c_c is the CO₂ concentration in chloroplast stroma).

Plants discriminate against ¹³CO₂ during photosynthetic carbon assimilation. This phenomenon was quantified as the deviation (Δ) in isotopic compositions between CO₂ in ambient air (δ_a), and leaf assimilates or dry mass (δ_l) as the product of photosynthetic CO₂ fixation: $\Delta = (\delta_a - \delta_l)/(1 + \delta_l)$. The isotopic composition δ shows a relative shift in the ¹³C/¹²C ratio of the sample ($R = [^{13}\text{C}/^{12}\text{C}]$) from the isotopic ratio of PDB carbonate standard (R_s): $\delta = (R - R_s)/R_s$ (for details see for example Farquhar et al. 1989). ¹³C discrimination (Δ) in C₃ photosynthesis is related to CO₂ concentrations inside the leaf by a relationship that partitions the overall discrimination into two components: discrimination due to (i) diffusion through stomata and (ii) carboxylation by Rubisco (Farquhar et al. 1982):

$$\Delta = a \cdot \frac{(c_a - c_b)}{c_a} + b \cdot \frac{c_b}{c_a}, \quad (8)$$

where a is the carbon isotope fractionation factor during diffusion of CO₂ across the stomata (4.4‰), and b is the net discrimination due to Rubisco carboxylation, CO₂ dissolution and diffusion in water (29–30‰). The relationship assumes no CO₂ drawdown from the substomatal cavities to the chloroplasts ($c_b = c_d = c_c$).

Carbon isotope composition of CO₂ in the leaf transection

Photosynthetic assimilation of CO₂ penetrating the hypostomatous leaf results in CO₂ concentration drawdown (the difference between c_b and c_d). Further, diffusion through and assimilation by mesophyll change ¹³CO₂ abundance in the IAS and create the difference between δ_b and δ_d . Two opposite effects on $\delta_b - \delta_d$ can be anticipated: (i) diffusion across the IAS depletes ¹³CO₂ due to kinetic fractionation in the same way as diffusion from the ambient atmosphere adjoining the leaf into the leaf [the first term in Eq. (8)], and (ii) discrimination against ¹³CO₂ during RuBP carboxylation by Rubisco [the second term in Eq. (8)] enriches the IAS gas in ¹³CO₂ diffusing back out of chloroplasts into the IAS. The isotopic depletion due to (i), shown schematically by the line ‘D’ in Fig. 10, can be expressed as

$$(\delta_b - \delta_d)|_D = a \frac{c_b - c_d}{c_b}, \quad (9)$$

where the notation $|_D$ indicates the partial effect of diffusion in the IAS on $\delta_b - \delta_d$. The partial effect due to (ii), $(\delta_b - \delta_d)|_C$ (line ‘C’ in Fig. 10), can be approximated using

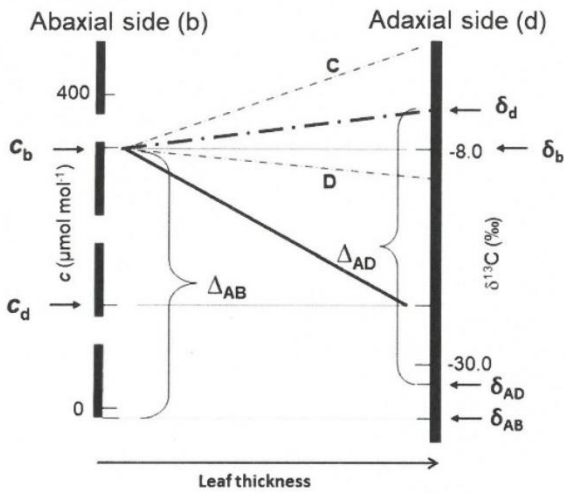


Fig. 10 Schematic of ^{13}C discrimination processes occurring during CO_2 transport and assimilation across the leaf. CO_2 concentration c , indicated on the left-hand vertical axis, which also represents the abaxial stomatous epidermis, decreases as CO_2 diffuses across the leaf and is assimilated in photosynthesis. This process is approximated by the full line connecting the CO_2 concentrations at the inner side of abaxial and adaxial epidermis c_b and c_d , respectively. The isotopic composition of leaf internal CO_2 , scaled on the right-hand vertical axis, which also represents the adaxial astomatous epidermis, changes across the mesophyll due to convolution of two processes indicated by the thin dot-dash lines: **a** slower diffusion of $^{13}\text{CO}_2$ than $^{12}\text{CO}_2$ depleting the intercellular air close to the adaxial epidermis in ^{13}C (line D) and **b** preferential assimilation of the lighter $^{12}\text{CO}_2$ molecules by Rubisco, leaving the inorganic carbon in chloroplasts close to the adaxial side enriched in $^{13}\text{CO}_2$ compared to those near the abaxial side (line C). Combination of these processes eventually results in different isotopic composition of CO_2 in chloroplasts near the abaxial (δ_b) and adaxial (δ_d) leaf sides, represented by the bold dot-dash line. ^{13}C discrimination during photosynthetic CO_2 fixation, Δ , is side-specific due to different c_b and c_d and δ_b and δ_d . We hypothesize that isotopic composition of cuticles and waxes from opposite leaf sides, δ_{AB} and δ_{AD} , mirrors the transectional differences in chloroplastic CO_2 concentration and isotopic composition. The lines showing the transectional course of c and δ indicate qualitative changes only, not the quantitative pattern

the relationship developed by Evans et al. (1986) for on-line measurements of $^{13}\text{CO}_2$ discrimination. The authors related discrimination in photosynthesizing tissue against $^{13}\text{CO}_2$ in surrounding air (Δ_L) to accumulation of $^{13}\text{CO}_2$ in air passing the leaf (Δ_a) as

$$\Delta_a = -\frac{\Delta_L}{\xi \cdot (1 + \Delta_L)}, \tag{10}$$

where $\xi = c_b/(c_b - c_d)$. In Evans et al.'s notation, c_b and c_d were the CO_2 concentrations at the chamber inlet (c_i in Evans et al.) and outlet (c_o), respectively. Δ_L showed the discrimination of leaf carbon against $^{13}\text{CO}_2$ in ambient air [and was defined as the isotopic ratio of the source CO_2 in air, R_a , to that of carbon in leaf assimilates, R_L : $\Delta_L = (R_a/R_L) - 1$],

and Δ_a was the discrimination in well-mixed air inside the leaf chamber relative to the source air at the leaf chamber inlet [$\Delta_a = (R_i/R_o) - 1$ with the original inlet, outlet notation]. Therefore, Δ_a had negative values as the air around the leaf becomes enriched ($R_o > R_i$). Our case of CO_2 diffusion across the leaf resembles the on-line discrimination experiment and the relation (10) can be derived using similar steps as in Evans's original work. The main difference is that CO_2 entering the leaf in our case is not transported by turbulent mass flow of air with a flow rate u [mol s^{-1} , see Eq. (7) in Evans et al. 1986] but by diffusion with diffusion conductance g_{IAS} ($\text{mol m}^{-2} \text{s}^{-1}$). Therefore, in analogy to Evans's Eq. (A1), we rearrange our Eq. (7) and write for the balance of carbon (i) entering the leaf by diffusion on the one side and (ii) leaving the leaf by backward diffusion plus incorporation in leaf matter by assimilation: $c_b \cdot g_{IAS} = c_d \cdot g_{IAS} + A$. Since isotopic mass conservation remains valid for both mass flow and diffusion, the derivation leads to the relationship (10), identical to A10 in Evans et al. (1986). At the leaf mesophyll scale, we consider the "input" as identical to the abaxial IAS ($i = b$), and "output" denotes the isotopically modified and CO_2 concentration-reduced adaxial IAS ($o = d$). However, to accept the analogy, we must take the intercellular air in bulk IAS as being isotopically homogeneous, with its CO_2 concentration averaging $(c_b + c_d)/2$. Then, the discrimination of the averaged IAS against "input" air ($\Delta_a = \Delta_{bd}$) relates to isotopic compositions δ as $\Delta_{bd} = [1/2(\delta_b - \delta_d)]/(1 + \delta_d)$, and the 'xi' parameter in fractionation due to carboxylation, ξ_C , is twice the previously defined ξ , i.e., $\xi_C = 2c_b/(c_b - c_d)$. Similarly, discrimination of bulk leaf tissue against $^{13}\text{CO}_2$ in IAS, Δ_L , can be expressed as $\Delta_L = [1/2(\delta_b + \delta_d)] - \delta_L/(1 + \delta_L)$. Substituting Δ_{bd} for Δ_a as well as the new Δ_L into Eq. (10) and rearrangement yields

$$(\delta_b - \delta_d)|_C = \frac{[\delta_L - \frac{1}{2}(\delta_b + \delta_d)] \cdot (2 + \delta_b + \delta_d)}{\xi_C [1 + \frac{1}{2}(\delta_b + \delta_d)]}. \tag{11}$$

The values of $\delta_b + \delta_d$ as well as of $1/2(\delta_b + \delta_d)$ are much smaller than 2 and 1, respectively, and $\delta_L - 1/2(\delta_b + \delta_d)$ is $-\Delta_L$. This allows us to simplify the relation (11):

$$(\delta_b - \delta_d)|_C = -\frac{1}{\xi} \Delta_L. \tag{12}$$

The total effect of diffusion and carboxylation on the isotopic change of CO_2 in the IAS ($\delta_b - \delta_d$) is obtained by adding up the contributions of diffusion (9) and carboxylation (12):

$$(\delta_b - \delta_d) = \frac{1}{\xi} (a - \Delta_L). \tag{13}$$

It is shown by the thick dot-dash line in Fig. 10.

Comparison of cuticles from opposite leaf sides as a proxy for changes in δ of CO₂ across the leaf

The relationship (13) does not provide any feasible way to estimate the relative CO₂ drawdown c_d/c_b ($c_d/c_b = -[(1/\xi) - 1]$) because the isotopic compositions of abaxial and adaxial intercellular air (δ_b and δ_d) cannot be measured directly. However, as mentioned above, δ_b and δ_d and the relevant concentrations are imprinted in δ of the assimilates synthesized in chloroplasts located in the respective regions of the leaf: c_b and δ_b in assimilates from near the stomatous (abaxial) epidermis, incorporated in the abaxial cuticle, and c_d and δ_d in assimilates synthesized close to the adaxial leaf side and sent to the adaxial cuticle. δ_L derives from the leaf bulk tissue. Therefore, we have tried to find a relationship between the isotopic composition of abaxial and adaxial cuticles or their waxes (δ_{AB} , δ_{AD}) and the isotopic composition and concentration of CO₂ in substomatal and palisade intercellular air (δ_b , δ_d and c_b , c_d , respectively).

¹³C discriminations imprinted in abaxial and adaxial cuticles (Δ_{AB} and Δ_{AD}) are defined as:

$$\Delta_{AB} = \frac{\delta_b - \delta_{AB}}{1 + \delta_{AB}} \tag{14a}$$

and

$$\Delta_{AD} = \frac{\delta_d - \delta_{AD}}{1 + \delta_{AD}} \tag{14b}$$

Given that the denominators are close to one, the ¹³C depletions of cuticles are approximated by the differences in the numerators. Mechanistically, the ¹³C content in cuticles can be attributed to fractionation effects during (i) CO₂ transport from the IAS to chloroplast stroma (a_w), (ii) carboxylation by Rubisco (b) and (iii) post-photosynthetic fractionation during fatty acid and wax synthesis (h). The fractionation effects (i)–(iii) are additive and the first two components depend on the CO₂ drawdown from IAS at cell wall (c_b or c_d) to the chloroplast interior (c_{cb} or c_{cd}):

$$\delta_b - \delta_{AB} = a_w \frac{c_b - c_{cb}}{c_b} + b \frac{c_{cb}}{c_b} + h \tag{15a}$$

and

$$\delta_d - \delta_{AD} = a_w \frac{c_d - c_{cd}}{c_d} + b \frac{c_{cd}}{c_d} + h. \tag{15b}$$

Equations 15a, b require the assumption that ¹³C fractionation during synthesis of cuticular compounds (h) is identical for the adaxial and abaxial leaf sides. Similarly, we will assume that the relative drawdown of CO₂ from the IAS to chloroplast stroma is not leaf side-specific ($c_{cb}/c_b = c_{cd}/c_d$, i.e., the CO₂ gradient in the cells across the leaf is homogeneous). Isotopic fractionation due to respiration and photorespiration was assumed to be negligible (Farquhar et al.

1982) and not included in Eqs. (15a), (15b); here, we may alleviate the assumption and allow this fractionation to be non-zero but identical in magnitude at opposite leaf sides. These assumptions simplify the estimation of the isotopic difference between abaxial and adaxial cuticles obtained by subtraction of Eqs. (15b) and (15a):

$$\delta_b - \delta_d = \delta_{AB} - \delta_{AD} \tag{16}$$

which yields an expression for $\delta_b - \delta_d$ alternative to that shown in Eq. (13).

Relative drawdown of CO₂ concentration in the gas phase

Substitution of Eq. (16) into (13) and rearrangement allows to factor out the $\delta_b - \delta_d$ term:

$$\delta_{AB} - \delta_{AD} = \frac{1}{\xi} (a - \Delta_L). \tag{17}$$

Rearrangement and expression of ξ in terms of CO₂ concentrations yield

$$\xi = \frac{c_b}{c_b - c_d} = \frac{a - \Delta_L}{\delta_{AB} - \delta_{AD}} \tag{18}$$

and the relative drawdown of CO₂ in the IAS, c_d/c_b , is:

$$\frac{c_d}{c_b} = 1 - \frac{\delta_{AB} - \delta_{AD}}{a - \Delta_L}. \tag{19}$$

Typically, leaf tissue is depleted in ¹³C compared to the source CO₂ (Δ has a positive value) by more than the value of a , so the term $a - \Delta_L$ is negative. We expect that the abaxial cuticle should be more depleted than the adaxial one, thus $(\delta_{AB} - \delta_{AD}) < 0$. Therefore, the second term on the right side of Eq. (19) should be positive and less than 1 and, thus, the drawdown c_d/c_b range between zero and one. The variable Δ_L represents ¹³C discrimination in bulk leaf assimilates against ¹³CO₂ in air inside the leaf. Assuming in first approximation that the IAS air is isotopically identical with ‘adaxial air’ ($\Delta_L \cong \delta_d - \delta_L$) and substituting δ_d with δ_b from (16), relation (19) can be reformulated as:

$$\frac{c_d}{c_b} = 1 - \frac{1}{1 + \frac{\delta_L - \delta_b + a}{\delta_{AB} - \delta_{AD}}}. \tag{20}$$

In a more rigorous alternative, if Δ_L is defined against ‘average’ IAS air [$\Delta_L = (\delta_{bd} - \delta_L)/(1 + \delta_L)$, where δ_{bd} is the isotopic composition of the average IAS air: $\delta_{bd} = \delta_b - 1/2(\delta_b - \delta_d) = \delta_b - 1/2(\delta_{AB} - \delta_{AD})$], Eq. (19) is transformed to the following formula:

$$\frac{c_d}{c_b} = 1 - \frac{(\delta_{AB} - \delta_{AD})(1 + \delta_L)}{(a + \delta_L)(1 + \delta_L) + \frac{1}{2}(\delta_{AB} - \delta_{AD}) - \delta_b}. \tag{21}$$

Relative drawdown of CO₂ concentration in the liquid phase

In analogy to Eq. (15), we can write for the discrimination in mesophyll cells against ¹³CO₂ in the IAS with the mean concentration $c_{bd} = 1/2(c_b + c_d)$ and ¹³C abundance $\delta_{bd} = 1/2(\delta_b + \delta_d)$:

$$\delta_{bd} - \delta_L = a_w \cdot \left(1 - \frac{c_c}{c_{bd}} \right) + b \frac{c_c}{c_{bd}}, \tag{22}$$

where a_w is the combined fractionation factor for CO₂ dissolution (1.2‰) and diffusion (0.6‰) in cell walls and cell interior ($a_w = 1.8‰$). Rearrangement yields the expression that we have used in assessment of the CO₂ drawdown in the cellular liquid phase, c_c/c_{bd} , in C₃ plants:

$$\frac{c_c}{c_{bd}} = \frac{\Delta_L - a_w}{b - a_w}, \tag{23}$$

where $\Delta_L = (\delta_{bd} - \delta_L)/(1 + \delta_L)$ and $\delta_{bd} = \delta_b - 1/2(\delta_{AB} - \delta_{AD})$. Finally, c_c/c_{bd} can be expressed in terms of δ_L , $(\delta_{AB} - \delta_{AD})$ and δ_b as:

$$\frac{c_c}{c_{bd}} = \frac{\delta_b - \delta_L - a_w(1 + \delta_L) - 0.5(\delta_{AB} - \delta_{AD})}{(b - a_w)(1 + \delta_L)}. \tag{24}$$

The magnitude of δ_b in Eqs. (21) and (24) may be approximated by evaluating the isotopic effect of CO₂ diffusion from ambient air at the leaf surface into substomatal cavities as $\delta_b = \delta_a - a(1 - c_i/c_a)$. Values of -8.0‰, 4.4‰ and 0.75 were used for δ_a , a and c_i/c_a , respectively, which yields $\delta_b = -9.1‰$ as the value typical for C₃ plants. It should be noted that the relations (21) and (24) are derived for δ and isotope fractionation factors expressed in fractional notation (values add up to 1). For calculations in per mille, the term $(1 + \delta_L)$ has to be substituted by $(1 + \delta_L/1000)$.

Partitioning of mesophyll conductance

Net photosynthesis rate integrated over the intracellular pathways across the leaf profile can be expressed in an alternative form to Eq. (7) as

$$A = g_{liq}(c_{bd} - c_c). \tag{25}$$

Resistances (the inverse values of conductances) for diffusion of CO₂ in the IAS (r_{IAS}), the cell interior (r_{liq}) and the whole mesophyll (r_m) are

$$r_{IAS} = \frac{c_b - c_d}{A}, \tag{26a}$$

$$r_{liq} = \frac{c_{bd} - c_c}{A}, \tag{26b}$$

$$r_m = r_{IAS} + r_{liq} \tag{26c}$$

which, provided that c_b and c_{bd} are not far apart, yields the relative portion of IAS in total mesophyll diffusion resistance or conductance (r_{IAS}/r_m and g_{IAS}/g_m):

$$\frac{r_{IAS}}{r_m} \cong \frac{1}{1 + \frac{1 - \frac{c_c}{c_{bd}}}{1 - \frac{c_d}{c_b}}}, \tag{27a}$$

$$\frac{g_{IAS}}{g_m} \cong 1 + \frac{1 - \frac{c_c}{c_{bd}}}{1 - \frac{c_d}{c_b}}. \tag{27b}$$

The analog expressions for the cellular (liquid) path are:

$$\frac{r_{liq}}{r_m} \cong \frac{1}{1 + \frac{1 - \frac{c_d}{c_b}}{1 - \frac{c_c}{c_{bd}}}}, \tag{28a}$$

$$\frac{g_{liq}}{g_m} \cong 1 + \frac{1 - \frac{c_d}{c_b}}{1 - \frac{c_c}{c_{bd}}}. \tag{28b}$$

References

Aalto T, Juurola E (2002) A three-dimensional model of CO₂ transport in airspaces and mesophyll cells of a silver birch leaf. *Plant Cell Environ* 25(11):1399–1409. <https://doi.org/10.1046/j.0016-8025.2002.00906.x>

Buschhaus C, Jetter R (2011) Composition differences between epicuticular and intracuticular wax substructures: how do plants seal their epidermal surfaces? *J Exp Bot* 62(3):841–853. <https://doi.org/10.1093/jxb/erq366>

Cernusak LA, Ubierna N, Winter K, Holtum JAM, Marshall JD, Farquhar GD (2013) Environmental and physiological determinants of carbon isotope discrimination in terrestrial plants. *N Phytol* 200(4):950–965. <https://doi.org/10.1111/nph.12423>

Chikaraishi Y, Naraoka H (2001) Organic hydrogen–carbon isotope signatures of terrestrial higher plants during biosynthesis for distinctive photosynthetic pathways. *Geochem J* 35(6):451–458. <https://doi.org/10.2343/geochemj.35.451>

Chikaraishi Y, Naraoka H (2003) Compound-specific delta D-delta C-13 analyses of n-alkanes extracted from terrestrial and aquatic plants. *Phytochemistry* 63(3):361–371. [https://doi.org/10.1016/S0031-9422\(02\)00749-5](https://doi.org/10.1016/S0031-9422(02)00749-5)

Chikaraishi Y, Naraoka H, Poulson SR (2004) Hydrogen and carbon isotopic fractionations of lipid biosynthesis among terrestrial (C₃, C₄ and CAM) and aquatic plants. *Phytochemistry* 65(10):1369–1381. <https://doi.org/10.1016/j.phytochem.2004.03.036>

Evans JR, Sharkey TD, Berry JA, Farquhar GD (1986) Carbon isotope discrimination measured concurrently with gas-exchange to investigate CO₂ diffusion in leaves of higher plants. *Aust J Plant Physiol* 13(2):281–292

Evans JR, Kaldenhoff R, Genty B, Terashima I (2009) Resistances along the CO₂ diffusion pathway inside leaves. *J Exp Bot* 60(8):2235–2248. <https://doi.org/10.1093/jxb/erp117>

- Farquhar GD, Lloyd J (1993) Carbon and oxygen isotope effects in the exchange of carbon dioxide between terrestrial plants and the atmosphere. In: Ehleringer JR, Hall AE, Farquhar GD (eds) Stable isotopes and plant carbon–water relations. Academic, San Diego, pp 47–70
- Farquhar GD, Richards RA (1984) Isotopic composition of plant carbon correlates with water-use efficiency of wheat genotypes. *Aust J Plant Physiol* 11(6):539–552
- Farquhar GD, O'Leary MH, Berry JA (1982) On the relationship between carbon isotope discrimination and the intercellular carbon dioxide concentration in leaves. *Aust J Plant Physiol* 9(2):121–137
- Farquhar GD, Ehleringer JR, Hubick KT (1989) Carbon isotope discrimination and photosynthesis. *Annu Rev Plant Physiol Plant Mol Biol* 40:503–537
- Flexas J, Ribas-Carbo M, Diaz-Espejo A, Galmes J, Medrano H (2008) Mesophyll conductance to CO₂: current knowledge and future prospects. *Plant Cell Environ* 31(5):602–621. <https://doi.org/10.1111/j.1365-3040.2007.01757.x>
- Flexas J, Barbour MM, Brendel O, Cabrera HM, Carriqui M, Diaz-Espejo A, Douthe C, Dreyer E, Ferrio JP, Gago J, Galle A, Galmes J, Kodama N, Medrano H, Niinemets U, Peguero-Pina JJ, Pou A, Ribas-Carbo M, Tomas M, Tosens T, Warren CR (2012) Mesophyll diffusion conductance to CO₂: an unappreciated central player in photosynthesis. *Plant Sci* 193:70–84. <https://doi.org/10.1016/j.plantsci.2012.05.009>
- Gao L, Burnier A, Huang YS (2012) Quantifying instantaneous regeneration rates of plant leaf waxes using stable hydrogen isotope labeling. *Rapid Commun Mass Spectrom* 26(2):115–122. <https://doi.org/10.1002/rcm.5313>
- Hassiotou F, Ludwig M, Renton M, Veneklaas EJ, Evans JR (2009) Influence of leaf dry mass per area, CO₂, and irradiance on mesophyll conductance in sclerophylls. *J Exp Bot* 60(8):2303–2314. <https://doi.org/10.1093/jxb/erp021>
- Hobbie EA, Werner RA (2004) Intramolecular, compound-specific, and bulk carbon isotope patterns in C-3 and C-4 plants: a review and synthesis. *N Phytol* 161(2):371–385. <https://doi.org/10.1111/j.1469-8137.2004.00970.x>
- Jeffree CE (2006) The fine structure of the plant cuticle. In: Riederer M, Muller C (eds) *Biology of the plant cuticle*. Blackwell Publishing Ltd., Oxford, pp 11–125
- Jetter R, Schaffer S (2001) Chemical composition of the *Prunus laurocerasus* leaf surface. Dynamic changes of the epicuticular wax film during leaf development. *Plant Physiol* 126(4):1725–1737. <https://doi.org/10.1104/pp.126.4.1725>
- Kerstiens G (1996) Cuticular water permeability and its physiological significance. *J Exp Bot* 47(305):1813–1832. <https://doi.org/10.1093/jxb/47.12.1813>
- Körner C (1999) *Alpine plant life*. Springer, Berlin
- Kunst L, Samuels AL (2003) Biosynthesis and secretion of plant cuticular wax. *Prog Lipid Res* 42(1):51–80. [https://doi.org/10.1016/s0163-7827\(02\)00045-0](https://doi.org/10.1016/s0163-7827(02)00045-0)
- Lawson T, Morison J (2006) Visualising patterns of CO₂ diffusion in leaves. *N Phytol* 169(4):641–643. <https://doi.org/10.1111/j.1469-8137.2006.01655.x>
- Lloyd J, Syvertsen JP, Kriedemann PE, Farquhar GD (1992) Low conductances for CO₂ diffusion from stomata to the sites of carboxylation in leaves of woody species. *Plant Cell Environ* 15(8):873–899. <https://doi.org/10.1111/j.1365-3040.1992.tb01021.x>
- Mackova J, Vaskova M, Macek P, Hronkova M, Schreiber L, Sant-rucek J (2013) Plant response to drought stress simulated by ABA application: changes in chemical composition of cuticular waxes. *Environ Exp Bot* 86:70–75. <https://doi.org/10.1016/j.envexpbot.2010.06.005>
- Maxwell K, von Caemmerer S, Evans JR (1997) Is a low internal conductance to CO₂ diffusion a consequence of succulence in plants with crassulacean acid metabolism? *Aust J Plant Physiol* 24(6):777–786. <https://doi.org/10.1071/pp97088>
- Muir CD (2015) Making pore choices: repeated regime shifts in stomatal ratio. *Proc R Soc B*. <https://doi.org/10.1098/rspb.2015.1498>
- Muir CD, Hangarter RP, Moyle LC, Davis PA (2014) Morphological and anatomical determinants of mesophyll conductance in wild relatives of tomato (*Solanum* sect. *Lycopersicon*, sect. *Lycopersicoideae*; Solanaceae). *Plant Cell Environ* 37(6):1415–1426. <https://doi.org/10.1111/pce.12245>
- Niinemets U, Diaz-Espejo A, Flexas J, Galmes J, Warren CR (2009) Role of mesophyll diffusion conductance in constraining potential photosynthetic productivity in the field. *J Exp Bot* 60(8):2249–2270. <https://doi.org/10.1093/jxb/erp036>
- Parkhurst DF (1994) Diffusion of CO₂ and other gases inside leaves. *N Phytol* 126(3):449–479. <https://doi.org/10.1111/j.1469-8137.1994.tb04244.x>
- Parkhurst DF, Mott KA (1990) Intercellular diffusion limits to CO₂ uptake in leaves. *Plant Physiol* 94(3):1024–1032
- Pieruschka R, Schurr U, Jensen M, Wolff WF, Jahnke S (2006) Lateral diffusion of CO₂ from shaded to illuminated leaf parts affects photosynthesis inside homobaric leaves. *N Phytol* 169(4):779–787. <https://doi.org/10.1111/j.1469-8137.2005.01605.x>
- Pons TL, Flexas J, von Caemmerer S, Evans JR, Genty B, Ribas-Carbo M, Brugnoli E (2009) Estimating mesophyll conductance to CO₂: methodology, potential errors, and recommendations. *J Exp Bot* 60(8):2217–2234. <https://doi.org/10.1093/jxb/erp081>
- Ramirez-Valiente JA, Sanchez-Gomez D, Aranda I, Valladares F (2010) Phenotypic plasticity and local adaptation in leaf eco-physiological traits of 13 contrasting cork oak populations under different water availabilities. *Tree Physiol* 30(5):618–627. <https://doi.org/10.1093/treephys/tpq013>
- Rumman R, Atkin OK, Bloomfield KJ, Eamus D (2018) Variation in bulk-leaf C-13 discrimination, leaf traits and water-use efficiency–trait relationships along a continental-scale climate gradient in Australia. *Glob Change Biol* 24(3):1186–1200. <https://doi.org/10.1111/gcb.13911>
- Schaufele R, Santrucek J, Schnyder H (2011) Dynamic changes of canopy-scale mesophyll conductance to CO₂ diffusion of sunflower as affected by CO₂ concentration and abscisic acid. *Plant Cell Environ* 34(1):127–136. <https://doi.org/10.1111/j.1365-3040.2010.02230.x>
- Schönherr J, Riederer M (1986) Plant cuticles sorb lipophilic compounds during enzymatic isolation. *Plant Cell Environ* 9(6):459–466. <https://doi.org/10.1111/j.1365-3040.1986.tb01761.x>
- Schreiber L (2010) Transport barriers made of cutin, suberin and associated waxes. *Trends Plant Sci* 15(10):546–553. <https://doi.org/10.1016/j.tplants.2010.06.004>
- Schreiber L, Riederer M (1996) Ecophysiology of cuticular transpiration: comparative investigation of cuticular water permeability of plant species from different habitats. *Oecologia* 107(4):426–432. <https://doi.org/10.1007/bf00333931>
- Sharkey TD, Imai K, Farquhar GD, Cowan IR (1982) A direct confirmation of the standard method of estimating intercellular partial pressure of CO₂. *Plant Physiol* 69(3):657–659. <https://doi.org/10.1104/pp.69.3.657>
- Tholen D, Ethier G, Genty B, Pepin S, Zhu XG (2012) Variable mesophyll conductance revisited: theoretical background and experimental implications. *Plant Cell Environ* 35(12):2087–2103. <https://doi.org/10.1111/j.1365-3040.2012.02538.x>
- Tipple BJ, Ehleringer JR (2018) Distinctions in heterotrophic and autotrophic-based metabolism as recorded in the hydrogen and carbon isotope ratios of normal alkanes. *Oecologia* 187(4):1053–1075. <https://doi.org/10.1007/s00442-018-4189-0>
- Tomas M, Flexas J, Copolovici L, Galmes J, Hallik L, Medrano H, Ribas-Carbo M, Tosens T, Vislap V, Niinemets U (2013)

- Importance of leaf anatomy in determining mesophyll diffusion conductance to CO₂ across species: quantitative limitations and scaling up by models. *J Exp Bot* 64(8):2269–2281. <https://doi.org/10.1093/jxb/ert086>
- Tominaga J, Shimada H, Kawamitsu Y (2018) Direct measurements solves overestimation of intercellular CO₂ concentration in leaf gas-exchange measurements. *J Exp Bot*. <https://doi.org/10.1093/jxb/ery044>
- von Caemmerer S, Farquhar GD (1981) Some relationships between the biochemistry of photosynthesis and the gas-exchange of leaves. *Planta* 153(4):376–387. <https://doi.org/10.1007/bf00384257>
- Vrabl D, Vaskova M, Hronkova M, Flexas J, Santrucek J (2009) Mesophyll conductance to CO₂ transport estimated by two independent methods: effect of variable CO₂ concentration and abscisic acid. *J Exp Bot* 60(8):2315–2323. <https://doi.org/10.1093/jxb/erp115>
- Warren CR (2008) Stand aside stomata, another actor deserves centre stage: the forgotten role of the internal conductance to CO₂ transfer. *J Exp Bot* 59(7):1475–1487. <https://doi.org/10.1093/jxb/erm245>
- Warren CR, Low M, Matyssek R, Tausz M (2007) Internal conductance to CO₂ transfer of adult *Fagus sylvatica*: variation between sun and shade leaves and due to free-air ozone fumigation. *Environ Exp Bot* 59(2):130–138. <https://doi.org/10.1016/j.envexpbot.2005.11.004>
- Xiao Y, Zhu X-G (2017) Components of mesophyll resistance and their environmental responses: a theoretical modelling analysis. *Plant Cell Environ* 40(11):2729–2742. <https://doi.org/10.1111/pce.13040>
- Yeats TH, Rose JKC (2013) The formation and function of plant cuticles. *Plant Physiol* 163(1):5–20. <https://doi.org/10.1104/pp.113.222737>
- Zhou YP, Stuart-Williams H, Grice K, Kayler ZE, Zavadlav S, Vogts A, Rommerskirchen F, Farquhar GD, Gessler A (2015) Allocate carbon for a reason: priorities are reflected in the C-13/C-12 ratios of plant lipids synthesized via three independent biosynthetic pathways. *Phytochemistry* 111:14–20. <https://doi.org/10.1016/j.phytochem.2014.12.005>

Publisher's Note Springer Nature remains neutral with regard to jurisdictional claims in published maps and institutional affiliations.

Article II

¹³CO₂ labelling as a tool for elucidating the mechanism of cuticle development: a case of *Clusia rosea*

Kubásek J; Kalistová T, Janová J; Askanbayeva B; Bednár J; Santrucek J
(2023).

New Phytologist **238**, 202-215. DOI: 10.1111/nph.18716

^{13}C labelling as a tool for elucidating the mechanism of cuticle development: a case of *Clusia rosea*

Jiří Kubásek¹ , Tereza Kalistová¹ , Jitka Janová¹ , Balzhan Askanbayeva¹, Jan Bednár² and Jiří Šantrůček¹ ¹Department of Experimental Plant Biology, Faculty of Science, University of South Bohemia, Branišovská 1760/31, České Budějovice, Czech Republic; ²Department of Ecosystem Biology, Faculty of Science, University of South Bohemia, Branišovská 1760/31, České Budějovice, Czech Republic

Summary

Author for correspondence:
Jiří Kubásek
Email: jirkak@prf.jcu.czReceived: 10 October 2022
Accepted: 22 December 2022New Phytologist (2023) 238: 202–215
doi: 10.1111/nph.18716**Key words:** ^{13}C labelling, cutin, development, gas exchange, photosynthesis, plant cuticle, wax regeneration.

- The plant cuticle is an important plant-atmosphere boundary, the synthesis and maintenance of which represents a significant metabolic cost. Only limited information regarding cuticle dynamics is available.
- We determined the composition and dynamics of *Clusia rosea* cuticular waxes and matrix using ^{13}C labelling, compound-specific and bulk isotope ratio mass spectrometry. Collodion was used for wax collection; gas exchange techniques to test for any collodion effects on living leaves.
- Cutin matrix (MX) area density did not vary between young and mature leaves and between leaf sides. Only young leaves incorporated new carbon into their MX. Collodion-based sampling discriminated between epicuticular (EW) and intracuticular wax (IW) effectively. Epicuticular differed in composition from IW. The newly synthesised wax was deposited in IW first and later in EW. Both young and mature leaves synthesised IW and EW. The faster dynamics in young leaves were due to lower wax coverage, not a faster synthesis rate. Longer-chain alkanes were deposited preferentially on the abaxial, stomatous leaf side, producing differences between leaf sides in wax composition.
- We introduce a new, sensitive isotope labelling method and demonstrate that cuticular wax is renewed during leaf ontogeny of *C. rosea*. We discuss the ecophysiological significance of the new insights.

Introduction

The plant cuticle is a multifunctional, hydrophobic biofilm covering aboveground plant surfaces (Riederer & Müller, 2006) and, remarkably, recently found also on the root cap (Berhin *et al.*, 2019). With an overall thickness of only $c.1\ \mu\text{m}$ in mesophytic leaves (Jeffree, 2018), its excellent gas barrier properties and self-cleaning ability have fascinated plant scientists and bio-engineers for many decades (Skoss, 1955; Barthlott & Neinhuis, 1997; Fernández *et al.*, 2017). Modern cuticles serve not only as a barrier but also as a communication interface between plants and their environment, as well as a developmental regulator; however, cuticles very probably arose primarily to aid plants' transition from water to land, by limiting uncontrolled water loss, *c.* 450 million years ago (Kerstiens, 1996b; Niklas *et al.*, 2017; Kong *et al.*, 2020). In concert with gas-filled intercellular spaces (ICSs) and adjustable gas valves – stomata – the cuticle enabled homoiohydric (i.e. decoupling of plant water regime from the external water potential) in plant sporophytes spanning from moss capsules to the biggest trees. Homoiohydricity was hypothesised to be a prerequisite of large plant size and high productivity (Proctor & Tuba, 2002) and thus to support the rich metazoan life including humanity.

A thin (rudimental) cuticle was found on many bryophyte gametophytes (where no stomata and ICSs are present) without any clear function (Matos *et al.*, 2021). On the contrary, moss sporophytes (Budke & Goffinet, 2016; Kubásek *et al.*, 2021) and vascular plant leaves and stems as well as various flower organs and fruits bear well-formed cuticles with very low conductance to water and CO_2 diffusion (Woolley, 1967; Boyer, 2015). Many studies measured environmental dependencies of cuticle properties (Baker, 1974; Kerstiens, 1996a, 1997). Increased relative air humidity (Schönherr & Schmidt, 1979; Schreiber *et al.*, 2001) and temperature (Riederer & Schreiber, 2001) have been found to increase cuticle conductance, but no correlation between this conductance and cuticle thickness, structure or composition has been found in large sets of plant species (Kerstiens, 1996b; Hauke & Schreiber, 1998; Riederer & Schreiber, 2001; Zeisler-Diehl *et al.*, 2017).

Even though the plant cuticle was studied as early as 1830 by Brongniart (Skoss, 1955), much remains still unknown. The fine structure of the plant cuticle is complex and variable (Jeffree, 2018). A simplified view distinguishes a polyester cutin matrix (MX), which consists of covalently bound C16, C18 hydroxy-fatty acids (and their derivatives), glycerol and phenolics, forming a 3D scaffold (Fich *et al.*, 2016). The MX is

impregnated with a variety of aliphatic and cyclic lipids (intracuticular wax, IW) and covered by a purely lipidic layer on the uppermost cuticle surface (epicuticular wax, EW; Haas & Rentschler, 1984; Jetter & Schäffer, 2001). Many plant species also incorporate cutan (nonester bound moieties) into their MX, and almost all species studied so far also accommodate various nonlipidic molecules (e.g. flavanols and phenolics) in small to dominant proportions (Karabourniotis *et al.*, 2001; Jetter *et al.*, 2018; Kong *et al.*, 2020). Waxes may be largely extracted using organic solvents (e.g. chloroform), and their removal leads to an increase in cuticular permeability for water by two or three orders of magnitude (Schönherr & Schmidt, 1979). The ultrastructure of the cuticle is even more complex. Cuticle proper, the outermost cutin-rich layer, descending from the embryonal procuticle, and cuticle layer, the polysaccharide-rich fraction in contact with the epidermal cell wall, are well-recognisable via transmission electron microscopy (TEM) in many plant species. Moreover, electron-lucent vs electron-dense micro-domains may be found in each layer (Jetter *et al.*, 2000; Jeffree, 2018). Traditionally, the cuticle is considered as a distinct layer on the epidermis since it may be isolated enzymatically (Skoss, 1955; Vráblová *et al.*, 2020). A more recent view, however, perceives a continuum of cell wall and cuticle (Guzmán *et al.*, 2014; Fernández *et al.*, 2016).

We currently have nearly complete pictures of the biosynthesis of many cuticle compounds (cutin monomers, triterpenes and phenolics), although restricted to several model species, for example *Arabidopsis* (Wen & Jetter, 2009; Bernard & Joubès, 2013; Wang *et al.*, 2020), tomato (Yeats *et al.*, 2012) or maize (Petit *et al.*, 2017). Much less is known, for example, about cutin monomer export and polymerisation (Fich *et al.*, 2016; Niklas *et al.*, 2017), lipid export to the apoplast (Pighin *et al.*, 2004; Panikashvili *et al.*, 2011) and assembly of the functional cuticle (Samuels *et al.*, 2008; Bourgault *et al.*, 2020; Seale, 2020).

Probably, the scarcest domain in our current understanding is cuticle dynamics. Gas chromatography – mass spectrometry revealed that the total wax amount and its composition change during the development of leaves or other organs (Hauke & Schreiber, 1998; Jetter *et al.*, 2018) and that IW and EW may be chemically distinct (Jetter & Schäffer, 2001). Changes in environmental factors and internal plant signalling are known to affect the cuticle quickly (Skoss, 1955; Baker, 1974; Koch *et al.*, 2004). For instance, just 7 d of irrigating *Lepidium sativum* seedlings with 10^{-4} M abscisic acid (ABA) led to a shift in cuticular wax to compounds with longer chains (Macková *et al.*, 2013). Atomic force microscopy and scanning electron microscopy have also proved useful for the study of EW regeneration (Neinhuis *et al.*, 2001; Koch *et al.*, 2004), revealing distinct groups of plants that differ in their ability to regenerate their EW (Neinhuis *et al.*, 2001).

Surprisingly, stable isotope labelling techniques have only been used in a few cuticular studies so far. Mostly, a heavy water (D_2O) irrigation approach was applied with the aim to detect whether and how fast cuticle components are renewed (Kahmen *et al.*, 2011; Gao *et al.*, 2012). However, the results remain controversial. It is not clear whether wax is deposited during the whole

leaf lifespan, as shown previously (Sachse *et al.*, 2009; Gao *et al.*, 2012), or only early in leaf ontogeny (Flore & Bukovac, 1974; Kahmen *et al.*, 2011). Compound-specific analyses revealed that turnover of cuticular fatty acids (C16 and C18) is much faster (2–3 d) than the turnover of long-chain lipids (5–128 d; Gao *et al.*, 2012). This may be the result of a noncuticular origin of those fatty acids (see the Discussion section). The dynamics of cutin MX and various wax compounds remain unknown.

The above-mentioned gaps are often related to the methods applied. Whole-leaf immersion in solvents (Medina *et al.*, 2004) and/or extraction of total leaf lipids may yield biased results with respect to the genuine lipid spectra of the cuticle. The GC–MS separation techniques may distinguish cuticular compounds thereafter, but their origin – IW, EW or lipids still present in ER of epidermal cells – cannot be distinguished. EW and IW, thus, we sampled separately, using selective techniques.

Clusiaceae is a tropical family of some 37 genera and 1610 species (very close to *Hypericaceae*) in the big order Malpighiales (Gustafsson *et al.*, 2002). Physiological and cuticular studies exist for many species in the genus *Clusia* (Medina *et al.*, 2004, 2006; Lüttge, 2008). There is a tendency for environmentally induced CAM metabolism in most *Clusia* species (Lüttge, 2008). *Clusia rosea* Jacq. is nowadays frequently cultivated in glasshouses and grown in frost-free outdoor sites world-wide. We chose this species for five reasons: (1) it grows vigorously and CO_2 assimilation is substantial under optimal conditions; (2) leaves are large, relatively thick and EW may be sampled easily without damage to the leaf; (3) leaves are hypostomatous and so, stomatous abaxial and astomatous adaxial cuticles may be compared; (4) wax composition is well-defined with several compounds prevailing in the total wax (Medina *et al.*, 2004, 2006); and (5) the cuticles may be isolated enzymatically and IW extracted subsequently.

Our aim was to reveal age-dependent and side-specific dynamics of the main cuticular wax compounds and the cutin matrix. We identified and quantified dominant EW and IW compounds in young and mature leaves of *Clusia rosea*, separately for adaxial and abaxial cuticles. We used the $^{13}CO_2$ pulse-chase approach to follow dynamics of deposition of the major wax compounds in EW, IW and cutin matrix. Methodologically, we tested the ability of collodion solution to discriminate between EW and IW. The impact of collodion treatment on leaf gas exchange and stomatal behaviour was also evaluated.

Materials and Methods

Plant material

Commercially obtained plants of autograph tree (*Clusia rosea* Jack.) were grown in a glasshouse (University of South Bohemia, České Budějovice, 48°58'40.5"N, 14°26'44.6"E) for 2 yr before the experiments. Temperature was maintained between 20 and 26°C during the day and at least 18°C at night. Relative humidity was 50–80%. The natural photoperiod at the time of the experiment (February to March 2020, *c.* 12 h) was extended to *c.* 16 h using metal halide high-pressure lamps with PPFD at *c.* 150 μmol photons $m^{-2} s^{-1}$.

¹³CO₂ Labelling and sampling strategy

Four plants (*c.* 30 cm tall) were transferred to a gas-tight Plexiglas box (internal dimensions were 60 × 60 × 60 cm and volume 190 l) for 2 h of assimilation in a ¹³CO₂-enriched atmosphere (Supporting Information Fig. S1). A fan inside the box reduced the resistance of the boundary layer. The box was placed in a cultivating room where the temperature was maintained at 20°C. PPF irradiation of *c.* 400 μmol photons m⁻² s⁻¹ was supplied by linear LED sources, two units above and two more on each side of the box, to achieve the most homogeneous light possible (see Fig. S2 for spectral output). At the beginning, we let the open box equilibrate with the atmosphere of the room. After a few minutes, steady state was reached, the box was hermetically sealed, and *c.* 95 ml of ¹³CO₂ (> 99% atoms, Sigma-Aldrich) was injected through a septum in the box wall, yielding *c.* 800 μmol CO₂ mol⁻¹ (twice the ambient level and about half of which is ¹³CO₂). The plants assimilated CO₂ for 2 h. Every 30 min, the box was opened, a new equilibrium was reached, and new ¹³CO₂ applied after closure. We previously found that the same plants were able to reduce the CO₂ concentration inside by *c.* 30% within 30 min (using a 6400XT unit; Li-Cor, Lincoln, NE, USA, and isotopically normal CO₂). After 2 h, the plants were transferred back to the glasshouse for the remainder of the experiment.

The overall sampling design was as follows: one young, more or less fully expanded leaf from the current year and one mature leaf from the previous year (typical projected leaf area 30–60 cm²) were collected from each plant before labelling (*t* = 0), immediately thereafter (*t* = 2 h), and 12, 24, 48, 96, 168 (1 wk), 336 (2 wk) and 504 h (3 wk) later. Epicuticular wax (EW) was removed separately from the adaxial and abaxial surfaces immediately after leaf excision (see below). One 2-cm-diameter disc (3.14 cm²) was then cut and dried at 80°C for 12 h to obtain dry mass, and two to four discs of the same size (depending on leaf area) were cut to isolate the cuticle. All this work was carried out within 1 h of harvest. Finally, the rest of the leaves were placed in a freezer (−80°C) for subsequent analysis of water-soluble compounds as a putative source for lipid biosynthesis.

Isolation of epicuticular and intracuticular waxes and wax-free cuticular matrices

Epicuticular wax was removed from each side of the leaf using a collodion solution (Haas & Rentschler, 1984) applied with a fine brush in two successive applications. The strips were peeled off after polymerisation (*c.* 1 min) and extracted in 4 ml of *n*-hexane in 20-ml scintillation vials on a roller overnight at room temperature (*n*-hexane was found to have comparable efficiency in extracting various compounds from collodion but not from cuticle, where chloroform was more efficient). It was then concentrated by evaporation under a gentle stream of air to 1 ml and transferred to 2-ml chromatographic vials for GC-IRMS analyses. The two strips from each side were able to remove *c.* 90% of the EW in the pilot experiment (Fig. S3), and we therefore chose

this protocol as a good compromise between efficiency and leaf damage. Two to four discs 2 cm in diameter were punched from EW-free leaves, and the cuticle was isolated enzymatically in a 2% mixture of cellulase and pectinase (Schönherr & Riederer, 1986). Isolated cuticles were separated into adaxial and abaxial ones (using a microscope), and IW was extracted in 1 ml chloroform in 2-ml vials at room temperature on a roller overnight. Then, the wax-free cuticular matrices (MX) were removed, dried, weighed (using a Mettler Toledo MT5 microbalance, Columbus, OH, USA) and analysed for ¹³C content using an elemental analyzer (Flash 2000; Thermo, Bremen, Germany) coupled to isotope MS (Delta XL; Thermo).

Gas chromatography, mass spectrometry and stable isotope analyses

The EW and IW extracts obtained with collodion were analysed on a gas chromatograph (Trace 1310; Thermo). A Restek Rxi-5MS-Sil column (30 m × 0.25 mm × 0.25 μm film thickness) was used, and the flow rate was 1.5 ml min⁻¹ of helium as carrier gas. The injection (at 300°C) was splitless for 1.5 min, then split flow at 100 ml min⁻¹ for another 1 min and 5 ml min⁻¹ for the rest of the time (gas saver). The oven temperature programme was set to 50°C during injection and for the following 2 min, then increased with a gradient of 40°C min⁻¹ to 200°C, then at 4°C min⁻¹ to 310°C, and was isothermal at 310°C for the rest of the analysis (*c.* 55 min in total). To maintain isotopic fidelity and avoid introducing additional isotopic noise, we chose to measure nonderivatised samples. The eluting compounds were oxidised to CO₂ via IsoLink II interphase (Thermo) at 1000°C and introduced into a continuous flow isotope ratio MS (Delta V Advantage; Thermo). The internal standard *n*-tetracosane (C24 alkane) calibrated at ¹³C against VPDB was added to the samples at a concentration of 10 or 20 μg ml⁻¹ to quantify the compounds and check for isotope shifts and/or potential memory effects. In addition, a GC calibration curve was developed for C10–C40 alkanes to correct for the decrease in GC sensitivity in high-boiling compounds. Finally, isotopic consistency across different carbon chain lengths was monitored using Arndt Schimmelmann's A7 isotope mixture of C16–C30 *n*-alkanes (Schimmelmann *et al.*, 2016). For compound identification, the same set-up and a capillary column with a GC-APCI-MS system (456-GC + Compact QToF; Bruker Daltonics; Billerica, MA, USA) were used. Compounds were identified using available standards and/or accurate molecular fragment masses. We also measured a subset of derivatised samples of both EW and IW from young and mature leaves (50 μl BSTFA + 100 μl pyridine, 2 h at 80°C; Hauke & Schreiber, 1998). Epicuticular wax did not contain additional compounds in substantial amounts (< 1% of total peak area), whereas IW of young leaves revealed some primary alcohols.

Isolation and measurement of water-soluble leaf carbon

To obtain the ¹³C content of the metabolically active pool, we isolated the water-soluble organic fraction of the leaves. Leaves

stored in a deep freezer (-80°C) were thawed, dried and homogenised to a fine powder using a ball mill (MM400; Retsch, Haan, Germany). Approximately 100 mg of this powder was mixed with 1 ml of deionised water, sonicated at room temperature for 2 h at 80°C and finally centrifuged at 10 000 g for 10 min. The supernatant was gently dropped into tin capsules and left to evaporate until the required dry weight (DW; *c.* 100 μg) was obtained. Samples were analysed for ^{13}C content by combustion using an elemental analyzer (Flash 2000; Thermo) coupled to isotope ratio MS (Delta XL; Thermo).

Gas exchange measurements before and after collodion treatment

Water and CO_2 exchange was measured separately for the adaxial and abaxial side of the leaf using two Li-6400XT units (Li-Cor, Lincoln, NE, USA) arranged 'in tandem' (see Fig. S4 for more details on the set-up of the two Li-6400XT units). Ambient conditions in the leaf chamber were as follows: 25°C , 400 $\mu\text{mol mol}^{-1}$ CO_2 and 40% to 60% relative humidity. A leaf acclimated in the dark for 1 h was placed in the leaf chamber. After a few minutes in the dark (to reach the steady state of the system), the light was switched to 1000 $\mu\text{mol m}^{-2}\text{s}^{-1}$, and CO_2 assimilation and stomatal conductance were recorded each 10 s for 1 h, separately for the adaxial and abaxial side. The leaf was then removed from the chamber and both sides treated with collodion as mentioned above. Gas exchange measurements were repeated on the same leaf *c.* 24 h later (Fig. S5).

Calculation of wax deposition and statistics

^{13}C excess (At%) of any particular labelled compound or structure is defined as the difference between the ^{13}C content after and before labelling. The variability in the natural content of ^{13}C in lipid substances (1.063 ± 0.003 At%) was small in comparison with the labelling-induced range (up to 1.5 At%), which ensured high sensitivity of the method.

We measured ^{13}C excess in water-soluble leaf carbon (SolC) as a proxy of the metabolic pool used in the synthesis of cutin and wax precursors (SolC values are able to even out differences between leaves in their labelling intensity over time).

Then, new wax deposition (NWD, $\mu\text{g cm}^{-2}$) may be calculated as:

$$\text{NWD} = \frac{{}^{13}\text{C compound excess} \times \text{compound mass per unit leaf surface}}{{}^{13}\text{C excess in SolC}}$$

Eqn 1

Statistical significance was tested using one-way or two-way factorial ANOVA followed by Tukey's *post hoc* HSD test. When normality and/or homoskedasticity (Shapiro–Wilks test) was violated (typically for EW wax load), a logarithmic transformation was used and log-transformed data tested instead.

Results

Leaf and cuticle characteristics

Leaf area was *c.* 35% smaller and stomatal density 27% greater in young leaves than in mature leaves, indicating an ongoing slight expansion of young leaves. Epicuticular wax formed 'flocs' on the leaf surface visible by cryo-SEM (Fig. 1). The amount of collodion-collected EW varied considerably and had a strongly and positively skewed distribution (Table 1; Fig. S6). Young leaves had a much lower EW load (0.20–0.41–1.58 $\mu\text{g cm}^{-2}$ (q25%–median–q75%, $n = 144$)) than mature leaves (3.1–7.4–27.7 $\mu\text{g cm}^{-2}$). Thus, mature leaves accumulate at least one order of magnitude more EW. EW-free cuticles had an area density of $329 \pm 110 \mu\text{g cm}^{-2}$, which may represent a thickness of *c.* 3.0 μm , assuming a mass density of 1.1 g cm^{-3} (Onoda *et al.*, 2012; Tsubaki *et al.*, 2012). Cutin matrix area density fitted well to Gaussian, and neither leaf age nor side had a significant effect (ANOVA, $F(1, 132) = 0.518$, $P = 0.472$, $n = 134$). The IW extracted from a subset of isolated cuticles accounted for *c.* 16.5% and 20% of cuticular mass in young and mature cuticles, respectively (ANOVA, $F(1, 12) = 7.67$, $P = 0.017$, $n = 16$; Table 1). The full GC data set yielded similar results. Young leaves had a lower IW load (2.1–3.0–4.6 $\mu\text{g cm}^{-2}$, $n = 144$) than mature leaves (3.1–4.9–7.1 $\mu\text{g cm}^{-2}$), and distribution of both data sets was slightly positively skewed (Fig. S6).

Relative abundance of epicuticular and intracuticular waxes

n-Alkanes, aldehydes and fatty acids were detected in native (non-derivatised) GC samples (Figs 2, S7). C29, C31 and C33 alkanes (*n*-nonacosane, *n*-hentriacontane and *n*-tritriacontane) were predominant in EW and together accounted for 88.8–90.9–93.8% (q25%–median–q75%) of all GC-amenable compounds, whereas they accounted for 24.6–36.4–50.5% in IW. The proportion of *n*-alkanes was always higher in mature cuticles (Table 1; Fig. 2). Aldehydes (C28–C36) were most abundant in the IW of young leaves (21%) and rarest in the EW of mature leaves (1.9%). Fatty acids (C16 and C18) were undetectable in EW but formed a surprisingly high percentage of IW from enzymatically isolated cuticles. Primary alcohols (with an even number of carbons) were also detected in small amounts (mainly in young leaves) in a subset of derivatised samples (not shown). Our approach was to detect the dynamics of major compounds. The difficulty of isotopic precision for derivatised and/or minor compounds led us to ignore them in further analyses. The absolute quantification of compound classes can be found in Table 1. Differences between opposite sides of leaves were minor and will be described separately.

Intracuticular and epicuticular wax extraction and dynamics

Cryo-SEM images indicated that two strips of collodion removed the visible wax on the leaf surface (Fig. 1). We tested the effectiveness of collodion for removing EW and its ability to distinguish between EW and IW. The efficiency of three subsequent

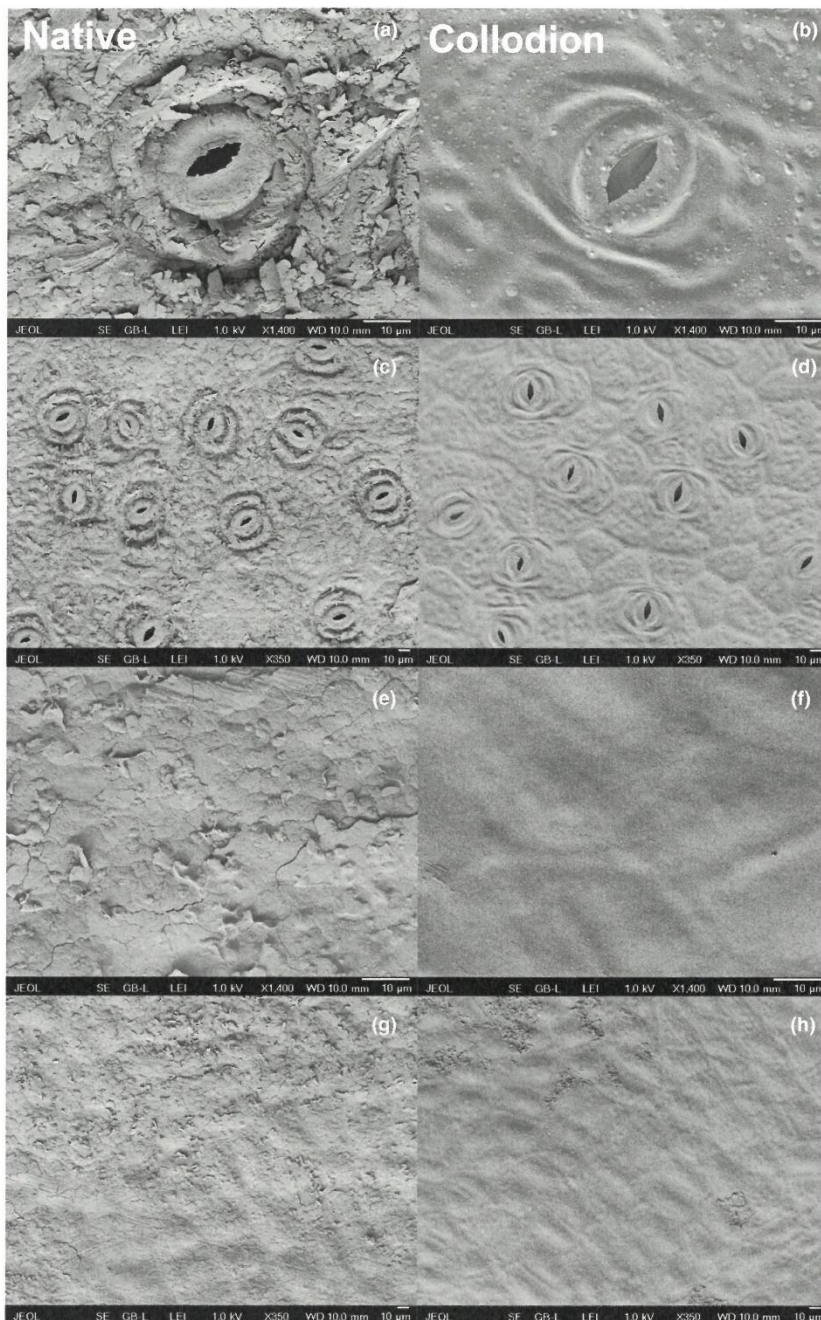


Fig. 1 Cryo-SEM images of leaf surfaces of *Clusia rosea* with and without collodion treatment. Intact surfaces (a, c, e, g) and surfaces after stripping with two layers of collodion applied subsequently (b, d, f, h). The upper four panels (a, b, c, d) show the abaxial, the bottom four panels (e, f, g, h) the adaxial leaf side. Two magnifications are shown (see scale bars).

collodion strips in removing EW can be seen in Fig. S3. Two strips removed at least 90% of EW (slightly more for alkanes than for semipolar compounds). We provide two lines of evidence that EW and IW are distinct and may be sampled selectively by collodion. First, individual compounds and compound classes (i.e. alkanes vs aldehydes) differed in their abundances between EW and IW (Table 1; Fig. 2). Second, assimilated carbon (^{13}C) was visible as early as 2 h after labelling in IW with a much later appearance in EW, which became progressively more

strongly labelled with time and could surpass IW by the end of the experiment (Figs 3, 4).

Cuticle compound-specific ^{13}C dynamics

Alkanes and aldehydes showed roughly similar ^{13}C dynamics, consistent with a common synthetic pathway, the 'alkane pathway' (Bernard & Joubès, 2013). They were more strongly and more rapidly labelled in young leaves than in mature ones

Table 1 Cuticle and wax characteristics of *Clusia rosea* leaves.

Parameter	Units	Young leaf		Mature leaf		n	Significance
		Adaxial	Abaxial	Adaxial	Abaxial		
Gravimetry							
EW-free cuticle area density (all)	µg cm ⁻²	325 ± 95 ^a	324 ± 84 ^a	348 ± 145 ^a	320 ± 111 ^a	34	ns
EW-free cuticle area density (subset)	µg cm ⁻²	317 ± 94 ^a	366 ± 56 ^a	287 ± 36 ^a	315 ± 50 ^a	4	ns
MX area density (subset)	µg cm ⁻²	266 ± 74 ^a	305 ± 44 ^a	234 ± 36 ^a	248 ± 38 ^a	4	ns
Total IW extracted (subset)	µg cm ⁻²	51.7 ± 19.8 ^a	62.1 ± 17 ^a	52.8 ± 5.8 ^a	66.9 ± 14.8 ^a	4	ns
Chromatography							
Total IW	µg cm ⁻²	0.2–0.6(1.6)–2.1–9.6 ^a	0.2–0.3(1.4)–1–10.2 ^a	3.8–7.6(17.3)–34.8–56.4 ^b	2–7.2(13.4)–23.3–38.4 ^c	34	*
EW alkanes	µg cm ⁻²	1.6–2.5(3)–4.3–6.8 ^a	2.4–3.1(3.8)–4.7–7.8 ^a	2.9–3.9(4.8)–6.5–11.7 ^b	3.4–6.5(6.5)–7.9–14.4 ^c	34	*
EW aldehydes	µg cm ⁻²	0.1–0.5(1.5)–1.9–9.2 ^a	0.2–0.28(1.3)–1.1–9.6 ^a	2.7–7.5(16.8)–34.1–53.6 ^b	2.0–7.0(13.1)–23.0–37.3 ^c	34	*
EW fatty acids	µg cm ⁻²	0.02–0.05(–0.09)–0.16–0.3 ^a	0–0.02(0.1)–0.1–0.4 ^a	0.08–0.20(0.35)–0.43–1.3 ^b	0–0.12(0.23)–0.39–0.81 ^c	34	*
IW alkanes	µg cm ⁻²	Not detectable	Not detectable	Not detectable	Not detectable	34	ns
IW aldehydes	µg cm ⁻²	0.37–0.62(0.77)–0.88–1.79 ^a	0.7–1(1.17)–1.37–3.59 ^b	0.9–1.2(2.2)–2.9–6.7 ^c	1.5–2.8(3.8)–5.0–11.1 ^d	34	*
IW fatty acids	µg cm ⁻²	0.08–0.44(0.69)–1–2.43 ^a	0.19–0.5(0.6)–0.79–2.17 ^a	0.19–0.24(0.4)–0.57–1.02 ^b	0.25–0.37(0.43)–0.53–1.13 ^b	34	*
EW ACL	C number	0–0.7–1.2(1.5)–2–4 ^a	0–1–1.6(1.8)2.4–3.7 ^a	0.3–1–1.4(1.6)–2.4–3.5 ^a	0–1–1.5(1.6)–2.2–3 ^a	34	ns
IW ACL	C number	30.73 ± 0.42 ^a	31 ± 0.41 ^b	31.2 ± 0.16 ^c	31.51 ± 0.2 ^d	34	*
EW OEP	Odd to even	31.31 ± 0.68 ^a	31.42 ± 0.73 ^a	31.65 ± 0.42 ^{ab}	31.85 ± 0.28 ^b	34	*
	C ratio	10.14 ± 5.17 ^a	13.27 ± 8.81 ^a	13.74 ± 4.63 ^a	20.6 ± 10.47 ^b	34	*
IW OEP	Odd to even	2.77 ± 2.04 ^a	3.21 ± 1.94 ^{ab}	4.51 ± 2.72 ^{bc}	5.23 ± 2.22 ^c	34	*
	C ratio						

Values with normal distributions are shown as mean ± 1 SD. Non-Gaussian distributions (predominantly positively skewed) are presented as q25%–median(mean)–q75%–q95%. EW and IW denote epicuticular and intracuticular waxes, respectively. Average carbon length (ACL) = $\sum([C_i] \times i) / \sum[C_i]$, where $[C_i]$ is the concentration of *n*-alkane containing *i* carbon atoms; odd to even preference index (OEP) = $\sum[C_i]_{\text{odd}} / \sum[C_i]_{\text{even}}$, where $[C_i]_{\text{odd}}$ are concentrations of odd carbon numbered compounds from C25 to C37 and $[C_i]_{\text{even}}$ are those of even numbered compounds from C26 to C38. Subset of cuticles is shown where cutin matrix (MX) and IW load were determined not only chromatographically but also gravimetrically. Subsets with different upper-key letters differ significantly. Two-way ANOVA and Tukey's HSD *post hoc* test were used. Significance criteria: ns, $P > 0.05$; *, $P < 0.05$ at least in one comparison.

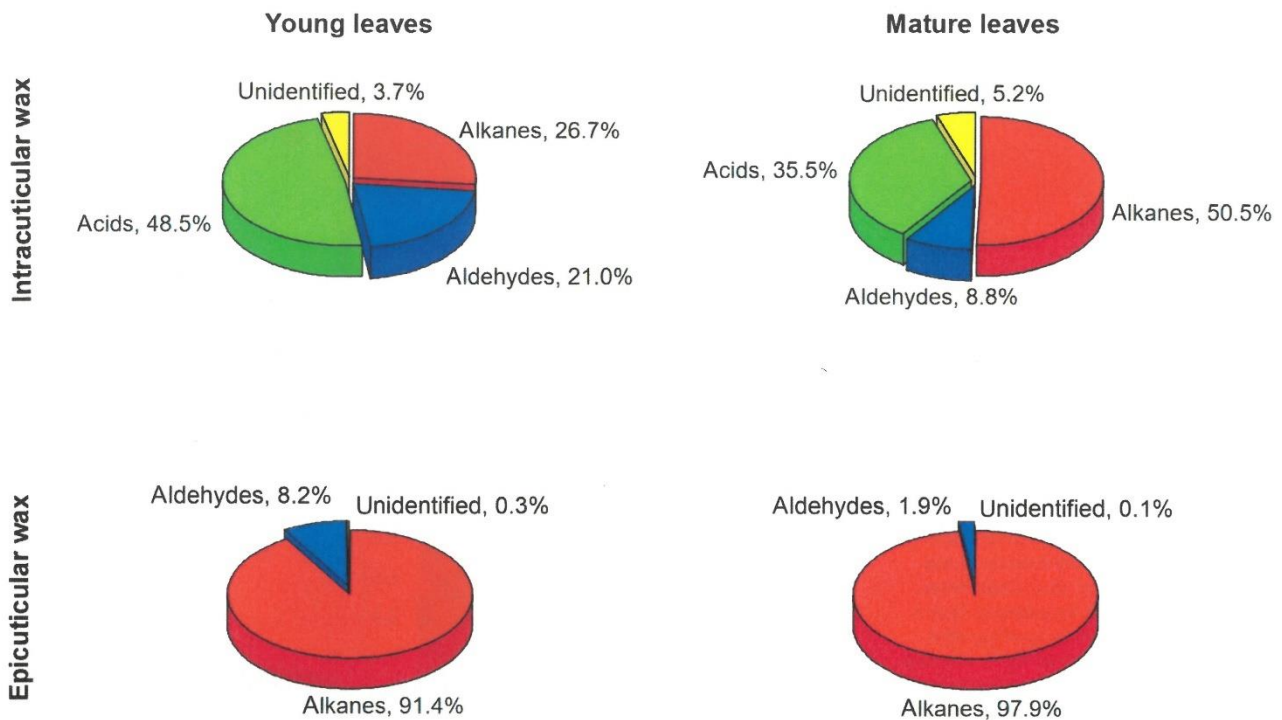


Fig. 2 Relative abundance of epicuticular and intracuticular wax compounds of *Clusia rosea* leaves. Percentages of alkanes, aldehydes and fatty acids measured in intracuticular and epicuticular waxes from young and mature leaves are shown. Adaxial and abaxial leaf sides are pooled due to insubstantial differences in overall compound class abundances. See Table 1 for side-specific absolute quantification of each compound class.

(Fig. 4). In IW, the fatty acids (C16 and C18) were labelled rapidly in the first hours after $^{13}\text{CO}_2$ treatment, which is very likely due to the noncuticular origin of these compounds indicated by the extremely tight correlation of ^{13}C excess between leaf sides (see Fig. S8).

Intracuticular wax alkanes, particularly in mature leaves, exhibited much faster ^{13}C enrichment in the early period after labelling compared with EW alkanes, suggesting deposition in the matrix before the cuticle surface. Absolute ^{13}C enrichment of a compound is a function of: (1) the rates of synthesis, transport and deposition; (2) the size of the unlabelled pool already present; and (3) the rate of wax loss (e.g. by abrasion) and reabsorption backward into epidermal cells. We assume in this study that (3) was negligible during the 3-wk duration of the experiment. ^{13}C enrichment recalculated according Eqn 1 as new wax deposition (NWD) shows that alkanes were preferentially allocated in IW in young leaves, whereas in mature leaves, the NWD was equal for IW and EW (Fig. 5). This recalculation also demonstrated about the same NWD of alkanes for young and mature leaves (Figs 5, S8E,F). The NWD of aldehydes was negligible due to their low abundance. We could not find any time-dependent pattern in either ^{13}C abundance or NWD between the differently elongated chains (e.g. C29, C31 and C33 alkanes) and between alkanes and aldehydes (data not shown).

The cutin matrix contained significant and highly variable amounts of new carbon ^{13}C (up to 1.2 At%) only in young leaves (Figs 3, S8). Moreover, the traces of ^{13}C excess in mature leaves (< 0.1 At% in most cases) may be the remnants of incompletely removed or even matrix-bound wax (Hauke & Schreiber, 1998).

Differences between the leaf sides

Despite the different adaxial (astomatous) vs abaxial (stomatous) leaf/cuticle morphology (Fig. 1), MX area density and EW and IW loads were similar for both leaf sides (Table 1). The chemical composition of EW and IW differed slightly but consistently between leaf sides. Both EW and IW compounds were significantly shifted towards longer carbon chains on the abaxial side (see greater average carbon length – ACL parameter in Table 1). The ratio of alkanes C29 and C33 is a major determinant of ACL in *C. rosea* leaves (Fig. S7). These ratios for adaxial and abaxial surfaces form distinct 2D data clusters (with a lower proportion of C29 in the abaxial cuticles), particularly in mature leaves (Fig. 6a,b). By contrast, the new carbon deposition expressed as ^{13}C excess in both alkanes showed no preference between adaxial and abaxial sides or IW and EW (Fig. 6c,d). Thus, the new wax deposition (NWD) is proportional to the amount of compound, that is higher for C29 alkane on the adaxial surface and higher for C33 alkane on the abaxial surface (Fig. 6e,f).

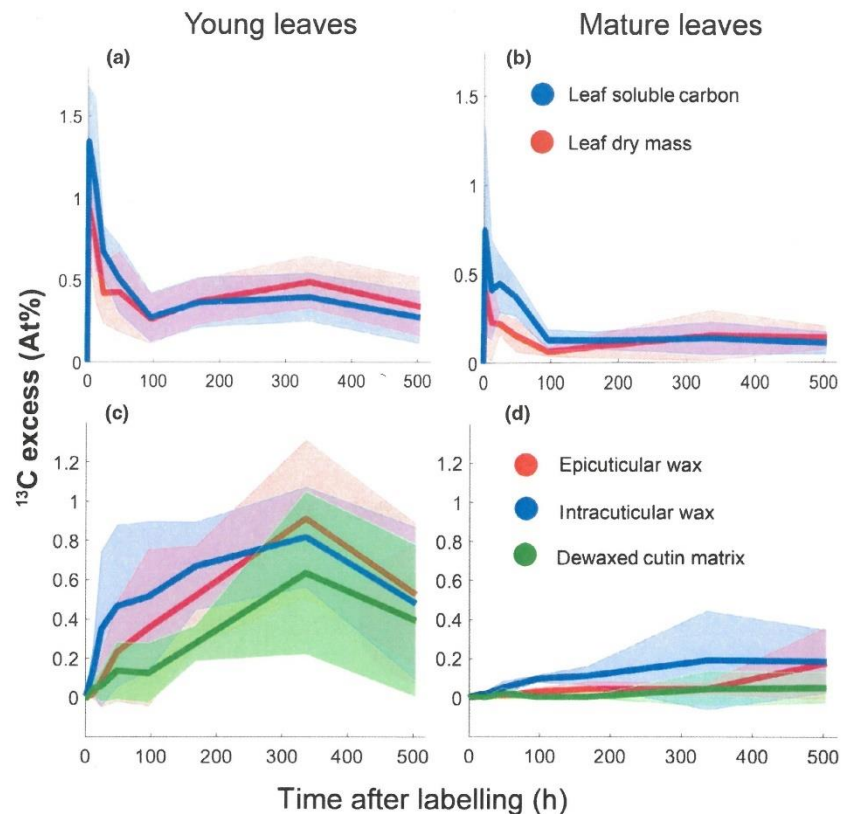


Fig. 3 Dynamics of ^{13}C abundance in leaf water-soluble fraction, dry mass (a, b) and cuticular constituents (c, d) of *Clusia rosea*. The dynamics is shown for young (a, c) and mature (b, d) leaves before labelling, after 2 h of CO_2 assimilation in air highly enriched in $^{13}\text{CO}_2$ (c. 50% of $^{13}\text{CO}_2$) and for the next 3 wk. ^{13}C excess shows ^{13}C abundance in the labelled leaf reduced by natural abundance of ^{13}C in the leaves before labelling. Thick lines represent mean and shaded areas 1 SD. $n = 4$.

Effect of collodion treatment on leaf gas exchange

The side-specific gas exchange measurements were carried out before and after leaf treatment with collodion with the aim to assessing the role of EW in gas exchange and any effect of collodion on stomata. CO_2 assimilation (Fig. S5A,B) and stomatal conductance (Fig. S5C,D) measured at the abaxial (stomatous) side of the leaf were highly variable (especially in mature leaves). However, the collodion treatment had little, if any, effect on photosynthesis and stomatal behaviour. Thus, the collodion treatment had no deleterious effect on the leaves and stomata of *C. rosea*. On the contrary, we could not detect any gas exchange, of either CO_2 or H_2O , on the adaxial (astomatous) side of the leaves, regardless of whether or not the collodion treatment had been applied (data not shown). Thus, the removal of EW by collodion did not significantly increase cuticular permeability.

Discussion

This is, to the best of our knowledge, the first study of the dynamics of all major parts of the plant cuticle and of individual chemical compounds using a ^{13}C tracer. We have shown that photosynthesis in air highly enriched in $^{13}\text{CO}_2$ resulted in a substantial labelling of the active metabolite pool and subsequently of cutin and wax in autograph tree (*C. rosea*) and broccoli (*Brassica oleracea* var. *gemmifera*).

Collodion discriminates between EW and IW and does not harm leaf of *Clusia rosea*

There is extensive discussion in the literature about the best method to sample EW and leaf IW as intact as possible. Collodion solution (Haas & Rentschler, 1984), gum Arabic (Jetter & Schäffer, 2001) and frozen water/liquids (Ensikat *et al.*, 2000) are among the most common techniques. Individual research groups mostly prefer the one they have developed. Collodion is a solution of c. 4% nitrocellulose in 1 : 1 diethyl ether and ethanol. Some researchers point out that these organic solvents may mobilise part of IW and recommend an aqueous solution of gum Arabic instead (Jetter *et al.*, 2000). Since gum Arabic is harder to work with, contains organic contaminants and is not suitable for working on isolated cuticles (Zeisler & Schreiber, 2016), collodion appears to be a more versatile option. Here, we confirm that EW and IW may be distinguished in *C. rosea* leaves by collodion sampling. Moreover, only two consecutive strips were sufficient to sample > 90% of the EW (Fig. S3). At the same time, no gas exchange of the upper (astomatous) side of leaves before and after the collodion treatment was detectable (with system noise: c. $0.001 \text{ mol m}^{-2} \text{ s}^{-1}$ for stomatal conductance and c. $0.1 \mu\text{mol m}^{-2} \text{ s}^{-1}$ for CO_2 exchange). Thus, we confirm that collodion does not have a detrimental effect on living leaves of *C. rosea* and their stomata (Fig. S5). This is in agreement with previous experiments on *Prunus laurocerasus* leaves and cuticles, where

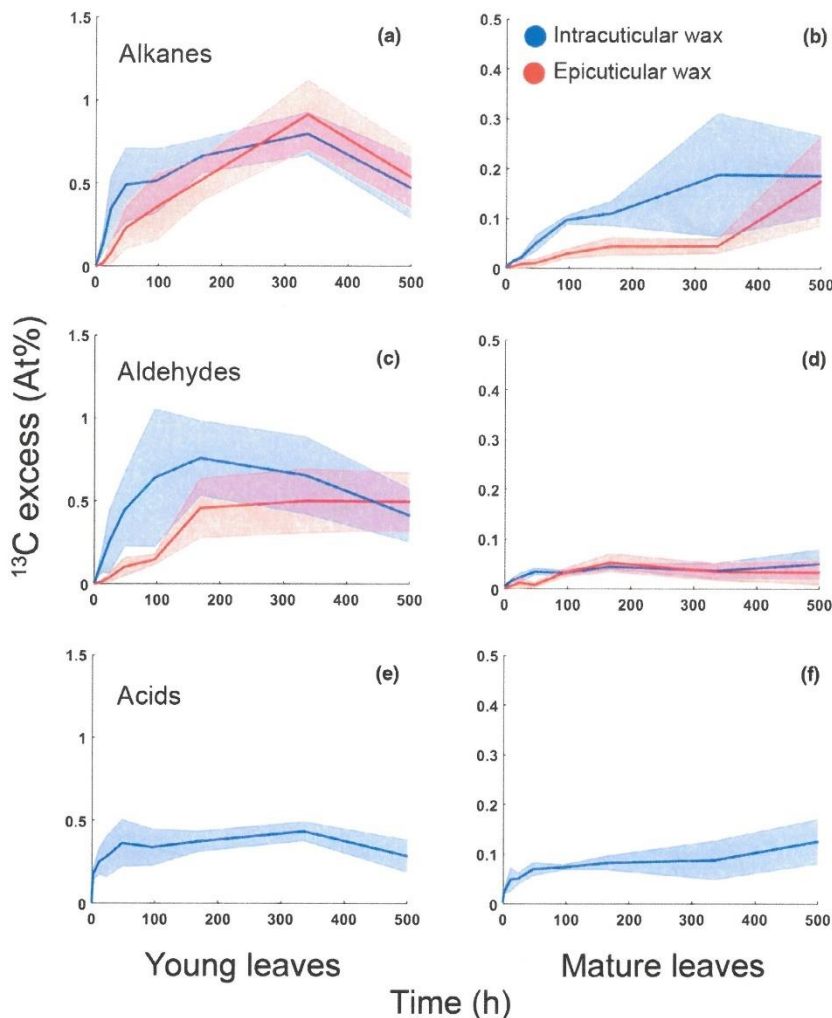


Fig. 4 Dynamics of ^{13}C abundance in main classes of wax compounds on *Clusia rosea* leaves. *n*-Alkanes (a, b), aldehydes (c, d) and fatty acids (e, f) of intracuticular (blue) and epicuticular (red) leaf wax are shown for young (a, c, e) and mature (b, d, f) leaves before labelling, after 2 h of CO_2 assimilation in air highly enriched in $^{13}\text{CO}_2$ (c. 50% of $^{13}\text{CO}_2$) and for the next 3 wk. Thick lines represent mean and shaded areas 1 SE of the mean. $n = 4$. Amount-weighted ^{13}C enrichment values of particular compounds were averaged. C29, C31, C33 (and much less C27, C28, C30, C32, C35, C37) alkanes, C28, C30, C32, C34 and C36 aldehydes and C16 and C18 fatty acids (only in IW) were detected and quantified. Note: different y-axis scaling for young and mature leaves.

collodion-derived EW contained only trace amounts of triterpenoids found exclusively in IW and up to five consecutive treatments did not disrupt the cuticle and its conductance (Zeisler & Schreiber, 2016).

Wax is deposited inside the cuticle before being exported to the leaf surface – the leaf lifespan perspective

New (^{13}C) carbon was detectable first (as early as 2 h after labelling) in IW, which remained enriched in comparison with EW for most of the experimental duration (Fig. 3), particularly in alkanes (Fig. 4). EW ^{13}C excess surpassed that of IW in young leaves 2 wk after labelling in. ^{13}C changes were smaller and slower in mature leaves (Figs 3, 4), due to the high wax load (Table 1). The ^{13}C excess more accurately depicts the amount of deposited wax in the two pools examined when converted to NWD (Fig. 5). This implies that the MX must first be filled with wax, and only small amount is exported to the leaf surface in young leaves (Fig. 5a). The very low EW

load of young leaves further supports this conclusion. Surprisingly, mature (last year) leaves with c. 10 times higher EW coverage (Table 1) allocated approximately equal amounts of alkanes in IW and EW (Fig. 5b). Intracuticular wax, not EW, has been recently identified as the main component of the gas transport barrier of leaf cuticles (Zeisler & Schreiber, 2016; Zeisler-Diehl *et al.*, 2017; Zeisler-Diehl & Müller, 2018). Sealing the young leaf by IW against desiccation stress seems to be the primary effort, followed by export of additional wax (EW) to the cuticle surface, which serves other cuticle-specific purposes. Mature leaves, on the contrary, may have saturated MX with IW during the earlier stages of their development, resulting in the increased deposition of EW providing an ‘armor’ against pathogens, xenobiotics and/or UV radiation penetrating the leaf (Lewandowska *et al.*, 2020). Interestingly, the rate of wax synthesis appears to be roughly comparable in young and mature leaves (Fig. 5). Thus, cuticular waxes are renewed in *C. rosea* throughout leaf ontogeny (except perhaps during senescence) despite the rate of loss of waxes from the leaf surface,

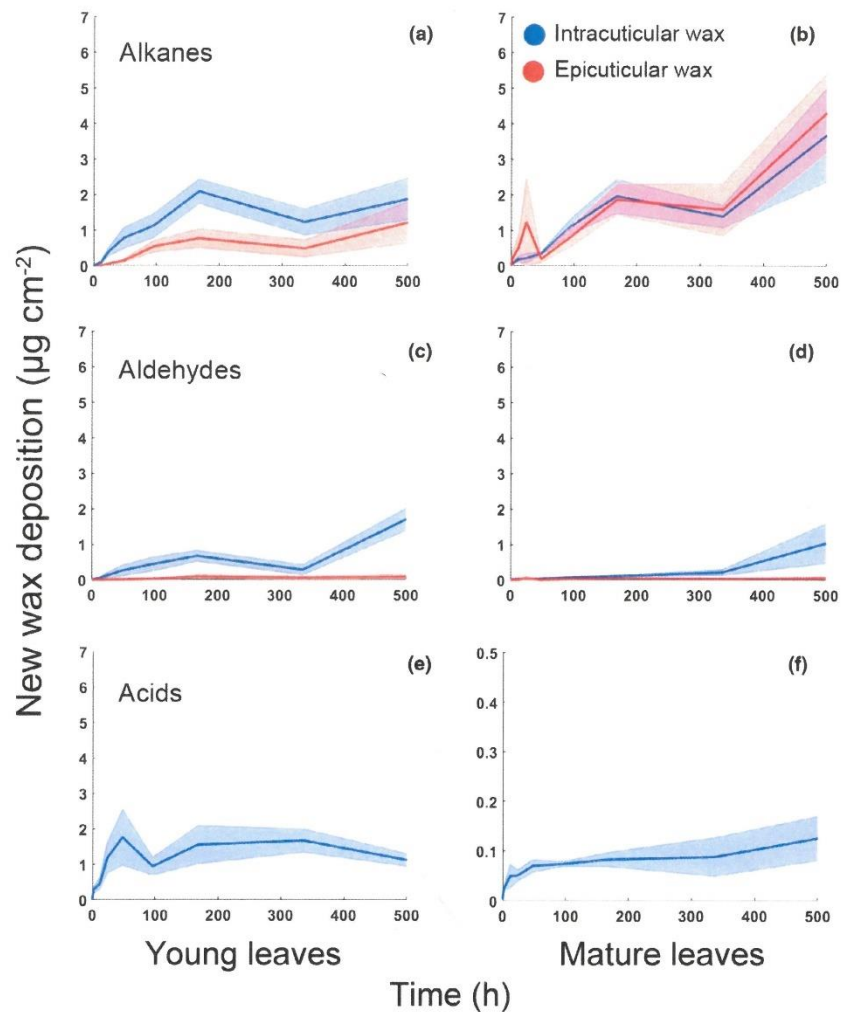


Fig. 5 New wax deposition (NWD) in main compound classes of *Clusia rosea* leaves. *n*-Alkanes (a, b), aldehydes (c, d) and fatty acids (e, f) of intracuticular (blue) and epicuticular (red) leaf wax are shown for young (a, c, e) and mature (b, d, f) leaves before labelling, after 2 h of CO₂ assimilation in air highly enriched in ¹³CO₂ (c. 50% of ¹³CO₂) and for the next 3 wk. New wax deposition was calculated as a product of ¹³C enrichment of the particular compound class (values in Fig. 4), amount of this compound class (Table 1) divided by ¹³C enrichment in soluble leaf fraction (Fig. 2), see the [Materials and Methods](#) section. Thick lines represent mean and shaded areas 1 SE of the mean. *n* = 4.

and thus the exact rate of wax turnover could not be inferred reliably from this study.

Wax renewal as an evolutionary trait reflecting climatic factors and plant/leaf life strategies

Lipid synthesis is one of the most energy-demanding processes in living cells (Buchanan *et al.*, 2015). The cuticle is usually thin but its mass is not negligible. Consider a 'typical' mesic leaf with a thickness of 0.2 mm. Two cuticles, on both sides, each 1 µm thick, represent 1% of the leaf cross-section. In addition, the weight of a leaf is usually reduced by 90% or more after drying, while the weight of the cuticle, containing mainly lipids, remains virtually unchanged. The cuticle therefore represents a significant proportion of leaf dry matter (up to 24%; on average 5–10%; Onoda *et al.*, 2012). Selective pressure should optimise cuticle dynamics in response to the environment and leaf longevity. It may explain the above-mentioned controversy in published data on wax renewal during leaf expansion or throughout the leaf lifespan (Sachse *et al.*, 2009; Kahmen *et al.*, 2011; Gao *et al.*, 2012).

Four distinct 'functional groups' with respect to EW regeneration were also found by Neinhuis *et al.* (2001) using SEM; however, ecological implications were not identified. Our recent data suggest that young *Brassica oleracea* leaves allocate much more wax per leaf area (by at least one order of magnitude) than leaves whose expansion has ceased (Fig. S9). Thus, annual leaves may save expending high-energy lipid resources on the renewal of wax in comparison with leaves with higher longevity (e.g. *C. rosea*), which must continuously allocate part of their energy and metabolites to wax turnover.

Wax elongation is very fast, and fatty acids detected are not of cuticular origin

The predominant compounds in the wax of *C. rosea* are various long-chain aliphatic compounds C25–C38 in length, mainly C29, C31 and C33 *n*-alkanes (nonacosane, hentriacontane and tritriacontane). Our efforts to detect differences in the relative amounts of newly synthesised compounds with different chain lengths, or between alkanes and aldehydes, did not provide a clear

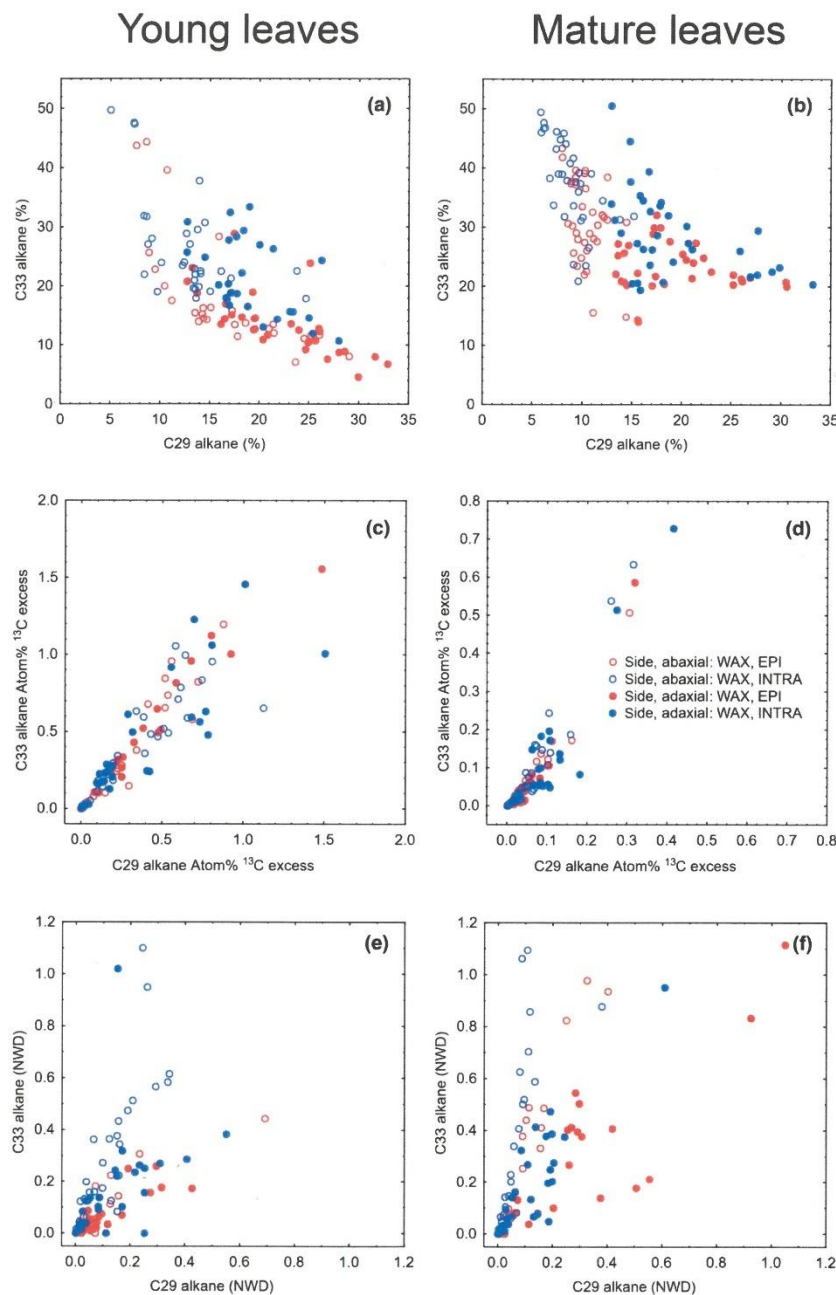


Fig. 6 Differences between adaxial and abaxial and intracuticular and epicuticular waxes of *Clusia rosea*. Percentage of C29 alkane (*n*-nonacosane, x-axis) and C33 alkane (*n*-tritriacontane, y-axis) of all alkane wax content (a, b), ¹³C excess (c, d) and new wax deposition, NWD ($\mu\text{g cm}^{-2}$, e, f) in those compounds for young (left column) and mature (right column) leaves. Waxes extracted from abaxial leaf side are shown as red symbols, waxes from adaxial leaf side as blue symbols. Open symbols represent epicuticular waxes, closed symbols intracuticular waxes, respectively. $n = 72$.

picture. There was a slight trend indicating that the ¹³C excess is higher for the shorter chain IW 2 h after labelling (EW was not sufficiently labelled at this time, data not shown). Thus, the elongation of fatty acids and formation of compounds with various functional groups and their transport to the uppermost leaf surface was surprisingly rapid. Shedding more light on these issues will require additional research.

Fatty acids, mainly C22 and longer, are frequently found in plant cuticles (Haas & Rentschler, 1984; Hauke & Schreiber, 1998; Bernard & Joubès, 2013). On the contrary, effective

adsorption of C16 and C18 fatty acids from tissue slurries was observed already in 1986 during enzymatic cuticle isolation (Schönherr & Riederer, 1986). We found substantial amounts of hexadecanoic and octadecanoic acids in IW of isolated cuticles but not in EW (Fig. 2). Based on ¹³C data, we argue these acids were not of cuticular origin. The extremely close correlation between adaxial and abaxial ¹³C excess observed (Fig. S8, $r^2 > 0.99$) is possible only if the following two conditions are met: the pool of fatty acids is the same, thus originating from leaf tissue; and the precision of the isotopic measurement is high.

This result proves the accuracy of our method and demonstrates that short fatty acids are not a major constituent of *C. rosea* cuticles.

Cuticle biosynthesis is coordinated between leaf sides

The abundances of major compounds and ^{13}C dynamics in the cuticles on opposite sides of *C. rosea* leaves were tightly correlated (Figs 6, S8), which contrasts with the differing morphology (Fig. 1) and presumably contrasting environmental conditions on opposite sides of the leaves (Bird & Gray, 2003). Moreover, *C. rosea* leaves are hypostomatous, implying a gradient of photosynthesis and CO_2 across the leaf (Terashima *et al.*, 2011). This side-specific coordination of cuticle development and renewal, first reported here using ^{13}C tracer, may be anticipated but mechanisms are unknown.

Probably, even more puzzling are the subtle and consistent side-specific differences in abundance of some compounds. For example, the ratio of C29 and C33 alkanes can predict the leaf side of *C. rosea* with nearly 100% confidence, particularly in mature leaves (Fig. 6b). The side-specific ^{13}C excess, in turn, was very similar for both leaf sides (Fig. 6c,d). This implies a proportionality of the rate of synthesis to the amount of a particular compound (Fig. 6e,f) and likely maintains the leaf-side-specific C29 : C33 ratio during development. Recently, we have found an even more striking contrast in EW of pepper. The ratio of the abundances of C29 : C33 alkanes was 0.98 ± 0.20 for the adaxial side but only 0.28 ± 0.20 for the abaxial side ($n = 60$, Fig. S10). These side-specific differences in cuticular wax chemistry have been known for a long time (Holloway *et al.*, 1977), but the physiological functions and mechanisms maintaining these contrasts are not clear. One possible explanation could arise from the side-specific presence or frequency of stomata. In most plant species, stomata are located preferentially on the abaxial leaf side, and the cuticle covering guard cells differs from the pavement cell cuticle in thickness and wax composition (Karabourniotis *et al.*, 2001; Bird & Gray, 2003). If the fraction of the leaf area taken up by guard cells increases, we might expect that the discrepancy in wax composition between opposite leaf sides will rise. However, this hypothesis remains to be tested in future studies. To the best of our knowledge, to date, only biotic interactions – microbial preferences for a particular leaf side – have been correlated with side-specific cuticular wax chemistry (Gniwotta *et al.*, 2005).

In conclusion, ^{13}C isotope labelling and tracing let us show that: both epicuticular and intracuticular waxes are renewed during the whole leaf lifespan; wax compounds are deposited in the cuticle as intracuticular wax first and may be exported to the leaf surface as epicuticular wax later on; only young, still expanding leaves incorporate new carbon into the cutin matrix; and differences in wax amount and composition between leaf sides are typically small but consistent, suggesting coordinated adaxial and abaxial cuticle formation. Methodically, we have shown that collodion is able to effectively discriminate between EW and IW and does not adversely affect leaves and stomata, at least in *Clusia rosea*, thus making it suitable for in-vivo wax regeneration studies.

Acknowledgements

The authors express their thanks to Petra Fialová for technical assistance with plant cultivation, Ladislav Marek for bulk-isotope analyses and Stanislav Svoboda for sequencing *C. rosea* specimen.

Competing interests

None declared.

Author contributions

JŠ and JK planned and designed the research (gas exchange, ^{13}C labelling and measurement). JK processed data and wrote the manuscript. TK sampled leaves and prepared samples for isotope analyses. JJ planned and designed the sampling during the experiment, planned and coordinated the pilot measurements, sample harvesting and preparing for isotopic analyses. BA sampled EW with collodion, isolated cuticles, obtained IW and processed some data. JB identified wax compounds using GC–MS–TOF. All authors approved the manuscript.

ORCID

Jitka Janová  <https://orcid.org/0000-0003-0743-535X>
Tereza Kalistová  <https://orcid.org/0000-0003-4557-7252>
Jiří Kubásek  <https://orcid.org/0000-0001-8540-6904>
Jiří Šantrůček  <https://orcid.org/0000-0003-0430-5795>

Data availability

The data that support the findings of this study are available from the corresponding author upon reasonable request.

References

- Baker EA. 1974. The influence of environment on leaf wax development in *Brassica oleracea* var. *gemmifera*. *New Phytologist* 73: 955–966.
- Barthlott W, Neinhuis C. 1997. Purity of the sacred lotus, or escape from contamination in biological surfaces. *Planta* 202: 1–8.
- Berhin A, de Bellis D, Franke RB, Andrade Buono R, Nowack M, Nawrath C. 2019. The root cap cuticle: a cell wall structure for seedling establishment and lateral root formation. *Cell* 176: 1367–1378.
- Bernard A, Joubès J. 2013. Arabidopsis cuticular waxes: advances in synthesis, export and regulation. *Progress in Lipid Research* 52: 110–129.
- Bird SM, Gray JE. 2003. Signals from the cuticle affect epidermal cell differentiation. *New Phytologist* 157: 9–23.
- Bourgault R, Matschi S, Vasquez M, Qiao P, Sonntag A, Charlebois C, Mohammadi M, Scanlon MJ, Smith LG, Molina I. 2020. Constructing functional cuticles: analysis of relationships between cuticle lipid composition, ultrastructure and water barrier function in developing adult maize leaves. *Annals of Botany* 125: 79–91.
- Boyer JS. 2015. Turgor and the transport of CO_2 and water across the cuticle (epidermis) of leaves. *Journal of Experimental Botany* 66: 2625–2633.
- Buchanan BB, Grisse W, Jones RL, eds. 2015. *Biochemistry and molecular biology of plants*, 2nd edn. Chichester, UK: John Wiley & Sons.
- Budke JM, Goffinet B. 2016. Comparative cuticle development reveals taller sporophytes are covered by thicker calyptra cuticles in mosses. *Frontiers in Plant Science* 7: 832.

- Ensikat HJ, Neinhuis C, Barthlott W. 2000. Direct access to plant epicuticular wax crystals by a new mechanical isolation method. *International Journal of Plant Sciences* 161: 143–148.
- Fernández V, Bahamonde HA, Javier Peguero-Pina J, Gil-Pelegrín E, Sancho-Knapik D, Gil L, Goldbach HE, Eichert T. 2017. Physico-chemical properties of plant cuticles and their functional and ecological significance. *Journal of Experimental Botany* 68: 5293–5306.
- Fernández V, Guzmán-Delgado P, Graça J, Santos S, Gil L. 2016. Cuticle structure in relation to chemical composition: re-assessing the prevailing model. *Frontiers in Plant Science* 7: 1–14.
- Fich EA, Segerson NA, Rose JKC. 2016. The plant polyester cutin: biosynthesis, structure, and biological roles. *Annual Review of Plant Biology* 67: 207–233.
- Flore JA, Bukovac MJ. 1974. Pesticide effects on the plant cuticle: I. Response of *Brassica oleracea* L. to EPTC as indexed by epicuticular wax production. *Journal of the American Society for Horticultural Science* 99: 34–37.
- Gao L, Burnier A, Huang Y. 2012. Quantifying instantaneous regeneration rates of plant leaf waxes using stable hydrogen isotope labeling. *Rapid Communications in Mass Spectrometry* 26: 115–122.
- Gniwotta F, Vogg G, Gartmann V, Carver TLW, Riederer M, Jetter R. 2005. What do microbes encounter at the plant surface? Chemical composition of pea leaf cuticular waxes. *Plant Physiology* 139: 519–530.
- Gustafsson MHG, Bitttrich V, Stevens PF. 2002. Phylogeny of Clusiaceae based on rbc L sequences. *International Journal of Plant Sciences* 163: 1045–1054.
- Guzmán P, Fernández V, García ML, Khayet M, Fernández A, Gil L. 2014. Localization of polysaccharides in isolated and intact cuticles of eucalypt, poplar and pear leaves by enzyme-gold labelling. *Plant Physiology and Biochemistry* 76: 1–6.
- Haas K, Rentschler I. 1984. Discrimination between epicuticular and intracuticular wax in blackberry leaves: ultrastructural and chemical evidence. *Plant Science Letters* 36: 143–147.
- Hauke V, Schreiber L. 1998. Ontogenetic and seasonal development of wax composition and cuticular transpiration of ivy (*Hedera helix* L.) sun and shade leaves. *Planta* 207: 67–75.
- Holloway PJ, Hunt GM, Baker EA, Macey MJK. 1977. Chemical composition and ultrastructure of the epicuticular wax in four mutants of *Pisum sativum* (L.). *Chemistry and Physics of Lipids* 20: 141–155.
- Jeffree CE. 2018. The fine structure of the plant cuticle. In: Riederer M, Müller C, eds. *Annual plant reviews online*, vol. 23. Chichester, UK: John Wiley & Sons, 11–125.
- Jetter R, Kunst L, Samuels AL. 2018. Composition of plant cuticular waxes. In: *Annual plant reviews online*. Chichester, UK: John Wiley & Sons, 145–181.
- Jetter R, Schäffer S. 2001. Chemical composition of the *Prunus laurocerasus* leaf surface. Dynamic changes of the epicuticular wax film during leaf development. *Plant Physiology* 126: 1725–1737.
- Jetter R, Schäffer S, Riederer M. 2000. Leaf cuticular waxes are arranged in chemically and mechanically distinct layers: evidence from *Prunus laurocerasus* L. *Plant, Cell & Environment* 23: 619–628.
- Kahmen A, Dawson TE, Vieth A, Sachse D. 2011. Leaf wax *n*-alkane δD values are determined early in the ontogeny of *Populus trichocarpa* leaves when grown under controlled environmental conditions. *Plant, Cell & Environment* 34: 1639–1651.
- Karabourniotis G, Tzobanoglou D, Nikolopoulos D, Liakopoulos G. 2001. Epicuticular phenolics over guard cells: exploitation for *in situ* stomatal counting by fluorescence microscopy and combined image analysis. *Annals of Botany* 87: 631–639.
- Kerstiens G. 1996a. Cuticular water permeability and its physiological significance. *Journal of Experimental Botany* 47: 1813–1832.
- Kerstiens G. 1996b. Signalling across the divide: a wider perspective of cuticular structure–function relationships. *Trends in Plant Science* 1: 125–129.
- Kerstiens G. 1997. *In vivo* manipulation of cuticular water permeance and its effect on stomatal response to air humidity. *New Phytologist* 137: 473–480.
- Koch K, Neinhuis C, Ensikat H, Barthlott W. 2004. Self assembly of epicuticular waxes on living plant surfaces imaged by atomic force microscopy (AFM). *Journal of Experimental Botany* 55: 711–718.
- Kong L, Liu Y, Zhi P, Wang X, Xu B, Gong Z, Chang C. 2020. Origins and evolution of cuticle biosynthetic machinery in land plants. *Plant Physiology* 184: 1998–2010.
- Kubásek J, Hájek T, Duckett J, Pressel S, Šantrůček J. 2021. Moss stomata do not respond to light and CO₂ concentration but facilitate carbon uptake by sporophytes: a gas exchange, stomatal aperture and ¹³C labelling study. *New Phytologist* 230: 1815–1828.
- Lewandowska M, Keyl A, Feussner I. 2020. Wax biosynthesis in response to danger: its regulation upon abiotic and biotic stress. *New Phytologist* 227: 698–713.
- Lüttge U. 2008. Clusia: holy grail and enigma. *Journal of Experimental Botany* 59: 1503–1514.
- Macková J, Vašková M, Macek P, Hronková M, Schreiber L, Šantrůček J. 2013. Plant response to drought stress simulated by ABA application: changes in chemical composition of cuticular waxes. *Environmental and Experimental Botany* 86: 70–75.
- Matos TM, Peralta DF, Roma LP, dos Santos DYAC. 2021. The morphology and chemical composition of cuticular waxes in some Brazilian liverworts and mosses. *Journal of Bryology* 43: 129–137.
- Medina E, Aguiar G, Gómez M, Aranda J, Medina JD, Winter K. 2006. Taxonomic significance of the epicuticular wax composition in species of the genus *Clusia* from Panama. *Biochemical Systematics and Ecology* 34: 319–326.
- Medina E, Aguiar G, Gómez M, Medina JD. 2004. Patterns of leaf epicuticular waxes in species of clusia: taxonomical implications. *Interciencia* 29: 579–582.
- Neinhuis C, Koch K, Barthlott W. 2001. Movement and regeneration of epicuticular waxes through plant cuticles. *Planta* 213: 427–434.
- Niklas KJ, Cobb ED, Matas AJ. 2017. The evolution of hydrophobic cell wall biopolymers: from algae to angiosperms. *Journal of Experimental Botany* 68: 5261–5269.
- Onoda Y, Richards L, Westoby M. 2012. The importance of leaf cuticle for carbon economy and mechanical strength. *New Phytologist* 196: 441–447.
- Panikashvili D, Shi JX, Schreiber L, Aharoni A. 2011. The Arabidopsis ABCG13 transporter is required for flower cuticle secretion and patterning of the petal epidermis. *New Phytologist* 190: 113–124.
- Petit J, Bres C, Mauxion J-P, Bakan B, Rothan C. 2017. Breeding for cuticle-associated traits in crop species: traits, targets, and strategies. *Journal of Experimental Botany* 68: 5369–5387.
- Pighin JA, Zheng H, Balakshin LJ, Goodman IP, Western TL, Jetter R, Kunst L, Samuels AL. 2004. Plant cuticular lipid export requires an ABC transporter. *Science* 306: 702–704.
- Proctor MCF, Tuba Z. 2002. Poikilohydry and homiohydric: antithesis or spectrum of possibilities? *New Phytologist* 156: 327–349.
- Riederer M, Müller C. 2006. *Biology of the plant cuticle*. Oxford, UK: Blackwell.
- Riederer M, Schreiber L. 2001. Protecting against water loss: analysis of the barrier properties of plant cuticles. *Journal of Experimental Botany* 52: 2023–2032.
- Sachse D, Kahmen A, Gleixner G. 2009. Significant seasonal variation in the hydrogen isotopic composition of leaf-wax lipids for two deciduous tree ecosystems (*Fagus sylvatica* and *Acer pseudoplatanus*). *Organic Geochemistry* 40: 732–742.
- Samuels L, Kunst L, Jetter R. 2008. Sealing plant surfaces: cuticular wax formation by epidermal cells. *Annual Review of Plant Biology* 59: 683–707.
- Schimmelmann A, Qi H, Coplen TB, Brand WA, Fong J, Meier-Augenstein W, Kemp HF, Toman B, Ackermann A, Assonov S *et al.* 2016. Organic reference materials for hydrogen, carbon, and nitrogen stable isotope-ratio measurements: caffeine, *n*-alkanes, fatty acid methyl esters, glycines, L-valines, polyethylenes, and oils. *Analytical Chemistry* 88: 4294–4302.
- Schönherr J, Riederer M. 1986. Plant cuticles sorb lipophilic compounds during enzymatic isolation. *Plant, Cell & Environment* 9: 459–466.
- Schönherr J, Schmidt HW. 1979. Water permeability of plant cuticles: dependence of permeability coefficients of cuticular transpiration on vapor pressure saturation deficit. *Planta* 144: 391–400.
- Schreiber L, Skrabs M, Hartmann KD, Diamantopoulos P, Simanova E, Santrucek J. 2001. Effect of humidity on cuticular water permeability of isolated cuticular membranes and leaf disks. *Planta* 214: 274–282.
- Seale M. 2020. The fat of the land: cuticle formation in terrestrial plants. *Plant Physiology* 184: 1622–1624.
- Skoss JD. 1955. Structure and composition of plant cuticle in relation to environmental factors and permeability. *Botanical Gazette* 117: 55–72.

- Terashima I, Hanba YT, Tholen D, Niinemets Ü. 2011. Leaf functional anatomy in relation to photosynthesis. *Plant Physiology* 155: 108–116.
- Tsubaki S, Ozaki Y, Yonemori K, Azuma J. 2012. Mechanical properties of fruit-cuticular membranes isolated from 27 cultivars of *Diospyros kaki* Thunb. *Food Chemistry* 132: 2135–2139.
- Vráblová M, Vrábl D, Sokolová B, Marková D, Hronková M. 2020. A modified method for enzymatic isolation of and subsequent wax extraction from *Arabidopsis thaliana* leaf cuticle. *Plant Methods* 16: 129.
- Wang X, Kong L, Zhi P, Chang C. 2020. Update on cuticular wax biosynthesis and its roles in plant disease resistance. *International Journal of Molecular Sciences* 21: 5514.
- Wen M, Jetter R. 2009. Composition of secondary alcohols, ketones, alkanediols, and ketols in *Arabidopsis thaliana* cuticular waxes. *Journal of Experimental Botany* 60: 1811–1821.
- Woolley JT. 1967. Relative permeabilities of plastic films to water and carbon dioxide. *Plant Physiology* 42: 641–643.
- Yeats TH, Buda GJ, Wang Z, Chehanovsky N, Moyle LC, Jetter R, Schaffer AA, Rose JKC. 2012. The fruit cuticles of wild tomato species exhibit architectural and chemical diversity, providing a new model for studying the evolution of cuticle function. *The Plant Journal* 69: 655–666.
- Zeisler V, Schreiber L. 2016. Epicuticular wax on cherry laurel (*Prunus laurocerasus*) leaves does not constitute the cuticular transpiration barrier. *Planta* 243: 65–81.
- Zeisler-Diehl V, Migdal B, Schreiber L. 2017. Quantitative characterization of cuticular barrier properties: methods, requirements, and problems. *Journal of Experimental Botany* 68: 5281–5291.
- Zeisler-Diehl V, Müller Y. 2018. Epicuticular wax on leaf cuticles does not establish the transpiration barrier, which is essentially formed by intracuticular wax. *Journal of Plant Physiology* 227: 66–74.

Supporting Information

Additional Supporting Information may be found online in the Supporting Information section at the end of the article.

Fig. S1 $^{13}\text{CO}_2$ labelling facility.

Fig. S2 Spectral output of LED modules used for plant acclimation and to drive photosynthesis during $^{13}\text{CO}_2$ labelling.

Fig. S3 Relative amounts of different epicuticular wax (EW) compounds removed by stripping with three subsequent collo-dion layers applied to the leaf surface (c. 30 cm²) of *Clusia rosea* plants (adaxial and abaxial sides pooled).

Fig. S4 Two Li-6400XT set-up.

Fig. S5 Photosynthetic induction of *Clusia rosea* leaves subjected to collo-dion treatment. Abaxial gas exchange.

Fig. S6 Statistical distribution of cuticular waxes and epicuticular wax-free, enzymatically isolated cuticles.

Fig. S7 Typical chromatograms of epicuticular waxes of abaxial and adaxial sides of *Clusia rosea* leaves.

Fig. S8 Correlation of ^{13}C excess between adaxial and abaxial cuticle compounds and dewaxed cutin matrix (MX).

Fig. S9 Epicuticular wax of *Brassica oleracea* var. *gemmifera* during pilot ^{13}C labelling experiment.

Fig. S10 Side-specific epicuticular wax of *Capsicum annuum* (pepper).

Please note: Wiley is not responsible for the content or functionality of any Supporting Information supplied by the authors. Any queries (other than missing material) should be directed to the *New Phytologist* Central Office.

Article III

Effect of light-induced changes in leaf anatomy on intercellular and cellular components of mesophyll resistance for CO₂ in *Fagus sylvatica*

Janová J; Kubásek J; Grams TE; Zeisler-Diehl V; Schreiber L; Šantrůček J
(2024).

Plant biology, DOI: 10.1111/plb.13655

Effect of light-induced changes in leaf anatomy on intercellular and cellular components of mesophyll resistance for CO₂ in *Fagus sylvatica*

Jitka Janová¹, Jiří Kubásek¹, Thorsten E. E. Grams², Viktoria Zeisler-Diehl³, Lukas Schreiber³, Jiří Šantrůček¹

¹ Faculty of Science, University of South Bohemia, Branišovská 1760, 37005 České Budějovice, Czech Republic

² Ecophysiology of Plants, Technical University of Munich, Von-Carlowitz-Platz 2, 85354 Freising, Germany

³ Institute of Cellular and Molecular Botany, University of Bonn, Kirschallee 1, 53115 Bonn, Germany

Abstract

Mesophyll resistance for CO₂ diffusion (r_m) is one of the main limitations for photosynthesis and plant growth. Breeding new varieties with lower r_m requires knowledge of its distinct components.

We tested new method for estimating the relative drawdowns of CO₂ concentration (c) across hypostomatous leaves of *Fagus sylvatica*. This technique yields values of the ratio of the internal CO₂ concentrations at the adaxial and abaxial leaf side, c_d/c_b , the drawdown in the *intercellular* air space (IAS), and *intracellular* drawdown between IAS and chloroplast stroma, c_c/c_{bd} . The method is based on carbon isotope composition of leaf dry matter and epicuticular wax isolated from upper and lower leaf sides. We investigated leaves from tree-canopy profile to analyse the effects of light and leaf anatomy on the drawdowns and partitioning of r_m into its inter- (r_{IAS}) and intracellular (r_{liq}) components. Validity of the new method was tested by independent measurements of r_m using conventional isotopic and gas exchange techniques.

73% of investigated leaves had adaxial epicuticular wax enriched in ¹³C compared to abaxial wax (by 0.50‰ on average), yielding 0.98 and 0.70 for average of c_d/c_b and c_c/c_{bd} , respectively. The r_{IAS} to r_{liq} proportion were 5.5:94.5 % in sun-exposed and

14.8:85.2 % in shaded leaves. c_c dropped to less than half of the atmospheric value in the sunlit and to about two-thirds of it in shaded leaves.

This method shows that r_{IAS} is minor but not negligible part of r_m and reflects leaf anatomy traits, i.e. leaf mass per area and thickness.

Article IV

Amphistomy: stomata patterning inferred from ^{13}C content and leaf-side specific deposition of epicuticular wax

Askanbayeva B; Janová J; Kubásek J; Zeisler-Diehl V; Schreiber L; Muir CD; Šantrůček J

(2024).

Annals of Botany.

Amphistomy: stomata patterning inferred from ^{13}C content and leaf-side specific deposition of epicuticular wax

Balzhan Askanbayeva¹, Jitka Janová¹, Jiří Kubásek¹, Viktoria V. Zeisler-Diehl², Lukas Schreiber², Christopher D. Muir³, Jiří Šantrůček¹

¹ Faculty of Science, Department of Experimental Plant Biology, University of South Bohemia, Branišovská 31, 370 05 České Budějovice, Czech Republic

² Institute of Cellular and Molecular Botany, University of Bonn, Kirschallee 1, 53115 Bonn, Germany

³ Department of Botany, University of Wisconsin, 143 Lincoln Drive, Madison, Wisconsin, USA 53711

Abstract

Background and Aims: The benefits and costs of amphistomy (AS) vs. hypostomy (HS) are not fully understood. Here, we quantify benefits of access of CO_2 through stomata on the upper (adaxial) leaf surface, using ^{13}C abundance in the adaxial and abaxial epicuticular wax. Additionally, a relationship between the distribution of stomata and epicuticular wax (EW) on the opposite leaf sides is studied.

Methods: We suggest that the ^{13}C content of long-chain aliphatic compounds of cuticular wax records the leaf internal CO_2 concentration in chloroplasts adjacent to the adaxial and abaxial epidermes. This unique property stems from (i) wax synthesis being located exclusively in epidermal cells and (ii) ongoing wax renewal over the whole leaf lifespan. Compound-specific and bulk wax ^{13}C abundance (δ) was related to amphistomy level (ASL, fraction of adaxial in all stomata) of four AS and five HS species grown under various levels of irradiance. The isotopic polarity of EW, i.e. the difference in abaxial and adaxial δ ($\delta_{\text{ab}} - \delta_{\text{ad}}$), was used to calculate the leaf dorsiventral CO_2 gradient. Leaf-side specific EW deposition, amphiwaxy level (AWL), was estimated and related to ASL.

Key Results: In HS species, the CO₂ concentration in the adaxial epidermis was lower than in the abaxial one independently of light conditions. In high-light and low-light grown AS leaves, the isotopic polarity and CO₂ gradient varied in parallel with ASL. AS leaves grown under high light increased ASL compared to low light, and $\delta_{ab}-\delta_{ad}$ approached near-zero values. Changes in ASL occurred concomitantly with changes in AWL.

Conclusions: The leaf wax isotopic polarity is a newly identified leaf trait, distinguishing between hypo- and amphistomatous species and indicating that increased ASL in sun-exposed AS leaves reduces the CO₂ gradient across the leaf mesophyll. Stomata and epicuticular wax deposition follow similar leaf-side patterning.

* ***Curriculum vitae***

Faculty of Science, University of South Bohemia in České Budějovice

Department of Experimental Plant Biology

370 05, České Budějovice, Czech Republic

Email: neuwij01@prf.jcu.cz, janovaj247@gmail.com

ACADEMIC QUALIFICATION:

- **Phd study** (2015-present, 2020-2023 on maternity leave)

Univesity of South Bohemia, Physiology and developmental biology

Topic: *Leaf cuticle as an archive of information on CO₂ supply*

Supervisor: prof. Ing. Jiří Šantrůček, CSc

- **Master study** (2012-2015)

Univesity of South Bohemia, Experimental biology

Topic: *Transport of carbon dioxide through the leaves of hypostomatous plants*

Supervisor: prof. Ing. Jiří Šantrůček, CSc

- **Bachelor study** (2009-2012)

Univesity of South Bohemia, Biology

Topic: *Effect of the quality of photosynthetically active radiation on diffusive limitations of photosynthesis*

Supervisor: Mgr. Daniel Vrábl

WORKING EXPERIENCE:

- Research assistant (2015 – present, 2020-2022 on maternity leave), Department of Experimental Plant Biology, Faculty of Science, University of South Bohemia, České Buějovice, Czech Republic.
- Organisation of conference *Methods in Plant Sciences 2023*, Srní, CZ
- Organisation of conference *Plant Biology CS 2019*, České Budějovice, CZ

- Internship at *James Cook University*, Centre for Tropical Environmental and Sustainability Science (10/2019-11/2019), lab head prof. Lucas Cernusak, Cairns, Australia
- Internship at *University of Bonn*, Institute for Cellular and Molecular Botany (11/2014, 1/2017 and 9/2018-10/2018), lab head prof. Lukas Schreiber, Bonn, Germany
- **Teaching activities:**

University of South Bohemia in České Budějovice, Faculty of Science

- › Courses: *Plant Cell Biology*, lecturing (in czech), 2019 - present

Stable isotopes Course, organising and lecturing (in english), 2017 – present

Plant physiology, practical training (in czech), 2016 - present

- › Bc. Student: *Tereza Kalistová*, topic: Development of the stomata of dicotyledonous plants: influence of environmental factors; successfully defended in 2019

CONFERENCES:

- **Plant Biology CS 2019.** České Budějovice, Czech Republic.
Oral presentation: *Effect of the light-induced changes in leaf anatomy on intercellular and cellular components of mesophyll resistance in Fagus sylvatica* (2019). CSEPB Young Researcher Award
- **CO₂ Assimilation in Plants from Genome to Biome, GRC.** USA.
Poster: *Effect of the light-induced changes in leaf anatomy on intercellular and cellular components of mesophyll resistance in Fagus sylvatica* (2019)
- **FESP/EPSO 2016.** Prague, Czech Republic
Oral presentation: *CO₂ gradient across hypostomatous leaves as revealed from carbon isotope composition of opposite-leaf-side cuticles* (2016)

- **Plant Cuticular Waxes: From Biosynthesis to Burial.** Ascona, Switzerland;
Poster: *CO₂ gradient across hypostomatous leaves as revealed from carbon isotope composition of opposite-leaf-side cuticles* (2015). Poster award
- **The Plant Biology Europe FESPB/EPSO Congress 2014.** Dublin, Ireland
Poster: *Stomatal development and CO₂ drawdowns in leaves of hypobaric plants* (2014)
- **13th Conference of Experimental Plant Biology.** Košice, Slovak Republic;
Poster: *Hypobaric plants: stomatal and leaf development* (2013)

* PUBLICATIONS

Šantrůček J; Vráblová M; Šimková M; Hronková M; Drtinová M; Květoň J; Vrábl D; Kubásek J; Macková J; Wiesnerová D; Neuwirthová J; Schreiber L (2014). Stomatal and pavement cell density linked to leaf internal CO₂ concentration. *Annals of Botany*, 114(2).

Santrucek J; Schreiber L; Macková J; Vráblová M; Kveton J; Macek P; Neuwirthová J (2019). Partitioning of mesophyll conductance for CO₂ into intercellular and cellular components using carbon isotope composition of cuticles from opposite leaf sides. *Photosynthesis Research* 141, 33-51.

Kubásek J; Kalistová T; Janová J; Askanbayeva B; Bednár J; Santrucek J (2023). ¹³CO₂ labelling as a tool for elucidating the mechanism of cuticle development: a case of *Clusia rosea*. *New Phytologist* 238, 202-215.

Janová J; Kubásek J; Grams TE; Zeisler-Diehl V; Schreiber L; Šantrůček J (2024). Effect of light-induced changes in leaf anatomy on intercellular and cellular components of mesophyll resistance for CO₂ in *Fagus sylvatica*. *Plant Biology*

Askanbayeva B; Janová J; Kubásek J; Zeisler-Diehl V; Schreiber L; Muir CD; Šantrůček J (2024). Amphistomy: stomata patterning inferred from ¹³C content and leaf-side specific deposition of epicuticular wax. *Annals of Botany*